MOBILITY PREDICTION OPTIMIZATION OF MOBILE HOSTS IN SMART ANTENNAS SYSTEM USING ADAPTIVE NEURO-FUZZY INFERENCE SYSTEM

NKAMWESIGA NICHOLAS

EE300-0012/15

Master of Science in Electrical Engineering (Telecommunication Engineering option)

A thesis submitted to Pan African University Institute for Basic Sciences, Technology and Innovation in partial fulfillment of the requirements for the award of the degree of Master of Science in Electrical Engineering (Telecommunication Engineering option)

March 2017

DECLARATION

I Nkamwesiga Nicholas declare that this research thesis is my original work, except where due acknowledgement is made in the text, and to the best of my knowledge has not been previously submitted to Pan African University or any other institution for the award of a degree or diploma.

Name: **Nkamwesiga Nicholas**

Reg. No.: **EE300-0012/15**

Signature: ..... Date: .....

TITLE OF THESIS: MOBILITY PREDICTION OPTIMIZATION OF MOBILE HOSTS IN SMART ANTENNAS SYSTEMS USING ADAPTIVE NEURO FUZZY INFERENCE SYSTEM

PROGRAMME: MASTER OF SCIENCE IN ELECTRICAL ENGINEERING

SUPERVISOR CONFIRMATION:

This research thesis has been submitted to the Pan African University Institute of Science, Technology and Innovation with our approval as the supervisors:

1. Name: **Prof. Dominic B. O. Konditi**

   Signature: ..... Date: .....
2. Name: **Prof. H. Ouma Absaloms**

   Signature: ..... Date: .....

ACKNOWLEDGMENT

First and foremost, I extend my sincere and profound gratitude to the almighty God who saw me through all the challenges and enabled me to complete this work.

I thank the management and the teaching staff of Pan African University Institute of Basic Sciences, Technology and Innovation for the excellent support they rendered me throughout the study. My indebtedness goes to African Union Commission for giving me an offer to be part of the second cohort of students at this University. Without their scholarship I would not have made it up this far.

Last but not least, I would like to acknowledge and appreciate both my supervisors. From the time Prof. Dominic B. O. Konditi and Prof. Heywood O. Absaloms acknowledged my request to supervise me, they have wholeheartedly guided me throughout this research.

DEDICATION

I dedicate this thesis to Rev. Fr. Emmanuel Baburworuganda, Mr. Kizito Tushabe, Sr. Lilian Beitwakakye, Sr. Jacinta Tusiime and Mr. Purtazio Aribatakeine (my father) who beefed-up the foundation for my education.

ABSTRACT

As the demand for wireless communication increases, there is need for better coverage, improved capacity, and higher transmission quality, all of which contribute to better Quality of Service (QoS). One of the promising technologies in achieving excellent QoS is the use of smart antenna systems (SASs) that dynamically radiate power beams to mobile nodes (MNs) in response to received signals to access a wireless link through a process known as beam forming. This has the effect of enhancing the performance characteristics (such as capacity and hand-over) in wireless systems. By using machine learning methods, it is possible to predict the upcoming change in the mobile location at an early stage and then carry out beam forming optimization to alleviate the reduction in network performance. This implies that with a dynamic SAS, a mobile user can be served relatively well while on the move. Efficient prediction of the position of mobile hosts in wireless networks by SASs requires an effective mobility optimization technique.

The use static samples of Received Signal Strength (RSS) in locating MNs has also been proposed in many research studies with positive results. This implies that prediction of RSS in wireless networks would form a strong base for mobility prediction and localization. However, these predictions are still challenging issues, which called for this research study.

One of the prediction techniques that has been proposed and used is the Grey prediction model (GM) which is associated with benefits of reduced overheads which is a serious issue in wireless cellular networks. This is due to its ability to perform prediction with little data and thus perform with little processing effort. In this research

we used of Adaptive Neuro-Fuzzy Inference System (ANFIS) to achieve better estimations of mobility than the prediction made by conventional models like Log-Normal Shadowing Model (LNSM) and GM. The mobility, in this study, was based on the RSS at the mobile node (MN) as it traverses towards or away from the transmitting antenna. This methodology performs prediction with a mean absolute error (MAE); between 0.0826m and 0.6904m in short distances, and between 0.3220m and 3.8765m in long distances which makes ANFIS one of the excellent methods that have been researched about to solve the mobility prediction issue. The study has also revealed that the average distance at which anomalies in the accuracy of mobility prediction occurs has been identified at 62.33% and 64.82% for short (1m to 100m) and long (100m to 1800m) distance communication environments respectively.

TABLE OF CONTENTS

LIST OF TABLES

LIST OF FIGURES

LIST OF APPENDICES

LIST OF ABBREVIATIONS

3G	Third Generation
4G	Fourth Generation
AGO	Accumulated Generation Operation
AI	Artificial Intelligence
ANFIS	Adaptive Neuro-Fuzzy Inference System
ANN	Adaptive Neural Networks
AP	Access Point
BTS	Base Transceiver Station
CN	Core Network
CS	Circuit Switched
dB	Decibel
FIS	Fuzzy Inference System
GGSN	Gateway GPRS Support Node
GMSC	Gateway Mobile Switching Centre
GPRS	General Packet Radio Service
GPS	Global Positioning System
HLR	Home Location Register

LAN	Local Area Network
LNSM	Log-Normal Shadowing Model
LTE	Long Term Evolution
MANETs	Mobile Adhoc Networks
MH	Mobile Host
MME	Mobility Management Entity
MN	Mobile Node
MS	Mobile Station
MSC	Mobile Switching Centre
NN	Neural Networks
P-GW	Packet Data Network Gateway
PS	Packet Switched
PSTN	Public Switched Telephone Network
QoS	Quality of Service
RAN	Radio Access Network
RF	Radio Frequency
RSS	Received Signal Strength
RSSI	Received Signal Strength Indicator
SAS	Smart Antenna System

SGSN	Serving GPRS Support Node
S-GW	Serving Gateway
UE	User Equipment
UMTS	Universal Mobile Telecommunication System
VLR	Visitor Location Register

CHAPTER ONE: INTRODUCTION

1.1 Mobility Prediction

With the current growth rates of mobile and high speed wireless communication networks, the mobile users expect of have a high Quality of Service (QoS) every time and wherever they traverse while they are communicating and accessing information. Telecommunication service providers are expected to provide high-speed data, superior quality voice and location based services [1]. With this motivation, smart antenna systems need to replace the conventional antenna systems and their smartness needs to be depicted in their support for real time services for mobile users with minimal signaling delays while enjoying global roaming.

It has also been evident that mobile communications technology has developed very rapidly over the past few decades. To achieve a high data rate, the concept of mobility is considered as a very important feature of wireless networks. A number of researches have been carried out on mobility [2], and it is seen that in all of the technologies that have been proposed, the mobile node (MN) has a point of attachment as the access point (AP) or a base station (BS) which serves its mobility needs. When a MN is active in a network, there is always a continuous exchange of radio signals between the MN and BS to which the antennas are attached. The non-smart or semi- smart antenna systems relies on the on the predefined parametric rules to make decisions regarding variation in their radiation characteristics. The future of wireless technology will necessitate the antenna systems to be fully equipped with learning intelligence in order to cope up with changing environmental characteristics.

In [3] algorithms for real-time tracking of the location and dynamic motion of a MN in a cellular network using the pilot signal strengths from neighboring BSs were studied. The modelling was based on a dynamic linear system driven by a discrete command process that determines the MN's acceleration. The command process was modeled as a semi-Markov process over a finite set of acceleration levels. The tracking algorithm proposed in [3] was used to predict future mobility behavior, which is useful in resource allocation applications. The numerical outputs of the methodology indicated good accuracy over a wide range of mobility parameter values. In [4] it was shown that good results are produced in case of regular movements and in irregular mobility conditions poor predictions were made.

Received Signal Strength Indicator (RSSI) is a property of a radio signal. RSSI does not require prior information relating to communication protocols. It is easy to observe by gathering the signal strength at the MN [5]. The methods involving mobility prediction using RSS are popular because they require no additional hardware and MNs in the networks have the ability to analyze the RSS [6]. The distance can then be estimated based on RSS data samples collected from a given channel. Calibration of models like the Log-normal Shadowing Model (LNSM) is done to adequately describe the environment through which the MNs traverse [6]. RSSI localization estimation is a feasible alternative to localization similar to GPS.

To add on the research in the area of mobility prediction, an approach based on Grey theory and model attracted attention because of the benefits associated with it. The Grey model (GM) reduces overheads in wireless cellular networks because it requires little data and thus little processing effort. The GM approach has relatively excellent

performance results as well as very short calculation time. The processing of the data needs few data points to get a prediction and is therefore suitable for use in real-time systems due to its quick response time [1] [7] [8].

It can therefore be noted that mobility prediction has remained an area of research seeking to come up with an optimal solution to track and locate mobiles in wireless networks. The methods available are not sufficient in estimating the next position of mobiles especially within the current environment having increased number of obstructions to the radio frequency signals. This is attributed to their failure to optimally reduce the errors made during predictions. Thus an ANFIS methodology, which is a learning system, needs to be investigated with a view to reduce the errors and thus make better predictions that would add on the intelligence of smart antenna systems when performing mobility prediction of mobiles nodes.

1.2 Problem Statement

Mobility in cellular networks is an everyday occurrence; the mobile users change their locations, moving from the proximity of one cell to another which are served by one or many Base Transceiver Stations (BTSs). This is usually done at the expense of reduced RSS of the RF signals transmitted from the transmitting antenna to the mobile node (MN) which reduces as the MN moves away from the transmitting station. Cooperation between or amongst antenna systems at different BTSs during handover is vital and may not be optimally exploited when the future location(s) of active MNs is unknown.

In dynamic smart antenna systems, once a mobile unit makes a call request to a BTS to access a wireless link or node, the antenna system in the BTS automatically concentrates its radiation pattern in that direction, a process known as beam forming. This has the effect of enhancing the performance characteristics, such as capacity and hand-over, in wireless systems [9]. The smart antenna technology has dramatically enhanced the capacity of wireless link through a combination of diversity gain, array gain and interference suppression. This implies that with dynamic smart antenna system, a mobile user can be served relatively well while on the move.

A number of models and optimization techniques have been investigated in the past to predict mobility of mobile nodes (MNs) in wireless network. These models include: Back Propagation (BP), Levenberg-Marquardt (LM), Feed-forward (FF), Bayesian Regularization (BR), Adaptive Neural Network (ANN), Multi-Layer Perceptron (MLP), Neural Networks (NN), and Hybrid (PSO-ANN) [10] [11] [12] [13] [14] [15]. However, the variations in the parameters that contribute to the RSS are not been considered. As a MN traverses in changing environments, the values of path loss, path loss exponent and relative distance between the MN and transmitter change. This has an impact on the overall prediction performance of mobility which depends on the RSS values. Also, the model complexities lead to a long processing time thus making mobility prediction remain an issue in mobile cellular and wireless networks.

To control the mobility prediction challenges, an alternative methodology based on Grey Model (GM) and Adaptive Neuro-Fuzzy Inference System (ANFIS) has been proposed. GM predicts RSS with minimal overheads in terms of processing time, memory, computation power or bandwidth. The ANFIS system learns the patterns of

the input-measured data to produce an optimal trend of RSS which is used to compute the distance of the mobile node (MN) from the transmitter serving it so that the smart antenna systems may serve well the mobility needs of MNs.

1.3 Justification

The current trend of mobile and cellular communication networks necessitates an improvement in the antenna technology especially in the area of mobility prediction. As indicated in [1], with the current growth rates of mobile and high speed wireless communication networks, high-speed data, superior quality voice and location based services are expected from service providers to facilitate both local and global roaming. A number of algorithms have been applied to make better predictions than the conventional models that are based on the RSS. However, these algorithms have not yielded optimal results.

In this research, ANFIS which is a hybrid of Fuzzy Logic and Artificial Neural Network (ANN) [16] [17] was used to come up with an optimal mobility prediction by effectively learning and minimizing errors that occur during localization and mobility prediction processes. The successful prediction of mobility improves wireless or cellular networks by increasing the intelligence of antenna systems thus improving the quality of service (QoS) by; reducing the complexity in mobility management which has been significant in many mobility prediction techniques, improving the handover prediction in wireless cellular networks as well as reducing the dependence of the communication systems on Global Positioning System (GPS) to update the antennas about their MNs' location.

1.4 Research Objectives

1.4.1 General Objective

The general objective of this research is to optimize mobility prediction of Mobile Hosts in Smart Antenna Systems using Adaptive Neuro-Fuzzy Inference System (ANFIS)

1.4.2 Specific Objectives

The specific objectives are as follows:

1. To design an adaptive neuro-fuzzy inference system for optimizing mobility prediction.
2. To optimize and validate the performance of designed mobility prediction methodology.
3. To evaluate the performance of the optimized mobility prediction methodology against reported methods.

1.5 Significance

The significance of the study is to:

a) Improve on the mobility prediction of Mobile nodes in wireless or cellular networks which can improve on dynamic smart antenna intelligence during the process of beam forming.
b) Provide an alternative approach for optimizing the mobility prediction with a keen focus on the smart antennas.

1.6 Scope

This research was limited to a computer simulations using theoretical and measured data. All the algorithms used in this research; the LNSM, GM and ANFIS technique were simulated. The key parameters were all considered in the simulation and these are: Received Signal Strength, Distance of the mobile from the transmitter, Path loss exponent and Path loss at reference distance.

1.5 Overview of Chapters

This thesis is structured as follows:

1. Chapter One covers the problem background together with the objectives of the research.
2. The literature review is elaborated in Chapter Two which presents concepts of mobility prediction and prediction methods like Grey model, antenna systems, and artificial intelligence techniques for example; ANN and ANFIS.
3. Chapter Three presents the research design methodology.
4. Chapter Four presents the research results with analysis and discussion of the simulation results.
5. Chapter Five consists of the conclusion and recommendations for future work.
6. Finally, the References and Appendices are presented at the end of the thesis.

CHAPTER TWO: LITERATURE REVIEW

2.1 Introduction

Mobility in wireless communication networks and mobile communications technology has developed very rapidly over the past few decades [1]. For achieving good Quality of Service (QoS) like high speed and high data rates, mobility is considered to be an important feature of antenna systems for wireless networks. A number of wireless technologies like wireless LAN, cellular networks, cellular 3G and satellite networks all need mobility prediction mechanisms to provide excellent wireless connectivity and roaming across the globe. Mobile users and mobile units especially in wireless cellular networks have drastically shifted from being static to mobile as phone and computer technology shifted from desk phones to mobile phones. The improvement in communication technology in favor of wireless cellular network has not adequately supported the mobile users as they traverse while communicating.

Mobility has become the order of the day with mobile users changing their positions at varying velocities and directions. Mobile users, thus, move from the proximity of one cell to another. Cooperation between different antenna systems during handover is vital and can be maximally exploited when the future location of mobiles are predicted. With the current technology of dynamic smart antenna systems [18], once a mobile unit makes a call or request to access a wireless link, the system automatically concentrates the directionality of its radiation patterns in response to the mobile unit's request. This has the effect of enhancing the performance characteristics (such as capacity and hand-over) in wireless systems.

In all the wireless technologies, whether providing voice, data or real multimedia applications, a mobile node (MN) has a point of attachment known as the access point (AP) or a base station (BS) which serves its mobility needs. An antenna as a part of the AP may thus serve as a reference point, to the mobiles that it serves within a given cell.

2.2 Theoretical Review

2.2.1 Cellular Networks

A cellular network has two main parts; the radio access network (RAN) and core network (CN), as shown in Figure 2.1 [19] for most popular 3G/4G systems; 3G Universal Mobile Telecommunications System (UMTS) and 4G Long-Term Evolution (LTE). UMTS is the most widely deployed 3G cellular network technology that offers both data and voice services while LTE is the only mainstream 4G standard. The overall architecture is similar in all types of cellular networks. 3G RAN is composed of the User Equipment (UE), the Base Station (BS) or Node B, and the Radio Network Controller (RNC). Each RNC manages tens or even hundreds of BSs via Iu-B interface, while exchanging calls/sessions and provisioning services with the core network. It provides central control for radio resource management in RAN including radio resource control, admission control, channel allocation, and mobility management. Each RNC communicates with the Packet-Switched (PS) and the Circuit Switched (CS) core networks to provide data and voice services. The BS is the physical unit providing network access services to UE via its air interface to the UE. The main functionalities of a BS include wireless link transmission/reception, modulation/

demodulation, fast link adaptation, packet scheduling, physical channel coding, error handling, and power control.

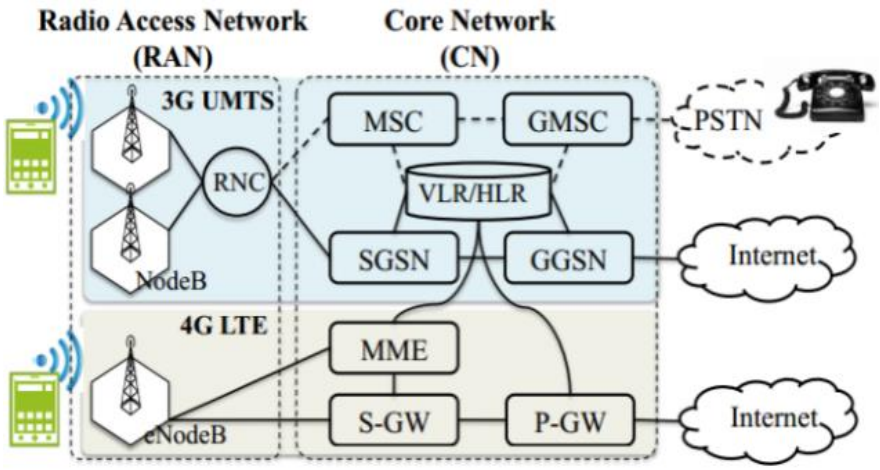

Figure 2.1: 3G/4G Cellular Network Architecture

2.2.2 Smart Antennas in Cellular Networks

The demand for increased capacity in wireless communication networks has motivated recent research activities toward wireless systems that exploit the concept of smart antenna and space selectivity [18] [20]. Efficient utilization of limited radio frequency spectrum is possible with the use of smart/adaptive antenna system. As shown in Figure 2.2 [20], smart antenna radiates not only narrow beam towards desired users exploiting signal processing capability but also places null towards interferers, thus optimizing the signal quality and enhancing capacity. Adaptive antenna systems form an array with main lobe towards user and null towards a co-channel interferer.

Adaptive antenna technology represents the most advanced smart antenna approach to date. Using a variety of new signal-processing algorithms, the adaptive system takes

advantage of its ability to effectively locate and track various types of signals to dynamically minimize interference and maximize intended signal reception.

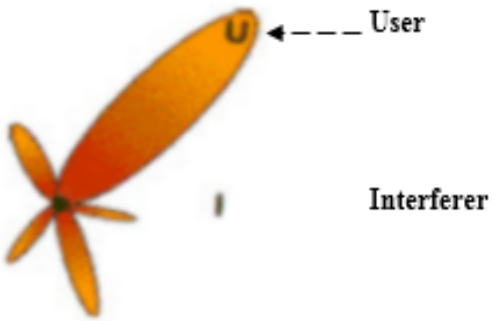

Figure 2.2: Adaptive array coverage

Both adaptive antenna and signal processing algorithms attempt to increase gain according to the location of the user; however, only the adaptive system provides optimal gain while simultaneously identifying, tracking, and minimizing interfering signals. To efficiently radiate to a desired direction, smart antennas usually incorporate the Least Mean Squares Algorithm in coded form which calculates complex weights according to the signal environment.

The functionality of an antenna depends on many factors including physical size of an antenna, impedance (radiation resistance), beam shape, beam width, directivity or gain and polarization among others [21]. By definition, an antenna array consists of more than one antenna element. The radiation pattern of an antenna array depends on the number of antenna elements used in array. The more elements they are, the narrower the beam that can be formed. Planar arrays are capable of making a narrow beam in the horizontal as well as vertical plane. Smart antennas with the ability of beam steering can be constructed by adding intelligence to planar arrays.

Receiver (R_x) smart antennas can be defined as antennas with multiple elements where signals from different elements are combined by an adaptive algorithm whereas transmit smart antennas are antennas in which the signals at the antenna elements are created by the algorithm. Increasing the antenna elements within an antenna array results into an increase in signal to noise ratio (SNR) compared with a single antenna. In a cellular system, each antenna has a fixed number of subscribers and increasing the number of antennas results in an increase in the number of subscribers that can be served by one BTS. By reducing the interference and increasing the signal power, a smart antenna improves link quality and this helps in combating large delay dispersion [22]. The current technology smart antennas [23], that is adaptive antenna as shown in Figure 2.2, exploits the array of antenna elements to achieve maximum gain in desired direction while rejecting interference coming from other directions.

An adaptive antenna can steer the maxima and nulls of its array pattern in nearly any direction in response to the changing environment [22]. The basic idea behind adaptive antenna is the same as in switched beam antenna, which is to maximize the SINR values. While the multiple switched beam antennas have a limited selection of directions to choose the best beam, an adaptive antenna can freely steer its beam in correspondence to the location of user. Smart antenna employs Direction of Arrival (DOA) algorithm to track the signal received from the user, and places nulls in the direction of interfering users and maxima in the direction of desired user. On the other hand, since adaptive antennas needs more signal processing, multiple switched beam antennas are easier to implement and have the advantage of being simpler, and less expensive compared to adaptive antennas. The overall capacity gain of smart antennas

is expected to be in the range of 100% to 200%, when compared with conventional antennas.

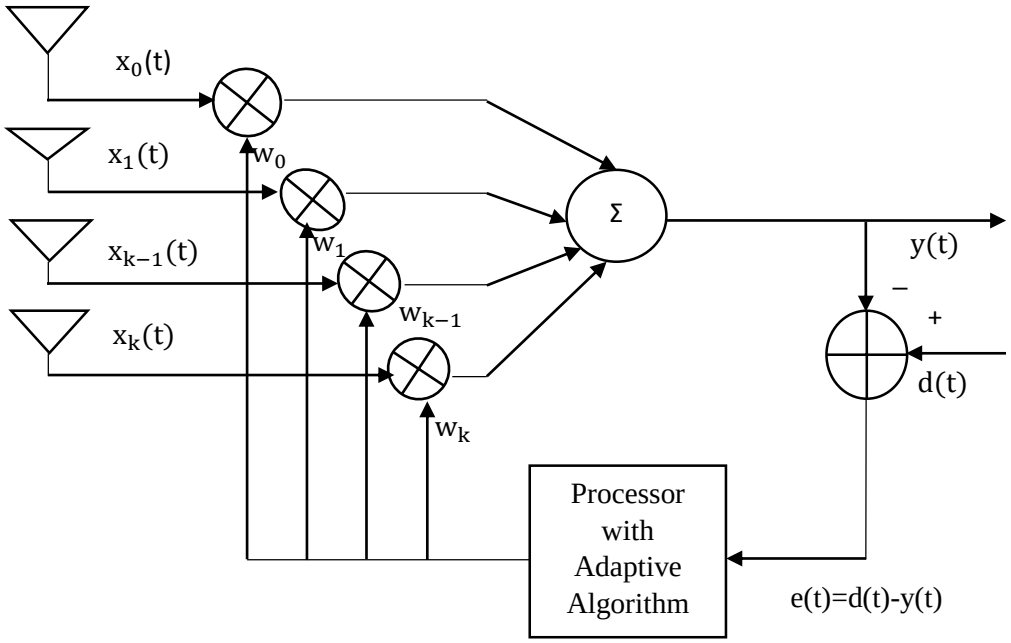

Figure 2.3: Adaptive Beam Forming System

Beam forming algorithms used in adaptive antennas are generally divided into two classes with respect to the usage of training signal: Blind Adaptive algorithm and Non-Blind Adaptive algorithm [23]. In a non-blind adaptive beam forming algorithm, a known training signal $d(t)$ is sent from transmitter to receiver during the training period. The beam former uses the information of the training signal to update its complex weight factor. Blind algorithm does not require any reference signal to update its weight vector; rather it uses some of the known properties of desired signal to manipulate the weight vector. Figure 2.3 [23] shows the generic beam forming system based on non-blind adaptive algorithm, which requires a training (reference) signal.

The output $y(t)$ of the beam former at time t is given by a linear combination of the data at the k antenna elements. The baseband received signal at each antenna

element is multiplied with the weighting factor which adjusts the phase and amplitude of the incoming signal accordingly. The sum of the weighted signals results in the array output $y(t)$. On the basis of adaptive algorithms, entries of weight vector w are adjusted to minimize the error $e(t)$ between the training signal $d(t)$ and the array output $y(t)$.

2.2.3 Load Balancing Algorithms

In [24], an investigation of a load balancing scheme for mobile networks that changes cellular coverage according to the geographic traffic distribution in real time was carried out using a bubble oscillation algorithm. The results indicated that the performance of the whole cellular network is improved by contracting the antenna pattern around a traffic hotspot and expanding adjacent cells coverage to fill in the coverage loss. It also shows that the system capacity is improved by adjusting the cell size and shape according to the existing geographic traffic distribution at a particular time.

In [25], we also see a sub-optimal Heaviest-First Load Balancing (HFLB) Algorithm that aimed at solving load imbalance that deteriorates the system performance in Long Term Evolution (LTE) networks. It was dealt with by proposing a load balancing framework, which aims at balancing the load in the entire network, while keeping the network throughput as high as possible. The results showed a significant load balancing while maintaining the same network throughput at the price of a bit more handover compared with the traditional signal strength based handover algorithm. Load imbalance that reduces network performance is a serious problem in LTE

Networks. Load imbalance occurs in communication networks due to non-uniform user deployment distribution.

2.2.4 Mobility Effect on the RSS

When an active mobile moves away from its reference antenna, the received signal strength (RSS) reduces with increase in travel distance. Wireless radio channel poses a severe challenge as a medium for reliable high-speed communication [26]. It is not only susceptible to noise, interference, and other channel impediments, but these impediments change over time in unpredictable ways due to user movement. Therefore, RSS [27] is a method to find distance from attenuation of propagation path. If the transmission power is known, the total attenuation of signal propagation through the path can be calculated by subtracting the received power from transmitted power. With the use of radio frequency (RF) transceiver, the received power can be measured and provided to an RSS ranging method. In most of the RF transceivers, a dedicated register is used to store the RSS indicator. Therefore, it is a low-cost and convenient way to measure distance.

In a report on the challenges of mobility prediction, published by the Institute of Eurecom [28], a number of mobility prediction methodologies were highlighted. One of the techniques was an integrated mobility and traffic model for resource allocation in wireless networks in which the RSS Indicators are periodically sampled from all the base stations (BSs) the mobile node (MN) connects to and then transmitted to the attached base station. This helps in obtaining course relative position estimates of mobiles. The MN and the attached BS coordinate to identify the next possible BS that the MN may move to in preparation for any handovers. It is observed here that the

mobility prediction is based on estimated positions obtained by the sampled RSSI from different BSs.

The mobility profile manager plays a major role in the handover prediction. It continuously monitors the mobility pattern of the MN concerned. The position of the MN is periodically computed basing on RSSI and then stored in the database. The mobility history is used in predicting the access point to which the MN is expected to have a handoff. RSS measurements uses historical values and optimal mobility predictions can be made when the predicted RSS measurements are used [29].

In [30], a mobility prediction algorithm based on dividing sensitive ranges was proposed. The division was based on the cell transformation probability. Different prediction methodologies were used according to the sensitivity of the defined ranges in order to gain high precision. A hierarchic position prediction algorithm was used basing on the user's movement history and instantaneous RSSI measurements of surrounding cells. This study proposed that the mobile user movement can be estimated by parameters like; current location, velocity and cell geometry which were estimated with the help of sampled instantaneous RSSIs. This method helped in setting up and reserving resources along a mobile's path, and planned quick handovers between BSs. Prediction performance was accurate at 75%. In this approach, the RSSI was just sampled to help them in locating positions. Greater accuracy in the prediction performance would be significant if the RSSIs were predicted instead of instantaneous sampling. This is because prediction yields a faster and timely response in locating new positions.

The changeover in IEEE 802.11 relies on the RSSI and many handover algorithms are based on RSSI [31]. For example; reduction in the RSSI of the currently associated Access Point (AP) beyond the preset thresholds can be used to trigger a handover. Depending on how the IEEE 802.11 standard is implemented on a mobile host device, the device may switch to another AP when the RSSI falls below a threshold. RSSI and other predictors like frame transmissions and frame losses play a vital role in mobility prediction and thus handover management. A handover may not be successful especially when the next access point is not discovered by the mobile host. However, effective prediction of the RSS measurements would yield an excellent mobility prediction and thus mobility prediction is necessary in handoff prediction.

RSS is used to determine distance based on the attenuation of propagation path. With known parameters for transmission power and received power, the total attenuation of signal propagation through the path can easily be obtained [32]. Using trilateration estimation approach, unknown location of a MN from several reference locations can be calculated. Trilateration approach uses the distances among the locations to estimate the coordinate of the unknown location. The distances between reference locations and the unknown location can be considered as the radii of many circles with centers at every reference location and the unknown location is obtained as the intersection of all the sphere surfaces. This method works well when the reference positions are at least three and for lower numbers of reference positions, a triangulation method may be used. Triangulation estimation is a trigonometric-based approach of determining an unknown location using two angles and a distance between them. This method was used in sensor networks; two reference nodes can be located on the horizontal axis or vertical axis.

The signal attenuation distance between two reference nodes on the baseline can be measured in preliminary stage and stored in the system's memory. By extrapolating this idea, it implies that prediction of the RSS of MNs at future locations can yield excellent performance in location prediction. Thus, mobility prediction basing on RSS is vital in wireless networks and smart antenna systems.

2.2.5 Capacity Enhancement in Cellular Networks through Sectorization

Cell sectorization [33] is an economical way to enhance system capacity of existing cellular networks without change of existing base transceiver station (BTSs). This reduces the additional cost for adoption of new technologies employed with smart antennas, adaptive beam antenna and steerable antennas. Sectorization technique is a widely used technique to reduce co-channel interference in cellular mobile radio systems. There are two important factors that influence the system performance when using sectorization technique. The first is the number of sectors per cell [21] [34]. By carefully controlling the transmission of signals to directions where they are really intended, directional antennas cut down the co-channel interference.

Cell sectorization is used extensively to increase the capacity of cellular systems [35] and typically, a cell within a cellular network grows from minimal number of sectors (Omni cell) to more sectors (3-sector or more) in response to the growth of tele-traffc demand. Presently cellular systems are working on three antennas with $120°$ or six antennas with $60°$ architectures. Researchers of cellular networks are always looking for techniques to improve the network capacity within the limited frequency spectrum.

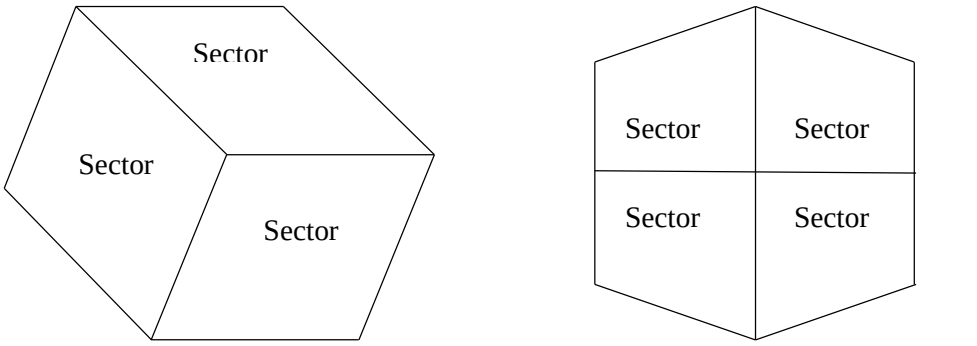

- 120^0 directional antennas
- 3 sectors per cell
- 3 transmit and receive antennas

- 90^0 directional antennas
- 4 sectors per cell
- 4 transmit and receive antennas

Figure 2.4: Cell Sector Configurations

As shown in Figure 2.4 [34], the network enhancement method is to increase the number of sectors per base station. The challenge with sectoring as indicated in [21][34] is that they require more antennas to be mounted on a BTS and they also require more frequent handoffs whenever MNs move across sectors.

2.2.6 Artificial Intelligence Techniques

Artificial intelligence (AI) is defined as the ability of a computer or any other machine to perform those activities that are normally thought to require intelligence by evaluating information and making decisions according to pre-established criteria [17]. AI borrows its meaning from the word intelligence which is defined as the ability to apply past and present experience to satisfactorily solve present and future problems. In AI, the basic paradigm of intelligent action is that of searching through a space of partial solutions (called the problem space) for a goal situation. Fuzzy logic, artificial neural networks, genetic algorithms, and particle swarm optimization, among others, are examples of AI techniques that are applicable in every day's life [1].

Artificial intelligence techniques have recently gained popularity in engineering design due to their efficiency and effectiveness and various papers have been published on the mobility prediction using AI techniques [4] [11] [36] [37].

2.2.7 Adaptive Neural Fuzzy Inference System (ANFIS)

ANFIS is about taking a Fuzzy Inference System (FIS) and tuning it with an Adaptive Neural Networks (ANN) algorithm based on some collection of input-output data [17]. Using a given input/output data set, the ANFIS constructs a FIS whose membership function parameters are tuned (adjusted) using either a back-propagation algorithm alone or in combination with a least squares type of method. This adjustment allows the fuzzy systems to learn from the data being modeled. The parameters associated with the membership function changes through the learning process. The computation of the parameters is facilitated by a gradient vector. This gradient vector provides a measure of how well the fuzzy inference system is modeling the input/output data for any given set of parameters. When the gradient vector is obtained, any of several optimization routines can be applied in order to adjust the parameters and to reduce some error measure. This error measure is usually defined by the sum of the squared difference between actual and desired outputs. This process is referred to as supervised learning in neural network literature. By combining the advantages of imprecise data sampling of fuzzy logic and the intelligence of ANN, the neuro-fuzzy outsmarts the two individual AI; Fuzzy systems and Neural Networks.

ANFIS structure consist of antecedent and conclusion parts. These two parts are linked by rules, to form a network. During the hybrid learning process, two steps are involved: a feed forward and feedback. In the feed forward, the parameters are first initialized

while keeping the antecedent parameters fixed, input data and functional signals propagate forward to compute the result of each layer node and the Least Square algorithm computes the consequent parameters. When the consequent parameters are identified, the functional signals continues in the forward motion until the error measure is computed and therefore known. In the feedback phase, the error rates propagate in a reverse order, from the output towards the input end [38] [39] [40]. The process is continued until the number of specified epochs (iterations) have been attained or error reaches a preset threshold.

Figure 2.5 [41] shows the architecture of an ANFIS. It assumes a system with two inputs *(x, y)*, four rules (Equation 2.1) and one output *(z)*. The ANFIS structure executes the rules and calculates the output through five layers: fuzzification, product, normalization, de-fuzzification and total output.

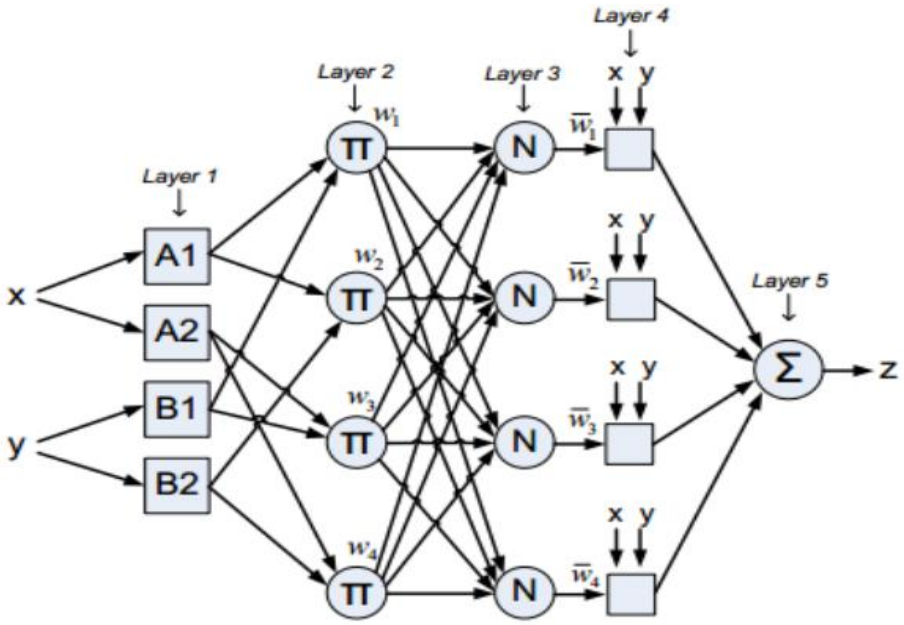

Figure 2.5: Structure of an ANFIS

This ANFIS structure has four rules and by using first-order Sugeno model, a typical set of fuzzy if-then rules are generated as

$$\text{If x is } A_1 \text{ and y is } B_1, \text{then } Z_1 = p_1x + q_1y + r_1 \quad (2.1a)$$

$$\text{If x is } A_1 \text{ and y is } B_2, \text{then } Z_2 = p_2x + q_2y + r_2 \quad (2.1b)$$

$$\text{If x is } A_2 \text{ and y is } B_1, \text{then } Z_3 = p_3x + q_3y + r_3 \quad (2.1c)$$

$$\text{If x is } A_2 \text{ and y is } B_2, \text{then } Z_4 = p_4x + q_4y + r_4 \quad (2.1d)$$

Where A_1, B_1, A_2, B_2 are fuzzy sets, p_i, q_i and r_i $(i = 1,2,3,4)$ are the coefficients of the first order polynomial linear functions. The different layers in Figure 2.5 are discussed next.

Layer 1: Fuzzification Layer

In this layer, the membership values are calculated from the membership relationship between input and output functions of layer 1 and they are identified as

$$O_{1,i} = \mu_{A_i}(x), \qquad i = 1, 2 \quad (2.2a)$$

$$O_{1,j} = \mu_{B_j}(y), \qquad j = 1, 2 \quad (2.2b)$$

Where $O_{1,i}$ and $O_{1,j}$ represent the output functions and μ_{A_i} and μ_{B_j} represent the membership functions.

Layer 2: Product Layer

This layer has four nodes and the output, w_j, of each rule has to be computed by means of a fuzzy AND operation.

The Equation 2.3 illustrates how this. w_j is the weight of the j^{th} rule and $O_{2,j}$ is the output

$$O_{2,j} = w_j = \mu_{A_i}(x)\,\mu_{B_i}(y),\ j = 1,2,3,4. \quad i = 1,2 \tag{2.3}$$

Layers 3: Normalized Layer

The purpose of this layer is to normalize the weight function, w_j, obtained from layer 2 to obtain the normalized output $\bar{w}_j$. The output $\bar{w}_j$ is calculated as the ratio of the j^{th} weight to the sum of the all weights. The output is denoted by

$$O_{3,j} = \bar{w}_j = \frac{w_j}{\sum_{i=1}^{4} w_i} \tag{2.4}$$

Layers 4: De-fuzzification Layer

In the layer 4, $\bar{w}_j$ multiplies the related output function (linear equations of the consequent part in Equation 2.4. The output of this layer is given by Equation 2.5.

$$O_{4,j} = z_j\,\bar{w}_j = \bar{w}_j(p_j x + q_j y + r_j) \tag{2.5}$$

Layers 5: Total Output Layer

This is the final layer with a single node which gives the overall output. The output, given in Equation 2.6, is the sum of the former nodes.

$$O_{4,j} = \sum_{j}^{4} z_j\,\bar{w}_j \tag{2.6}$$

The antecedents are tuned during the training process. Other parameters in the ANFIS training process are the coefficients of the output polynomials (as seen in Equation

2.1) and number of rules. The number of rules are defined by the number of inputs and membership functions [42].

2.3 Empirical Review

2.3.1 Mobility Prediction Techniques and Models

Mobility prediction of wireless users and units plays a major role in efficient planning and management of the bandwidth resources available in wireless networks [36]. In return, this efficiency allows better planning and improved overall QoS in terms of continuous service availability and efficient power management. In cellular networks, QoS degradation or forced termination may occur when there are insufficient resources to accommodate handoff requests. One solution is to predict the trajectory of mobile terminals so as to perform resource reservations in advance. With the vision that future mobile devices and thus smart antenna systems are likely to be equipped with reasonably accurate positioning capability, some new features for use in mobility prediction were investigated by Wee-Seng and Kim [43].

The application of mobility model is very important in the description of the movement pattern of mobile users. These patterns show how their location, velocity and acceleration among others change with respect to time. Every mobility prediction model has different characteristics as it performs location prediction of the target mobile node. A brief description of mobility prediction models which have been proposed and used are highlighted in this subsection of literature review.

2.3.2 Neural Network Techniques for Prediction in Mobile Networking

Neural Networks (NN) are very sophisticated modeling techniques capable of modeling extremely complex functions [11] [15] and they have non-linear structure networks which learn by example. Neural Networks gather representative data and then invokes training algorithms to automatically learn the structure of the data. NN methodology for location prediction is done in two steps. Firstly, NN is trained with observed motion pattern. In the second step the trained NN is used for prediction, the actual movement and time is used to feed the trained neural network to make location prediction. This approach gives good results in the case of regular movements, but poor prediction results are seen in irregular mobility conditions [4].

2.3.3 Random Walk Mobility Model

In this mobility model [44], mobile node (MN) moves from its current location to a new location by randomly choosing both the direction and speed. The new speed and direction are both chosen from ranges defined in advance; minimum speed-maximum speed and [0, 2π], respectively. The movement can be calculated in two ways; either with a constant time interval, t or with a constant distance traveled d. If the MN approaches a boundary, it bounces back with an angle determined by the next upcoming direction. This mobility model is memoryless with the next move totally independent from the previous one. As the name of the model states, MNs are considered to be random and depicts a memoryless mobility system where the next move is totally independent from the previous one.

2.3.4 Random Waypoint Mobility Model

The Random Waypoint Model was proposed by Johnson and Maltz [44]. This model includes pause times between changes in destination and speed. Firstly, the mobile node (MN) chooses a random location and considers it as its destination and then it moves towards its destination with constant velocity which is uniformly distributed between minimum velocity and maximum velocity. After arriving at the destination, the MN pauses for a specific time before choosing another random destination. The pause time can have the value zero (0), which means that it will continue its movement without any pause. This mobility model is also memoryless and the future movements of the future position MNs is independent of the previous movements [45]. From this brief description, this model is simple and is commonly studied in MANETs to evaluate their performance.

2.3.5 Gauss-Markov Mobility Model

From [19], the Gauss-Markov Mobility Model was planned to achieve randomness via one tuning parameter. Initially each mobile node (MN) is assigned a current speed and direction. At fixed intervals of time, *n*, movement occurs by updating the speed and direction of each MN. Specifically, the value of speed and direction at the n^{th} instance is calculated based on the value of speed and direction at the $(n-1)^{th}$ instance and a random variable using the following equations:

$$s_n = as_{n-1} + (1-a)\mu + \sqrt{(1-a^2)}s_{x_{n-1}} \tag{2.7a}$$

$$\alpha_n = a\alpha_{n-1} + (1-a)\mu + \sqrt{(1-a^2)}\alpha_{x_{n-1}} \tag{2.7b}$$

s_n and α_n denotes the new speed and direction of the MN at time interval n, a is a tuning parameter used to vary the randomness, $0 \leq a \leq 1$, $s_{x_{n-1}}$ and $\alpha_{x_{n-1}}$ are random variables drawn from a Gaussian distribution with zero mean and standard deviation equal to 1. The value of μ is usually fixed at 1. For $a = 0$, the equation yields totally random values, equivalent to Brownian motion. For $a = 1$, the equation yields fixed values, equivalent to linear motion. The value of a can be adjusted between these two extremities to obtain different levels of random movement. At every time interval the next location of the MN is calculated based on the current location, speed, and direction of movement. Specifically, at time interval n, an MN's position is given as

$$x_n = x_{n-1} + s_{n-1}\cos\alpha_{n-1} \tag{2.8a}$$

$$y_n = y_{n-1} + s_{n-1}\sin\alpha_{n-1} \tag{2.8b}$$

(x_n, y_n) and (x_{n-1}, y_{n-1}) are coordinates of the MNs position at the n^{th} and $(n-1)^{th}$ time intervals, respectively. s_{n-1} and α_{n-1} are the speed and direction of the MN at the $(n-1)^{th}$ time interval, respectively.

This model ensures that the MNs do not go beyond the boundaries grid which acts like a cell. This prevents the MN from remaining near an edge of the grid for a long period of time. This is done by modifying the mean direction variable α, for example; its value can be changed to 180° when it reaches the grid. In Gauss Markov model, the velocity of a MN at any time slot is a function of its previous velocity. This summarizes Gauss-Markov Model as a chronological dependency model with the degree of dependency being determined by the capacity of its memory to store parameter a which is a random

generator a that determines whether the model either behaves randomly in a Brownian form or in linear motion.

2.3.6 Reference Point Group Mobility Model

This model simulates group behavior [46], where each MN belongs to a group where every node follows a logical center, also known as a group leader. It is the leader that determines the group's motion behavior. The nodes in a group are usually randomly distributed around the reference point. The most vibrant contribution by this model is that different nodes use their own mobility model and are then added to the reference point which drives them in the direction of the group. At any given point in time, every node has a speed and direction that are derived by randomly deviating from that of the group leader. This general description of group mobility can be used to create a variety of models for different kinds of mobility applications. Group mobility as such can be used in military battlefield communications. One example of such mobility is that a number of soldiers may move together in a group. Another example is during disaster relief where various rescue crews, for example; firemen, policemen, and medical assistants form different groups and work together as a group.

This model considers nodes to be moving in a group and that they are randomly distributed around the reference point. The reference point is a leader of the group. The individual position is neglected as long as it is not the leader. This increases the QoS at the reference node at the expense of the individual nodes. However, on a good note, every node may use its own mobility model and are then added to the reference point. The reference model does the work of driving nodes in a given direction as a group.

The group mobility model can thus be used to create a number of models for various kinds of mobility applications.

2.4 Models under this Study

2.4.1 Log-Normal Shadowing Model

Signal propagation models are used to generate theoretical received signal strength (RSS) values. In this research, the log-normal shadowing model (LNSM) is proposed as the target signal propagation model. This is because of its ability to compensate the attenuating factors through the use a compensating factor X_{ξ}, which is a Gaussian random variable (measured in dB) [43].

In cellular or wireless networks, the location of the mobile node (MN) and its serving base transceiver stations (BTSs) is observable in the information that characterizes the forward link received signal strength indicator (RSSI) of all the active BTSs. The values of RSSI at the MN are measured at the mobile station and is modeled as a two-fold effect of path loss and shadow fading [47]. The path loss, $P_L(d_i)[dB]$, at any distance, $d_i(m)$, in an open space is in Equation 2.9 [43].

$$\mathrm{P_L(d_i)[dB]} = \mathrm{P_L(d_0)[dB]} + 10\mathrm{n}\log_{10}\left(\frac{\mathrm{d_i}}{\mathrm{d_0}}\right) \tag{2.9}$$

Where; d_i is the transmitter-receiver separation, n is the path loss exponent, $\mathrm{P_L(d_0)[dB]}$ is the path loss at known reference distance, d_0. The path loss exponent, *n*, is an empirical constant and it varies with the characteristics of the propagation environment.

The model shown in Equation 2.9 is considered to be unrealistic and with environmental factors like weather conditions, atmospheric absorption and space rays, the propagating signal is hindered by reflection, diffraction and scattering phenomenon. Basing on the empirical evidence, the path loss ($P_L(d_i)$) at any given distance d_i is modeled as a log-normally distributed random variable and a distance-dependent [47] [48] [49] [50]. This forms the log-normal shadowing model in Equation 2.10

$$P_L(d_i)[dB] = P_L(d_0)[dB] + 10n\log_{10}\left(\frac{d_i}{d_0}\right) + X_\xi \quad (2.10)$$

Where X_ξ (dB) is Gaussian random variable. The RSS at any given distance is modeled in Equation 2.11

$$RSSI = P_R = P_T - P_L(d_i)$$

$$= P_T - P_L(d_0)[dB] - 10n\log_{10}\left(\frac{d_i}{d_0}\right) - X_\xi \quad (2.11a)$$

$$RSSI = -10n\log_{10}(d) + A \quad (2.11b)$$

Where; RSSI denotes the signal power at the receiver, P_T denotes the transmitted power, n denotes the path loss exponent, $d = \frac{d_i}{d_0}$ is the normalized distance from the transmitter and A denotes $(P_T - P_L(d_0) - X_\xi)$. In this study, d_0 is set between 1m and 3.5m for short distance and 100m for long distance.

2.4.2 Grey Prediction Model

Grey prediction model is based on the Grey theory which organizes the original sequence of data so that a high degree of accuracy is achieved. Grey systems are

generic and may use colors to describe the subject under investigation. For example; a dark color may represent the degree of clarity of information. In a similar way, Black Box has been widely used to stand for a structure that is not known to the investigator. In Grey theory black symbolizes unknown information, white for known information and Grey for partially known information [1].

Grey and fuzzy concepts seem to be similar but different in the properties of internal meanings and external extensions of subjects under investigation. Grey systems emphasize the objects of definite external extensions and vague internal meanings, unlike fuzzy logic which studies the objects with definite internal meanings and vague external extensions [51]. Grey systems relies on the foundation of Grey numbers and their operations which are Grey matrices and equations. Some examples of research tasks with Grey systems are: control problems in industry, Grey systems analysis, modeling, forecasting and controlling intrinsic characteristics of systems. It is through organization of raw data that Grey systems can remove randomness, which is followed by series of operations for construction of the Grey model. The organization and operations of the Grey forecasting model are based on grey system theory which has got a strong adaptation ability since it requires less data and distribution information is not necessary. It requires a few discrete data values which are sufficient to characterize an unknown system in order to formulate a real world problem associated with uncertainty [52] [53] [54].

The prediction method of Grey systems theory has the following features:

a. It is composed of a dynamic model expressed by an ordinary differential equation.

b. The right hand side of the differential equation can have various factors of fluctuation (mainly input factors).
c. The algorithm is relatively easy to understand and requires only a few calculations.

The Grey system prediction methodology is achieved through: conversion of original data into a new data sequence, a process called Accumulated Generation Operation (AGO); and parameter determination through the use of least squares method using the new data series. As already mentioned, the theory relies on objects that are known as Grey numbers, together with operations, matrices and equations. It is also already known that Grey theory treats raw data using suitable laws to transform it into processed data. The randomness in the data is reduced by the AGO on the raw data to make it meaningful. The AGO is illustrated below: Consider

$$\times (0) = 1, 2.5, 3, 4.5, 5, 3.5 \tag{2.12}$$

This sequence in Equation 2.12 does not have clear rule. After the application of AGO, the sequence in Equation 2.13 has a steady increase in the numbers which are generated.

$$\times (1) = 1, 3.5, 6.5, 11, 16, 19.5 \tag{2.13}$$

The AGO method removes the irregularities in the raw data and this is the basis of Grey theory. AGO transforms the original data into data with an exponential curve which is illustrated in Figure 2.6

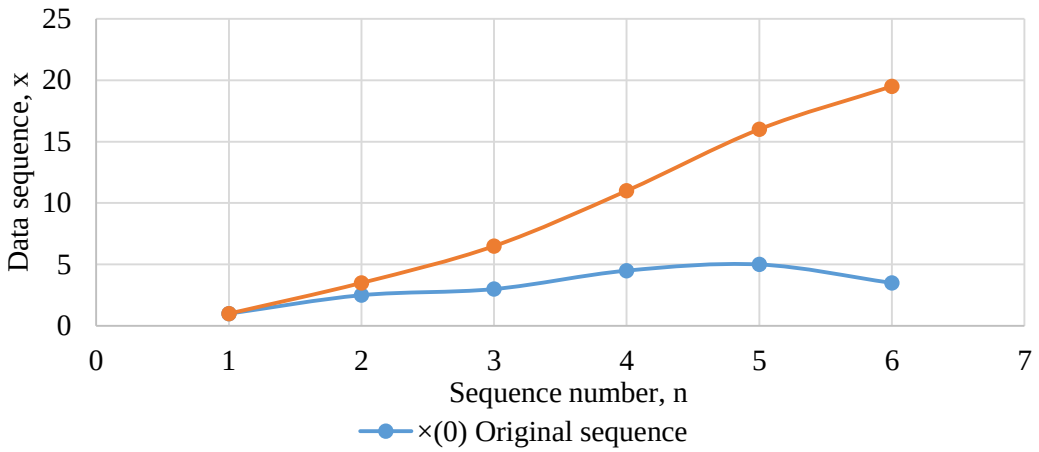

Figure 2.6; Data transformation for AGO operation in the Grey model

The Grey model GM(1,1) is the most widely used Grey forecasting model. GM(1,1) is a single variable first-order Grey model, which weakens the randomness of the original data series. It relies on the original data to search the intrinsic regularity of the data. It is achieved through the following steps:

Step 1: Generate the initial time series

$$x^{(0)}(t) = x^{(0)}(1), x^{(0)}(2), \ldots, x^{(0)}(k) \tag{2.14}$$

Step 2: Generate regular data sequence by applying the AGO on the initial irregular data sequence in Equation 2.14.

$$x^{(1)}(k) = x^{(1)}(1), x^{(1)}(2), \ldots, x^{(1)}(n) \tag{2.15}$$

Where $x^{(1)}(n)$ is the n^{th} value of the regular sequence. The result of the AGO is summarized as

$$x^{(1)}(k) = \sum_{t=1}^{k} x^{(0)}(t) \tag{2.16}$$

Step 3: Formulate the first-order Grey differential equation.

The first-order differential equations of the Grey model GM(1,1) is formulated as follows:

$$\frac{dx^{(1)}}{dt} + ax^{(1)} = b \tag{2.17}$$

Where; a is the development coefficient for reflecting the development trends of x^0 and x^1, b is the Grey input. The values of a and b are obtained by applying a least square method to Equation 18.

$$\begin{bmatrix} a \\ b \end{bmatrix} = (\mathbf{B}^T\mathbf{B})^{-1}(\mathbf{B}Y_N)^T \tag{2.18}$$

Where;

$$\mathbf{B} = \begin{bmatrix} -\frac{1}{2}\left[x^{(1)}(2) + x^{(1)}(1)\right] & 1 \\ -\frac{1}{2}\left[x^{(1)}(3) + x^{(1)}(2)\right] & 1 \\ \vdots & \vdots \\ -\frac{1}{2}\left[x^{(1)}(n) + x^{(1)}(n-1)\right] & 1 \end{bmatrix} \text{ and } \mathbf{Y}_N = \left[x^{(0)}(2), x^{(0)}(3), \dots, x^{(0)}(n)\right]$$

The first column of the B-matrix consists of the background sequence and each point in the sequence forms part of the background value. The values of a and b are obtained by substituting the values of $\boldsymbol{B}$ and $\boldsymbol{Y}_N$ into Equation 2.18.

Step 4: Solve the differential equation

Using the solution of step 3 and Equation 2.17, the prediction model GM(1,1) is obtained as

$$x^{(1)}(k+1) = \left[x^{(1)}(0) - \frac{b}{a}\right]e^{-ak} + \frac{b}{a}, \quad k = 1,2,3, \dots, n \tag{2.19}$$

Step 5: Apply Inverse Accumulated Generating Operation (IAGO)

The IAGO is applied to obtain a prediction value corresponding to the original data series.

$$\hat{x}^{(0)}(k+1) = x^{(1)}(k+1) - x^{(1)}(k) = (1 - e^{-a})\left[x^{(1)}(0) - \frac{b}{a} \right] e^{-ak} \quad (2.20)$$

Step 6: Validation of the accuracy of prediction

The accuracy of the GM(1,1) model is inspected by testing the accuracy of the prediction and prediction error made by the modelling algorithm. The original data series $x^{(0)}(k) = \{x^{(0)}(1), x^{(0)}(2), \ldots, x^{(0)}(n)\}$ and formulated predicted data series $\hat{x}^{(0)} = \{\hat{x}^{(0)}(1),\ \hat{x}^{(0)}(2), \ldots,\ \hat{x}^{(0)}(n)\}$ are used in calculating of residual error, relative error and mean relative error.

The absolute residual error is calculated as shown in Equation 2.21.

$$\varepsilon_k^{(0)} = \left| x^{(0)}(k) - \hat{x}^{(0)}(k) \right|, k = 1, 2, 3, \ldots, n \quad (2.21)$$

The relative error is calculated as shown in Equation 2.22.

$$\Delta_k = \frac{\varepsilon^{(0)}(k)}{x^{(0)}(k)} = \frac{\left| x^{(0)}(k) - \hat{x}^{(0)}(k) \right|}{x^{(0)}(k)}, k = 1,2,3, \ldots, n \quad (2.22)$$

The mean relative error is calculated as

$$e_k = \overline{\Delta_k} = \frac{1}{n} \sum_{k=1}^{n} \Delta_k \quad (2.23)$$

The prediction accuracy is $(1 - e_k) * 100\%$. When $e_k \leq 0.3$, the grey model GM(1,1) is suitable for medium and long term forecasting [52].

Step 7: Introduce weights in GM(1,1)

Introduce weights, w_1 and w_2, in Equation 8 and Equation 14 to form a new a weighted-prediction sequence.

$$\hat{x}_N^{(0)}(k+1) = w_1 x^{(0)}(k) + w_2 \hat{x}^{(0)}(k+1) \quad (2.24)$$

Where $\hat{x}_N^{(0)}(k+1)$ is the weighted GM, which is a generic prediction based on GM. Step 6 was performed to validate the prediction accuracy.

2.5 Identified Research Gap

From the current methodologies used in studying mobility prediction, as highlighted in the literature review, we learn that many of the proposed models do not consider using Received Signal Strength (RSS) during mobility prediction. A few methods which partially use the RSS measurements to perform localization and mobility prediction only use the historical measurements of the RSS accompanied with other parameters that describe the motion or map the path of mobile nodes (MNs) like current location, velocity and cell geometry. Optimum utilization of RSS measurements would be of a great importance in achieving accurate mobility prediction of MNs in current and future generation wireless networks and smart antenna systems. In this research, an ANFIS methodology that utilizes RSS values to perform localization of MNs has been studied. This method is very efficient since using RSS does not require any additional hardware components on both the transmitter and receiver ends.

CHAPTER THREE: RESEARCH METHODOLOGY

3.1 Rationale of the Study

Mobility prediction in smart antenna systems is of vital importance in predicting the position of mobile hosts as well as any future handovers. Prediction, in this research, is based on the Received Signal Strengths (RSS), at the reception of the mobile node (MN), from the base station (BS) to which the node is connected. With a good prediction of the RSSI values it is possible to achieve excellent future location and the related advantages like handoff predictions. The proposed methodology uses the RSS to predict the movement of the MN.

By benchmarking with the similar studies carried out in [10] [11] [12] [13] [14] [15], a log-normal shadowing model (LNSM) was chosen to provide a basis of this research.

This model was chosen because of its ability to compensate for the shadow fading, which is either as a result of multipath propagation or due to shadowing from obstacles affecting the wave propagation, in RSS through the inclusion of the Gaussian random variable. The Grey model is then used to predict RSS values based on the data supplied by the LNSM [43] [55] [56].

It is known that the major goal of wireless communications is to allow a user to access the capabilities of global networks at any time without encountering problems of location and mobility, the technology of future smart antenna systems needs to make right predictions about Mobile Nodes' movement. Therefore, an ANFIS technique that demonstrates inherent learning abilities due to the neural network (NN) training algorithm incorporated for the tuning of the nonlinear parameters was chosen to

optimize the RSS values at the MN. The tuned RSS are used in the optimal estimation of the Mobile Node's distance from the transmitter. The proposed technique also has a rule-based structure that performs fuzzy reasoning to extract the dynamics of the studied phenomenon.

3.2 Conceptual Design Flow of ANFIS in Mobility Prediction

In this study, the Grey prediction model and its weighted version perform prediction of RSS using the data generated by the LNSM. Both LNSM and the ANFIS models are supplied with the same parameter values. The RSS values are contributed by three parameters, which include path loss at reference distance, distance and path loss exponent.

Optimization of mobility prediction using ANFIS technique is therefore achieved by using a three-steps below:

1. Process the input data so as to construct the mobility model according to the Grey theory to predict the RSS values.
2. Feed the ANFIS with both the training and testing data.
3. Run the ANFIS to generate the optimal RSS values.

In Figure 3.1 the ANFIS simulates the relationship between the input and output data through training and learning processes. This study used secondary data as the training dataset. This data was gathered from published journals as indicated in Table 3.1 [10] [47] [43] [48] [57]**.** The testing data was generated by the Grey model. The inputs of the GM were the RSS values generated by the Log-normal Shadowing Model (LNSM). Through its learning, the ANFIS optimizes the RSS values indicated by

RSS_A. The error in the output of ANFIS was determined by the number of epochs which was limited to 800 epochs.

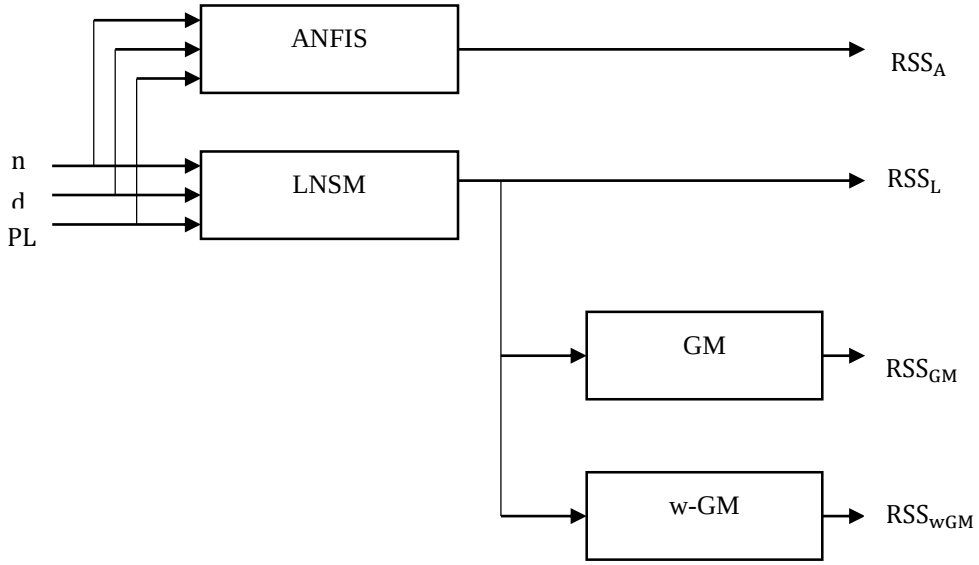

Figure 3.1: RSS Prediction Set-up for ANFIS and Other Models

Table 3.1: Simulation Parameters

Index, x	Path loss exponent, n	Path loss at reference distance (dB)	Reference Distance (m)	Distance (m)	Standard Deviation (dB)	Transmitter Power (dBm)	References
1	1.613	39.00	1.0	1.5 – 61.5	0.4510	0.000	[10]
2	2.200	45.00	1.0	1.0 – 10.0	0.2721	0.000	[48]
3	3.800	47.30	1.0	2.5 – 35.0	0.7270	3.802	[57]
4	3.11	89.77	100.0	100.0– 1250	6.000	44.771	[47]
5	3.55	106.00	100.0	100.0– 1800	8.000	0.000	[43]
6	2.57	95.00	100.0	100.0– 1800	5.400	0.000	[43]
7	1.701	41.00	3.0	3.0 – 48.0	2.157	0.000	[10]

3.3 Logical Design Flow of ANFIS Methodology

All the models used in this research; which are Log-normal Shadowing Model (LNSM), Grey model (GM) and ANFIS were simulated in MATLAB (R2012b). The ANFIS model which forms the heart of this research is logically presented in Figure

3.2. The simulation begins with the LNSM which provided the inputs to the Grey model. The simulation parameters highlighted in Table 3.1 provided the inputs to the LNSM. Both the LNSM and GM are simulated together and this is captured in Appendix A-1. The Received Signal Strength (RSS_L) is processed by the GM and w-GM to produce outputs; RSS_{GM} and RSS_{wGM} respectively. The output of the GM, RSS_{GM}, together with input parameters of the LNSM formed the testing data set to the ANFIS.

The training data set to the ANFIS was gathered from the published papers [10] [47] [43] [48] [57]**.** This data is captured in Appendix A-2. The training and testing data was organized in corresponding rows and columns before the execution of the MATLAB programme.

During the simulation process, 106 datasets was used for training and testing. The input data to the ANFIS as shown in Figure 3.1**,** was the path loss, path loss exponent and distance. The output of the system was the optimized RSS values, RSS_A. The input data consisted of set of [4 4 5] membership functions which generated 80 (4x4x5) rules. The selection of these membership functions was reached basing on a series of simulations that were performed to check the performance of the system. A hybrid learning algorithm constituting of error back propagation and gradient descent method was used in this research for ANFIS learning.

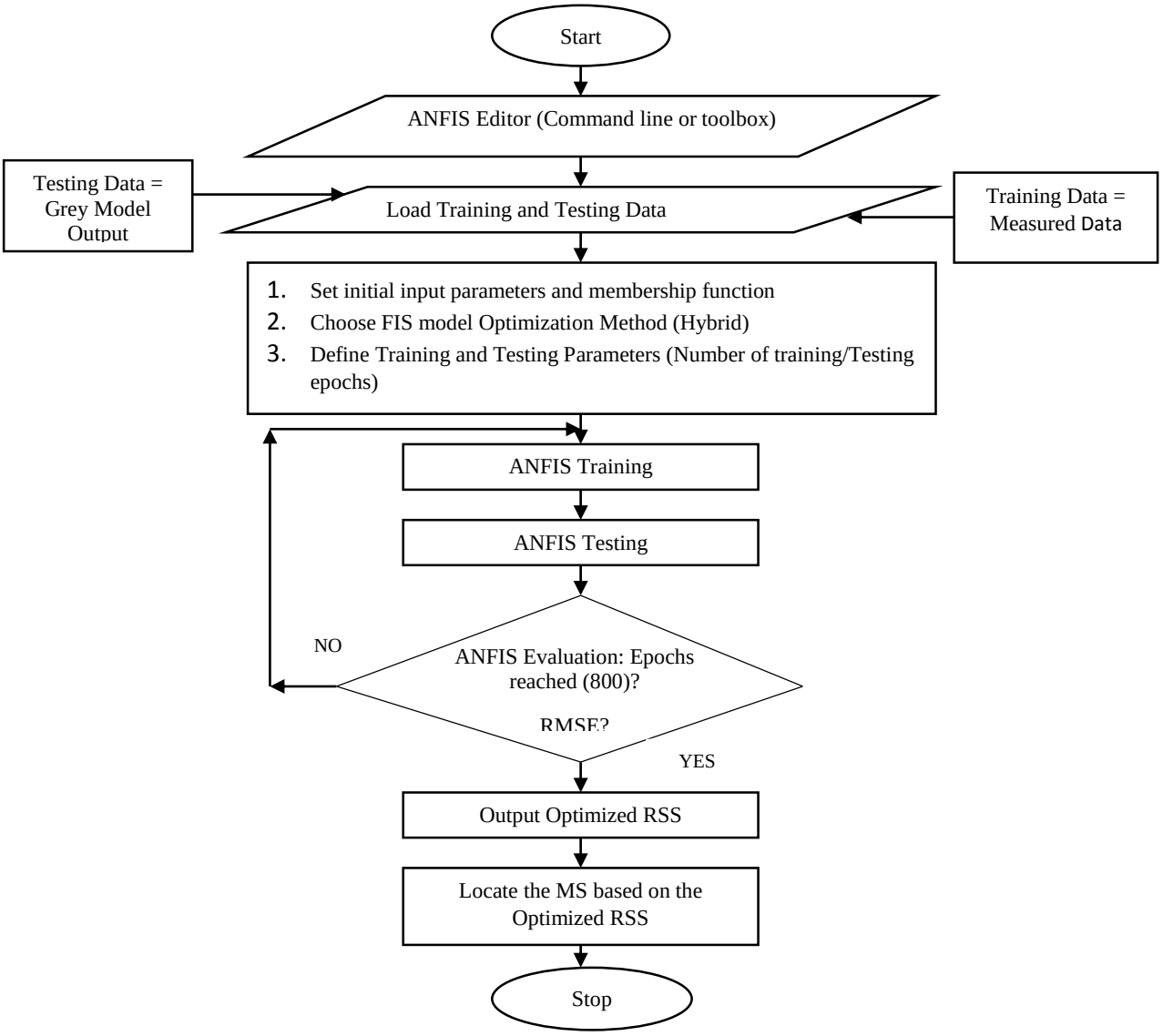

Figure 3.2: Mobility Prediction Optimization

During the learning process, the premise parameters of the fuzzification layer and consequent parameters in the de-fuzzification layer are tuned for a desired output. Once the preset number of epochs are reached, ANFIS uses Equation 3.1 to obtain the Root Mean Square Error (RMSE) incurred during training.

$$\mathrm{RMSE} = \sqrt{\frac{1}{\mathrm{N}}\sum_{\mathrm{i}=1}^{\mathrm{N}}(\mathrm{d_i} - \mathrm{o_i})^2} \qquad (3.1)$$

Where d_i denotes the desired output, o_i denotes the ANFIS output for the i^{th} sample from training data and N is the training sample count.

The optimized RSS and distance parameters were used to generate regression models which were used in distance estimations. The outputs of ANFIS simulation were exported to and analyzed using Microsoft Excel. The exported RSS data was used to generate the approximate distances. During the validation of ANFIS performance, the error between the distance values generated by ANFIS and the measured and published distances was computed. The mean average error was calculated and used to compare with the reported errors in other methods.

CHAPTER FOUR: RESULTS AND DISCUSSION

4.1 Introduction

The output data, from the ANFIS programme, which was exported to excel was analyzed at this point. The column for the RSS values was pivotal in computing the corresponding distances and gaining deeper insights about the behavior of the designed methodology. This involved generating regression models for each data sets. To validate the performance of ANFIS in estimating mobility or the distance of Mobile Node (MN) from the transmitting stations in wireless or cellular networks, a comparison of the mean absolute errors produced by ANFIS estimates and those produced by other methods highlighted in [10] [11] [12] [13] [14] [15] was performed.

4.2 Simulation of Models

All the models used in this research; which are Log-normal Shadowing Model (LNSM), Grey model (GM) and ANFIS were implemented in MATLAB (R2012b). The simulation begun with the LNSM which provided the inputs to the Grey model. The Received Signal Strength (RSS_{LN}) is processed by the GM to produce an output Received Signal Strength (RSS_{GM}). The RSS_{GM} together with the input parameters of the LNSM formed the testing data set to the ANFIS. The testing data was organized in corresponding rows and columns before the execution of the MATLAB code.

4.2.1 LNSM and Grey Model

Using Equation 2.20 and 2.24, Grey and weighted Grey models were simulated. As shown in Appendix A-1, the LNSM provided the inputs to the GM. When plotted, the results of this simulation produced Figure 4.1.

In Figure 4.1, a plot of GM is seen having the same nature as the LNSM with a reducing difference (error) from the starting point (100m) up to the second last point (1200m). There a notable anomaly at the last point. This is caused by the nature of GM which uses a sliding window while performing predictions. At every point of its prediction, GM searches for a value at $n + 1$ point. On failing to get the next point, GM drops the search that falls out of the window and the output becomes a random value on the right hand side of the sliding window.

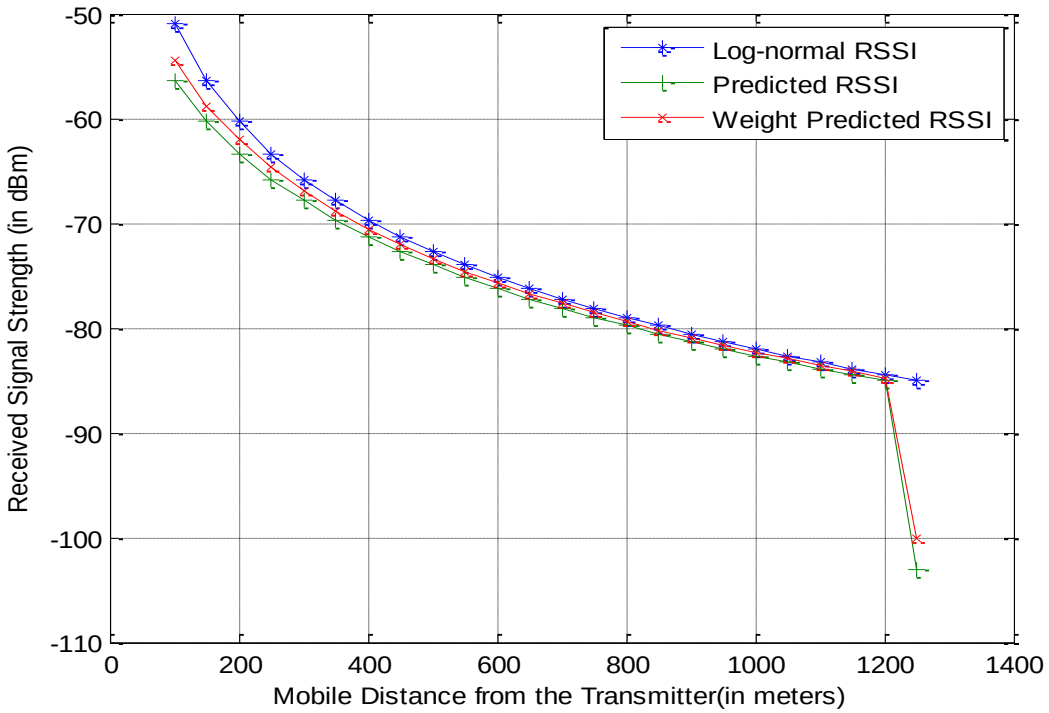

Figure 4.1: RSS versus Distance with Endpoint Error

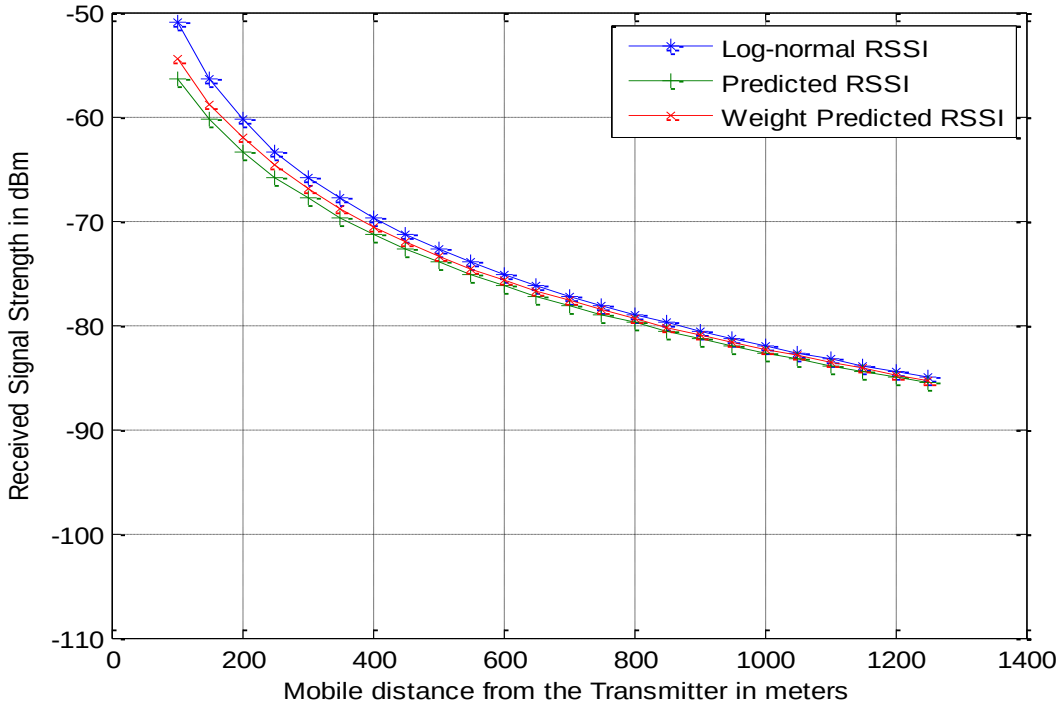

Figure 4.2: RSS versus Distance without Endpoint Error

The end point error contributed to a large mean average error in the outputs of GM. In order to eliminate the endpoint diversion of the last values in GM predictions, as shown in Figure 4.1, the value that corresponds to the endpoint was eliminated to give Figure 4.2. Figure 4.2a-b show en enlarged view of Figure 4.2. This was done to give a clear view of the congested plots in Figure 4.2. On average, this reduced the average mean error by 0.0572 as well as reduced the average run time in its processing. An alternative approach towards the elimination of the endpoint error was to predict the $(n+1)^{th}$ data points, where n is the expected number of data points. After predicting with one extra point the last point can then be discarded. The execution times of the two versions of GM Prediction were compared under the same hardware and software conditions. The version of the GM with end point error took a longer time to converge

than the version whose endpoint error was eliminated. Without the endpoint error the running time reduced by 12.83%. The endpoint error inherent in the GM prediction is attributed to the sliding window operation to which GM model relies on. The model tries to search for the matching value in the RSS which doesn't exist. The output to this is a random value which is less than the second last prediction.

The illustrations of Figures 4.1 and 4.2 are a representative of dataset corresponding to index 4 of Table 3.1. The others datasets corresponding to indices 1, 2, 3, 5, 6 and 7 exhibit similar characteristics like the data set in index 4.

Another study on the GM was done to reduce the error magnitude between the GM and LNSM. This reduced the error by 0.7696dBm (from 1.9436 to 1.1740). This was done by applying weighted averages in the primitive data and the GM predicted data to form a generic version. The weights of $w_1 = 0.5$ and $w_2 = 0.5$ were randomly chosen and used in Equation 2.24 for all the datasets used in the study. After the application of weights, the resulting predicted data had a reduced error between the output values of LNSM and GM. The impact of the weighted averaging is shown in the third legend of the curves in both Figure 4.1 and 4.2.

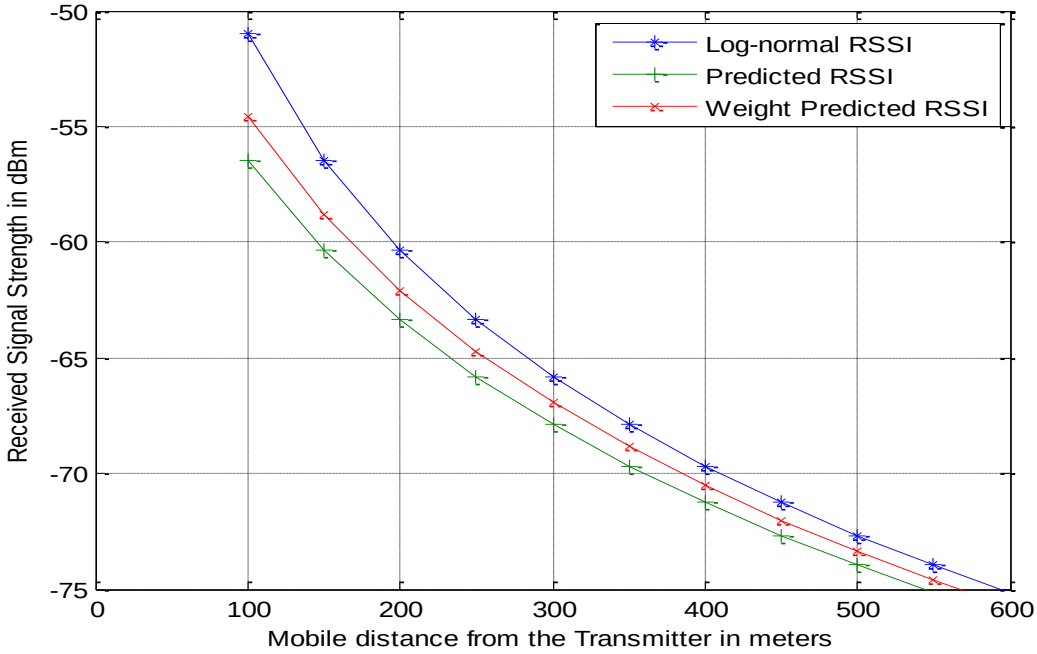

Figure 4.2a: Enlarged View of Figure 4.2 for Distance between 0m and 600m

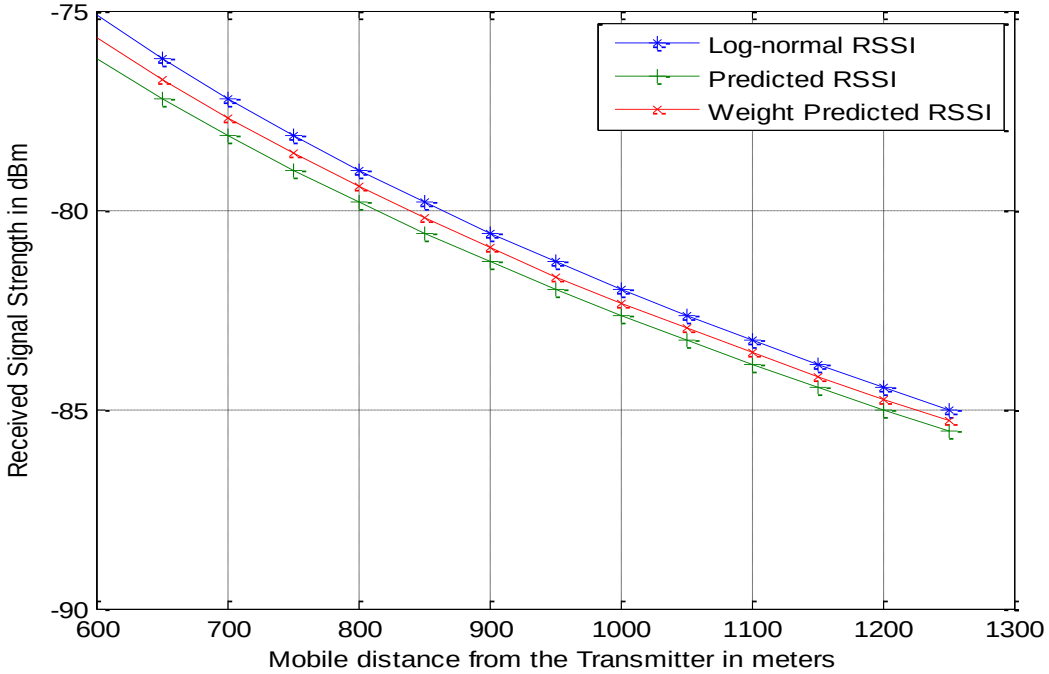

Figure 4.2b: Enlarged of RSS Figure 4.2 for Distance between 600m and 1400m

Using Equation 2.23, the accuracies of Grey Model and weighted Grey model were computed. On average, the accuracies of GM and weighted GM were 96.56% and 97.86% respectively. This shows that the prediction accuracy of weighted GM, in reference to the LNSM outputs, is better than that of ordinary GM. Table 4.1 summarizes the different prediction accuracies of first order Grey Model, GM(1,1), on different sets of data used in this research.

Table 4.1: Grey Model Prediction Accuracy

Index, x	**Grey Model(GM)**		**Weighted Grey Model(wGM)**	
	$\mathbf{e_k}$	$(\mathbf{1}-\mathbf{e_k})*\mathbf{100}\%$	$\mathbf{e_k}$	$(\mathbf{1}-\mathbf{e_k})*\mathbf{100}\%$
1	0.02053	97.9467	0.01208	98.7912
2	0.04249	95.7503	0.02566	97.4335
3	0.05292	94.7076	0.03490	96.5092
4	0.02278	97.7219	0.01310	98.6892
5	0.03753	96.2469	0.02411	97.5888
6	0.03011	96.9884	0.01826	98.1737
7	0.0212	97.8773	0.0119	98.8075

In Table 4.1, e_k denotes the average relative error and $(1-e_k)$ is the prediction accuracy. Using Equation 2.23, the relative errors in each dataset, indices 1-7, and the corresponding prediction accuracies were calculated. The results in Table 4.1 show that the prediction accuracy of both GM and wGM are excellent. However, it is evident that the prediction accuracy of wGM in relation to the LNSM outputs is better than that of ordinary GM.

4.2.2 ANFIS

As discussed in Chapter Three, the simulation of ANFIS was performed with input data consisting of a set of [4 4 5] membership functions which generated 80 (4x4x5) rules. This information is captured in Figure 4.3 that shows the relationship between

the input and output parameters of the proposed ANFIS model. The input parameters before and after the training are indicated in Figures 4.4 and 4.5. The selection of these membership functions was experimentally done based on a series of simulations that were carried out to check their performance.

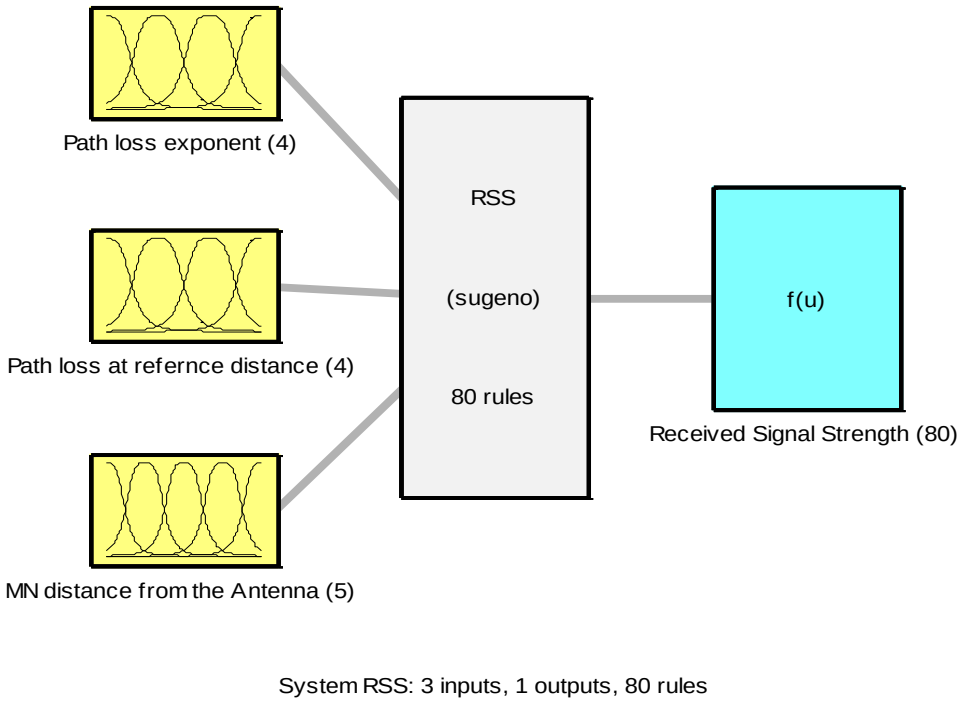

Figure 4.3: Input-Output Relationship for the ANFIS Model

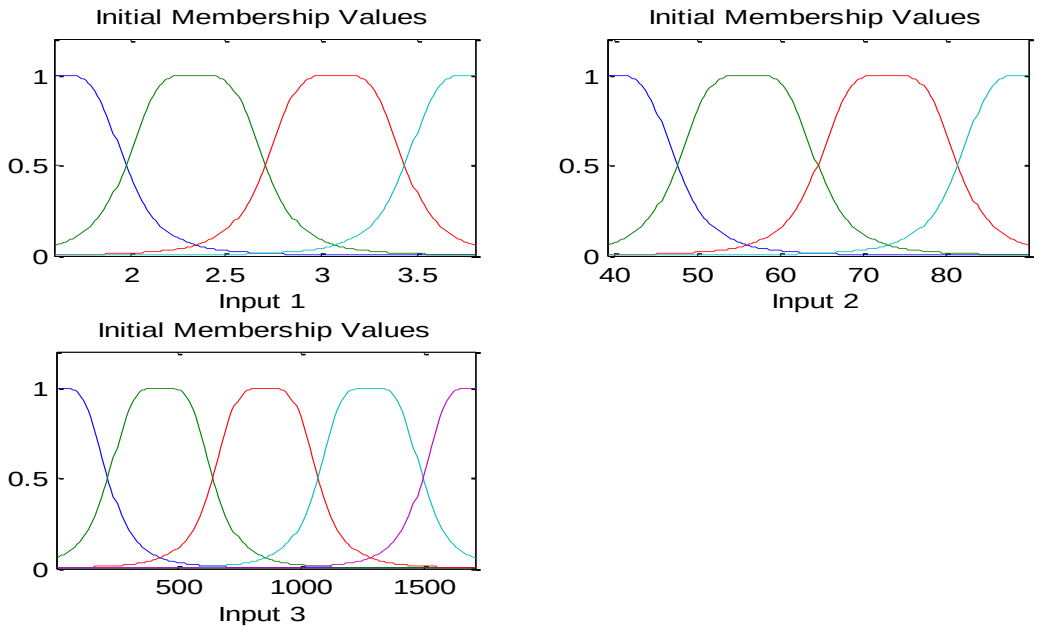

Figure 4.4: Membership of ANFIS Input Parameters before Training

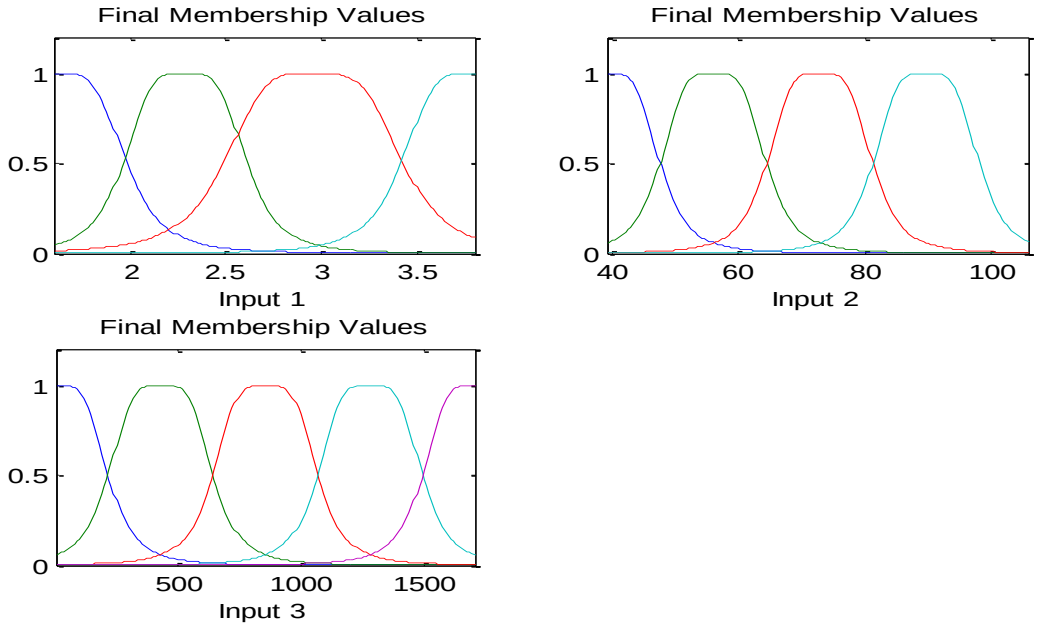

Figure 4.5: Membership of ANFIS Input parameters after Training

The performance indicators for the simulation were: convergence or run time, and training error size. The selected set of membership functions trained the data for approximately 120s (averaged time) with a training RMSE of 0.4016 which corresponded to the predefined 800 epochs. The run time depends on the amount of data and training error depends on the number of epochs in the ANFIS algorithms. Other sets of simulations performed here consisted a higher and lower number of membership functions and rules. In these other sets of simulations, the number of epochs were varied. Increase in the number of rules increased the execution time while reducing the RMSE and the reverse was true. The similar trend of behavior was significant with variation in the number of epochs; increase in the epochs improved the RSME at the expense of the execution time.

Three independent studies were performed on ANFIS by subjecting the system to different sets of testing data: the first study involved the use of GM's output; the second one involved the use of LNSM output; and in the last one the wGM outputs were used. Under all these testing data, the trained outputs of ANFIS exhibited the same behavior with the same results.

As already mentioned, the study was carried out on data gathered from both short and long distance communication environments. Data plots of RSS versus distance have been shown in Figures 4.6-8, 4.15-17 and 4.26. In all these plots, five RSS parameter values are plotted against distance. These RSSs values are measured RSS from published data; optimal RSS which is the ANFIS output, RSS output from GM; RSS output from the weighted GM; and RSS output from LNSM.

The measured data used in this research consists of data gathered from both long and short distance environments. It is evident that the outputs of different predictions follow a general trend; the RSS at the MN reduces as the distance between the MN and the transmitter increases. The performance of the different prediction models in estimating distance was analyzed by studying the relationship between the RSS values and the logarithmic values of distance and the results are shown in Figures 4.9-11, 4.18-20 and 4.27. Each figure yielded a set of regression line approximations for the prediction models under study. These regression line approximations are presented in the Tables 4.2-3 and 4.5. The index x used here is similar and therefore corresponds to the indices used in Table 3.1.

4.2.2.1 Short Distance Outdoor Environment

In this research short distance environment considered distance less than 100m. Specifically, Table 3.1 highlights the short distance ranges as 1.0-10.0m, 2.5-35.0m, 3.0-48.0m and 1.5-61.5m. Figures 4.6-8 show plots of RSS versus distance for the four models (ANFIS, LNSM, GM, and wGM) plus a plot for the measured data used in this study for short distance communication environment. Figures 4.9-11 show the regression approximations for the datasets shown in Figures 4.6-8. Figures 4.12-14 show plots of localization error versus distance for the models indicated in Figures 4.6-8.

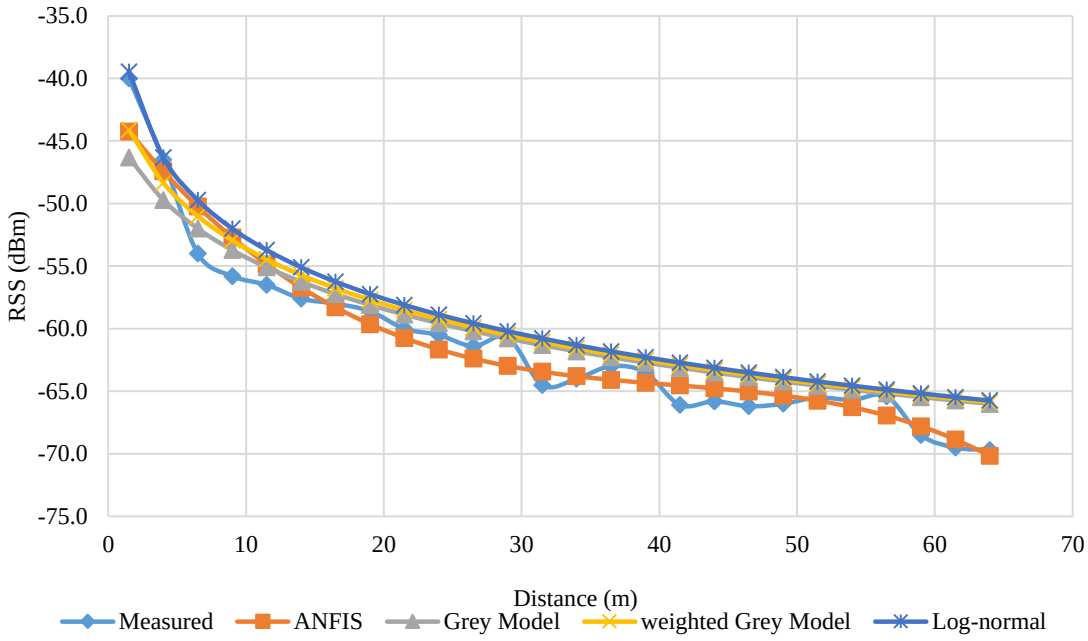

Figure 4.6: RSS versus Distance for Index 1

The vertical line in Figure 4.6 at a distance of 30m separates the display into two sections that are represented by Figure 4.6a-b. This was done to have a clear view of Figure 4.6.

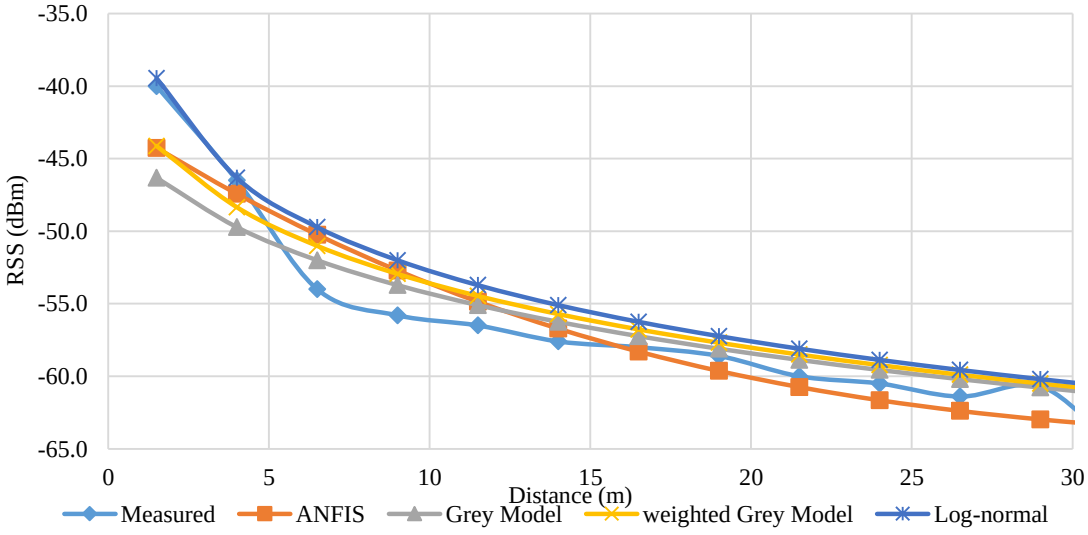

Figure 4.6a: Enlarged View of Figure 4.6 for Distance between 0m and 30m

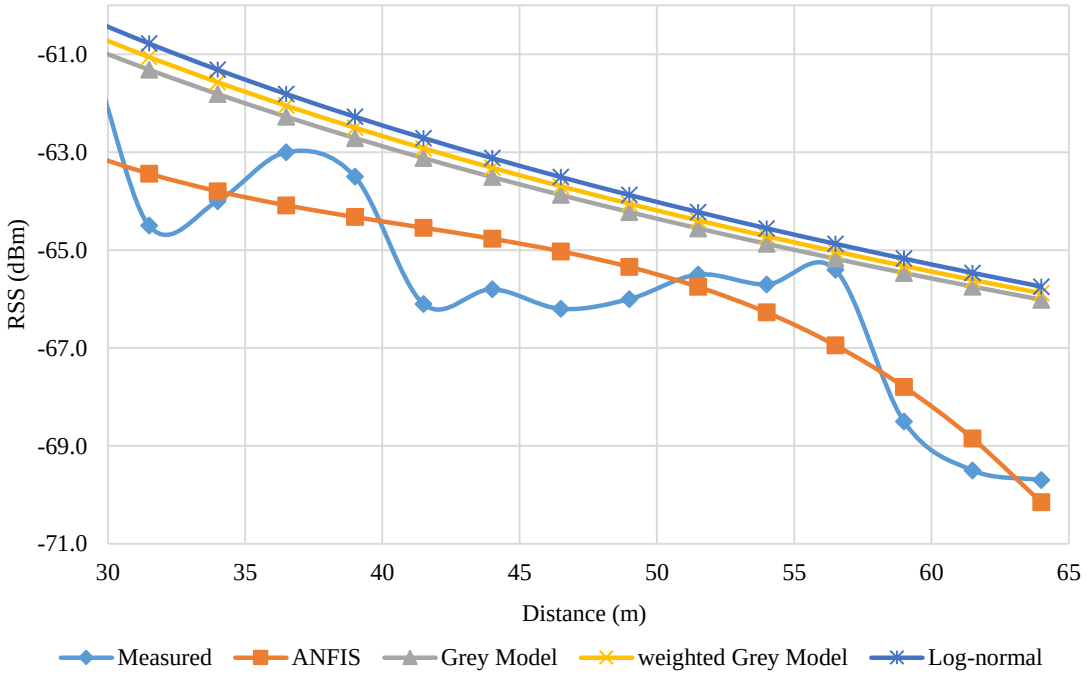

Figure 4.6b: Enlarged View of Figure 4.6 for Distance between 30m and 70m

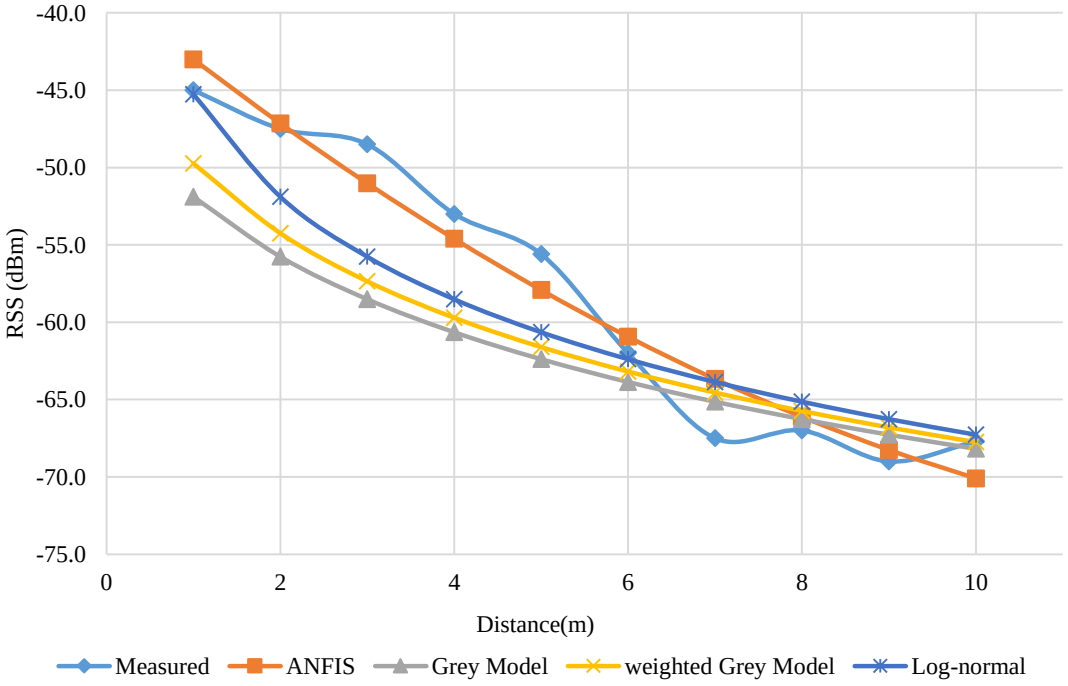

Figure 4.7: RSS versus Distance for Index 2

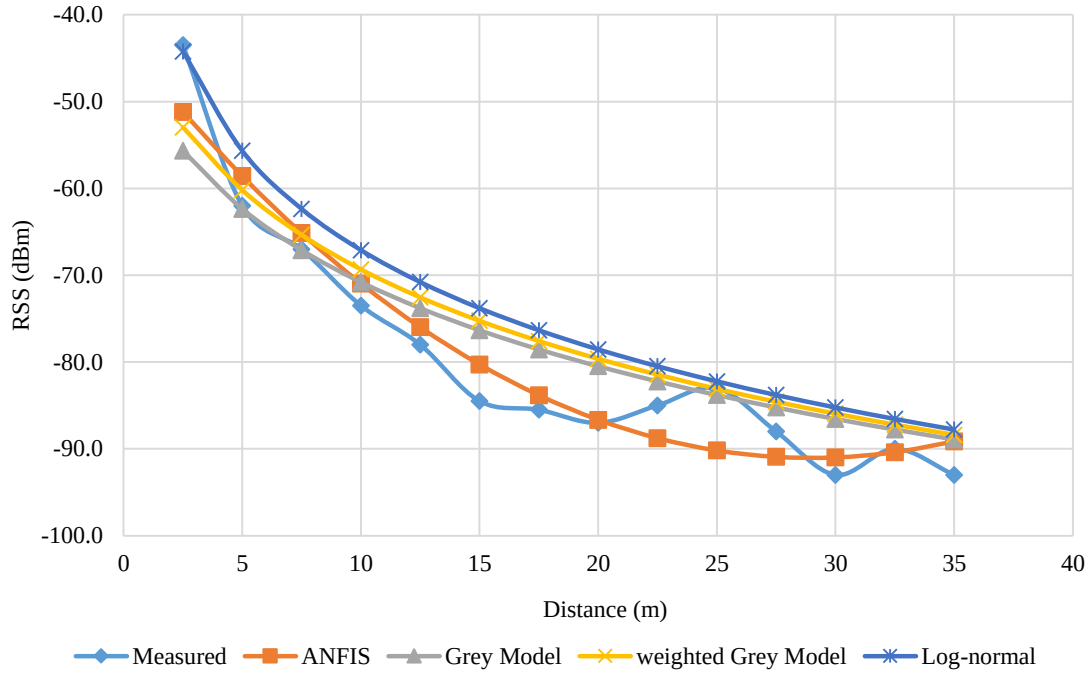

Figure 4.8: RSS versus Distance for Index 3

From Figures 4.6-8, it is observed that:

1. ANFIS outputs distribute themselves around the measured data forming curves that are almost normally distributed around curves formed by the measured data.
2. The ANFIS curves have a similar trend as the curves of the testing data in terms of linearity.
3. In each dataset, the ANFIS curves form multiple points of intersection with both the training data (measured data) and testing data (from the GM) with many cross-points being between the ANFIS output curves and the training data curves compared to the cross-points between ANFIS output curves and the testing data curves.
4. For each dataset, the recorded RSS and ANFIS output values deviate away from the general trend of the previously recorded and generated data. For Figure 4.6,

this occurs at 38m distance; for Figure 4.7 it occurs at 6m distance; and for Figure 4.8, it occurs at 23m distance.

From the Figures 4.9-11, the regression lines formed by the ANFIS outputs are very close to the ones formed by the measured data compared to other models considered under this study. The nature of these regression lines depicts the observations made from Figures 4.6-8.

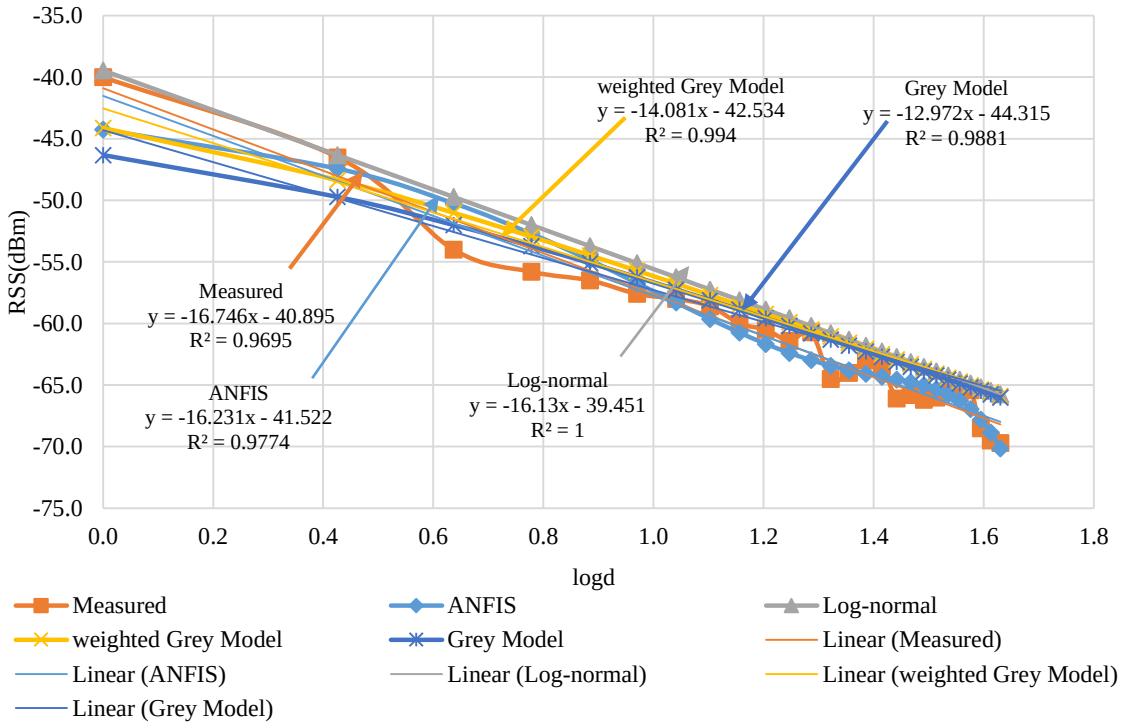

Figure 4.9: RSS versus $\log_{10}(d)$ for Index 1

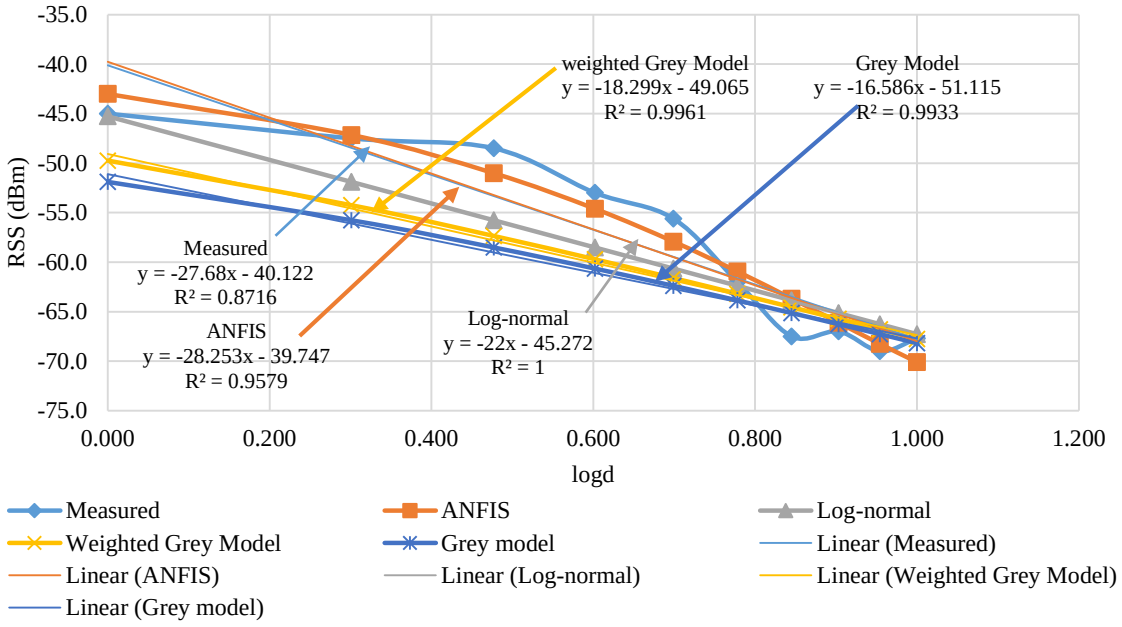

Figure 4.10: RSS versus $\log_{10}(d)$ for Index 2

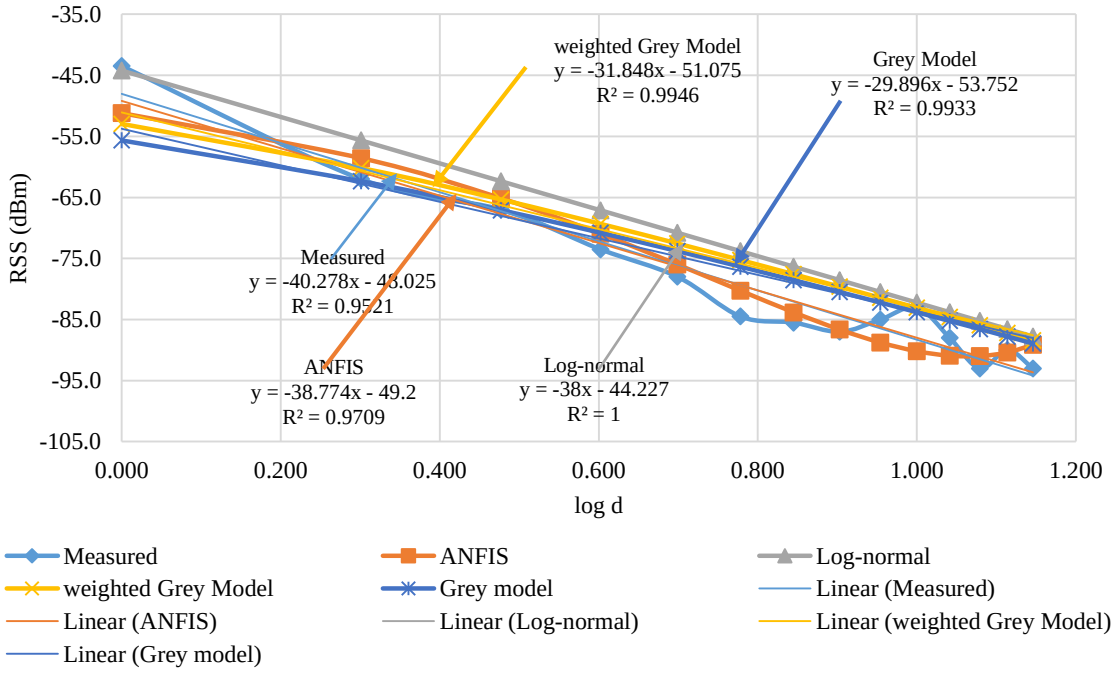

Figure 4.11: RSS versus $\log_{10}(d)$ for Index 3

From Figures 4.12-14, it is seen that the localization or mobility prediction is carried out with some errors as the mobile node (MN) moves away from the base station. A large increase in the prediction error for Figure 4.12 begins to occur at 38m distance; for Figure 4.13, it occurs at a distance of 6m; and in Figure 4.14, it occurs at 23m. In each dataset, a rise in the error magnitude is due to the deviation in the RSS values recorded at the MN which slightly or greatly deviates away from the trend of the previously collected data. The error changes as seen in Figures 4.12-14 correlate to the observations made from Figures 4.6-8. By comparing the distance covered by the MN before the RSS becomes erroneous to the entire distance under the study, it is seen that the magnitude of error correlates to the total distance of coverage. Thus, for longer distances, larger error values are observed. On average, a large increase in error occurs at 62.33% of the total distance in short distance communication environment.

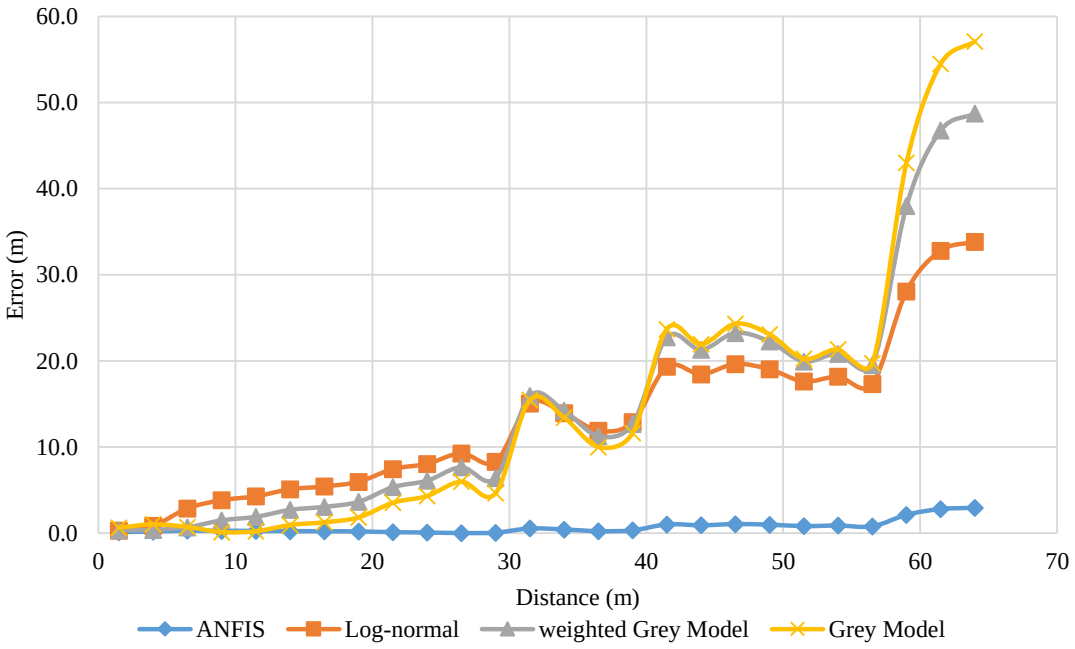

Figure 4.12: Localization Error for the Different Prediction Models for Index 1

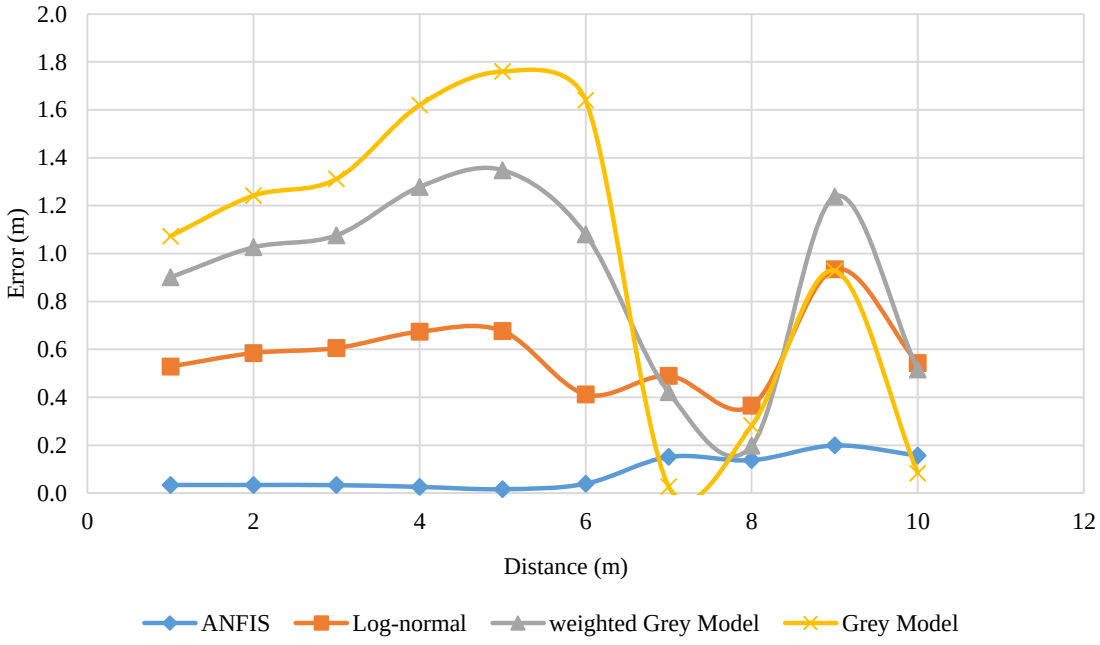

Figure 4.13: Localization Error for the Different Prediction Models for Index 2

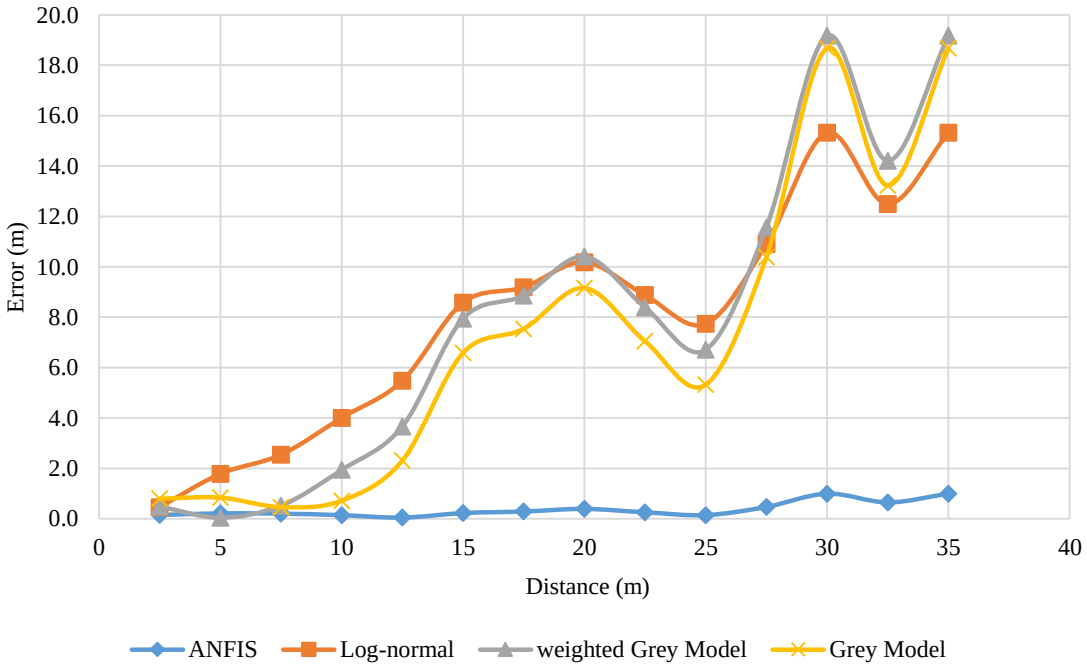

Figure 4.14: Localization Error for the Different Prediction Models for Index 3

Table 4.2: Regression Line Estimations for the Different Prediction Models for Index 1-3

Index, x	Regression Line Approximation	R^2
1	$\mathrm{RSS}_1(\mathrm{dBm}) = -16.746 * \log_{10}(\mathrm{d_m}) - 40.895$	0.9695
	$\mathrm{RSS}_1(\mathrm{dBm}) = -16.231 * \log_{10}(\mathrm{d_a}) - 41.522$	0.9774
	$\mathrm{RSS}_1(\mathrm{dBm}) = -16.13 * \log_{10}(\mathrm{d_l}) - 39.451$	1.000
	$\mathrm{RSS}_1(\mathrm{dBm}) = -14.081 * \log_{10}(\mathrm{d_{wg}}) - 42.534$	0.994
	$\mathrm{RSS}_1(\mathrm{dBm}) = -12.972 * \log_{10}(\mathrm{d_g}) - 44.315$	0.9881
2	$\mathrm{RSS}_2(\mathrm{dBm}) = -27.68 * \log_{10}(\mathrm{d_m}) - 40.122$	0.8716
	$\mathrm{RSS}_2(\mathrm{dBm}) = -28.253 * \log_{10}(\mathrm{d_a}) - 39.747$	0.9579
	$\mathrm{RSS}_2(\mathrm{dBm}) = -22 * \log_{10}(\mathrm{d_l}) - 45.272$	1.000
	$\mathrm{RSS}_2(\mathrm{dBm}) = -18.299 * \log_{10}(\mathrm{d_{wg}}) - 49.065$	0.9961
	$\mathrm{RSS}_2(\mathrm{dBm}) = -16.586 * \log_{10}(\mathrm{d_g}) - 51.115$	0.9933
3	$\mathrm{RSS}_3(\mathrm{dBm}) = -40.278 * \log_{10}(\mathrm{d_m}) - 48.025$	0.9521
	$\mathrm{RSS}_3(\mathrm{dBm}) = -38.774 * \log_{10}(\mathrm{d_a}) - 49.2$	0.9709
	$\mathrm{RSS}_3(\mathrm{dBm}) = -38 * \log_{10}(\mathrm{d_l}) - 44.227$	1.000
	$\mathrm{RSS}_3(\mathrm{dBm}) = -31.848 * \log_{10}(\mathrm{d_{wg}}) - 51.057$	0.9946
	$\mathrm{RSS}_3(\mathrm{dBm}) = -29.896 * \log_{10}(\mathrm{d_g}) - 53.752$	0.9933

In Tables 4.2-3, x is the index; d_m is the ratio d_i/d_0 for the measured data regression line; d_a is the ratio d_i/d_0 for the ANFIS regression line; d_l is the ratio d_i/d_0 for the LNSM regression line; d_{wg} is the ratio d_i/d_0 of the weighted Grey model regression line; d_g is the ratio d_i/d_0 of the Grey model regression line; and R^2 is the correlation coefficient of the estimated regression lines.

4.2.2.2 Long Distance Outdoor Environment

In this research long distance environment considered distance between 100m and 1800m as summarized in Table 3.1 with index 4-6. Figures 4.15, 4.16 and 4.17 show plots of RSS versus distance for the four models (ANFIS, LNSM, GM, and wGM) and a plot of measured data used in this study. Figures 4.18, 4.19 and 4.20 show the regression approximations for the datasets shown in Figures 4.15, 4.16 and 4.17.

Figures 4.21, 4.22 and 4.23 show plots of localization error against distance for the models indicated in Figures 4.15, 4.16 and 4.17.

From Figures 4.15-17, the following observations were made:

1. ANFIS outputs and the measured data form curves that are almost normally distributed around each other.
2. The ANFIS curves have an independent trend to the curves of the testing data in terms of linearity.
3. In each dataset, the ANFIS curves form multiple points of intersection with the training data (measured data) and very few points of intersection with the testing data (from the GM). Longer distances form more intersecting points than the shorter distance.
4. For each dataset, there is the deviation in the recorded RSS and ANFIS output values from the general trend of the previously recorded and generated data. For Figure 4.15, this occurs at 800m distance; for Figure 4.16 it occurs at 1100m distance; and for Figure 4.17, it occurs at 1200m distance.

The regression lines formed by the ANFIS outputs, as shown in Figures 4.18-20 are very close to the ones formed by the measured data unlike the other models used under this study. The nature of these regression lines also depicts the observations made from Figures 4.15-17.

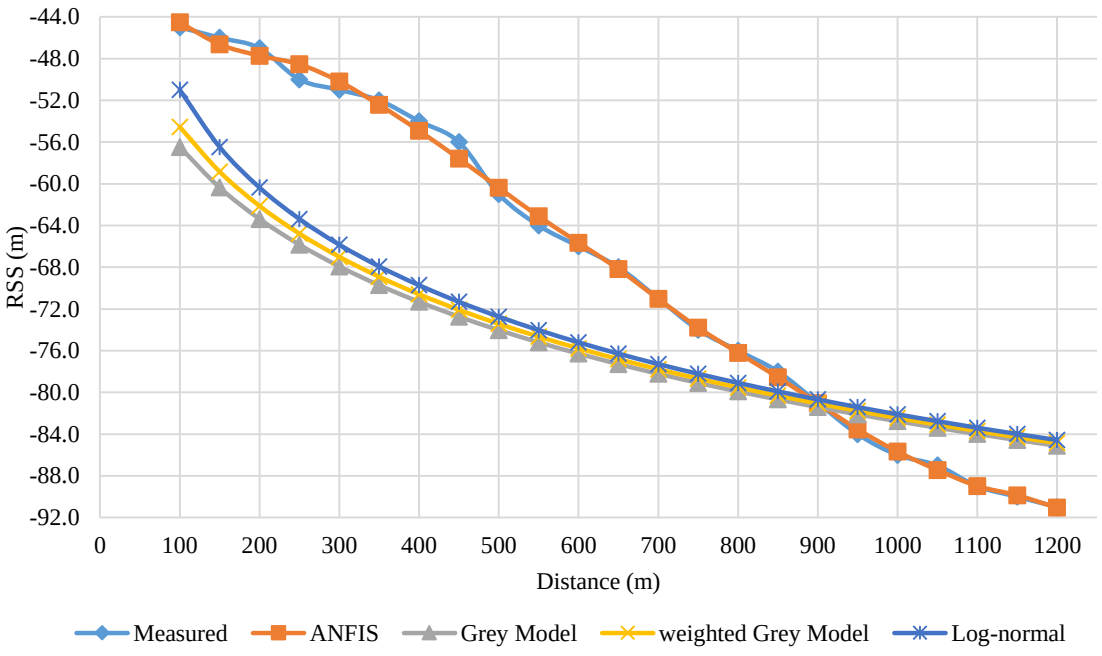

Figure 4.15: RSS versus Distance for Index 4

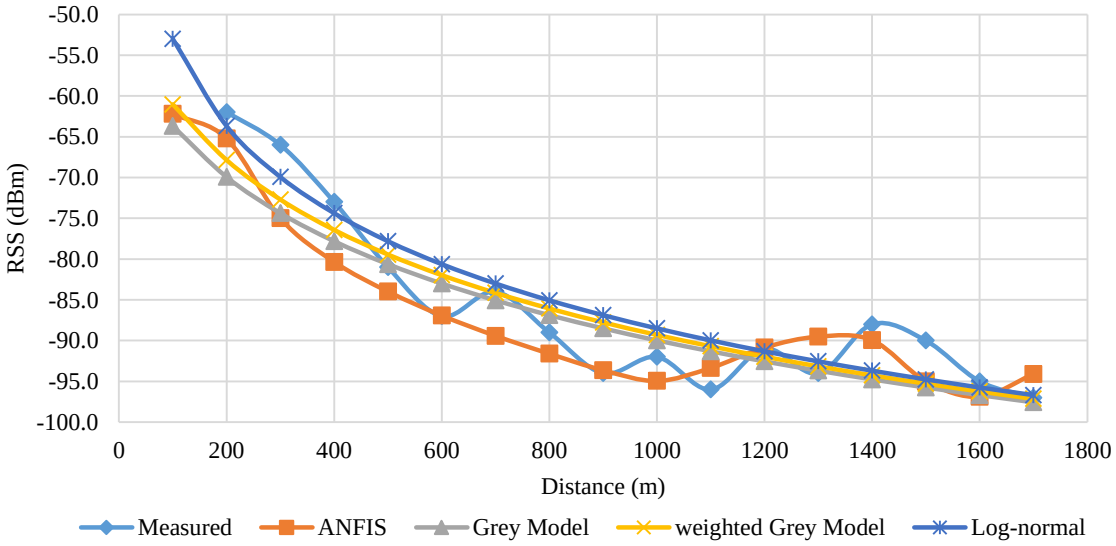

Figure 4.16: RSS versus Distance for Index 5

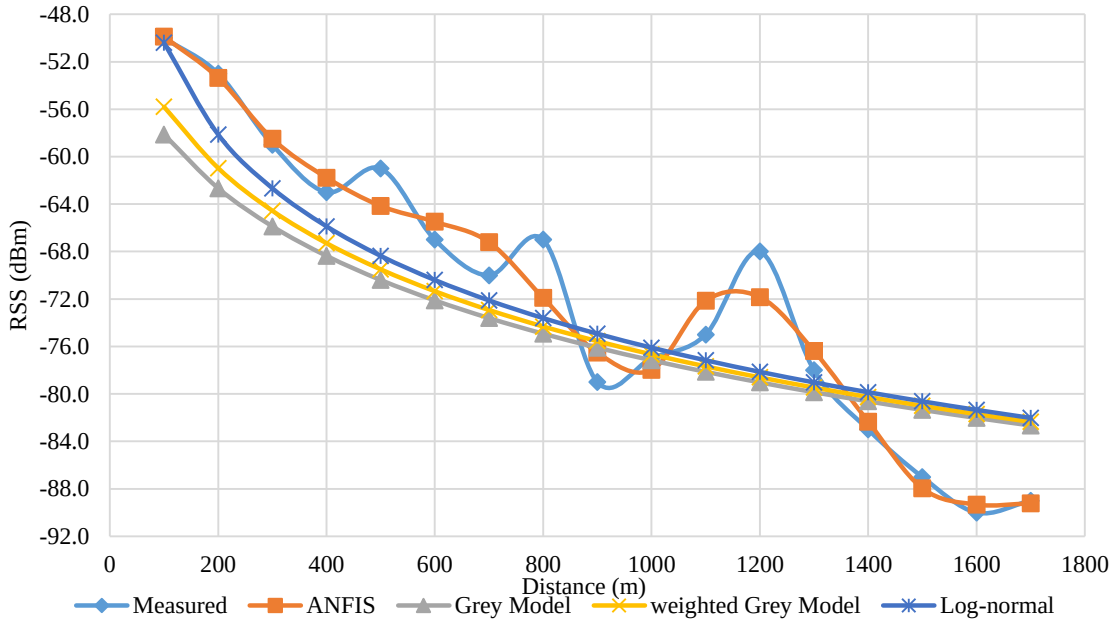

Figure 4.17: RSS versus Distance for Index 6

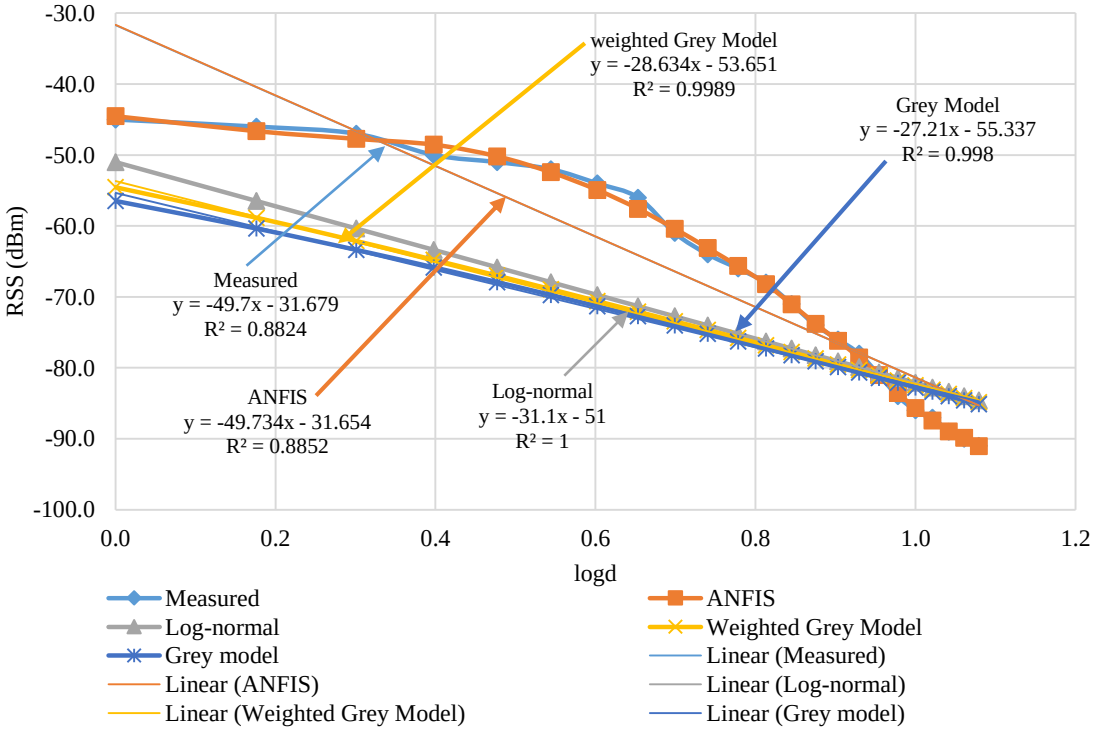

Figure 4.18: RSS versus $\log_{10}(d)$ for Index 4

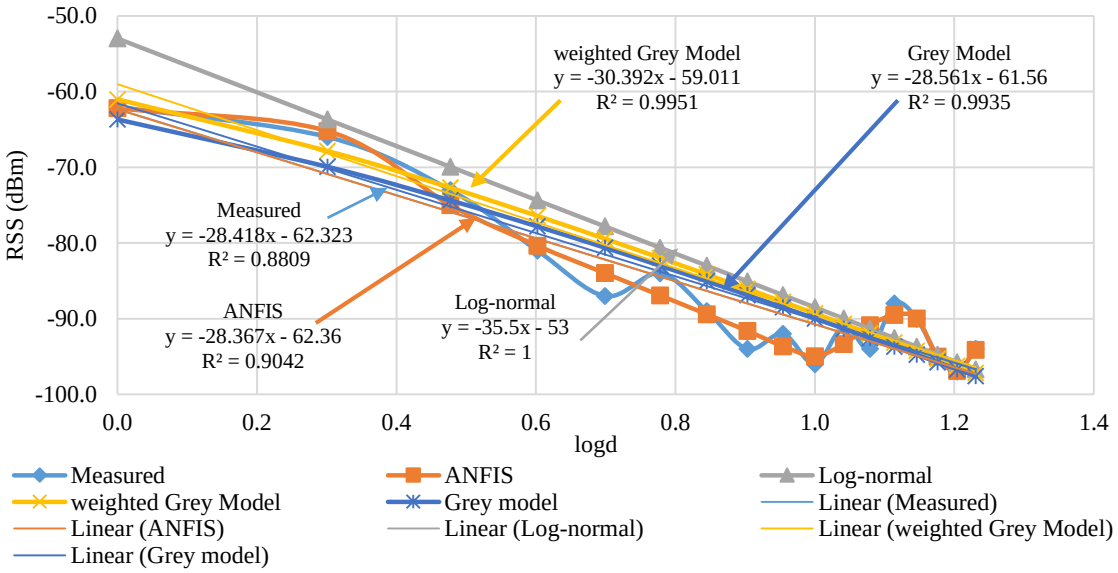

Figure 4.19: RSS versus $\log_{10}(d)$ for Index 5

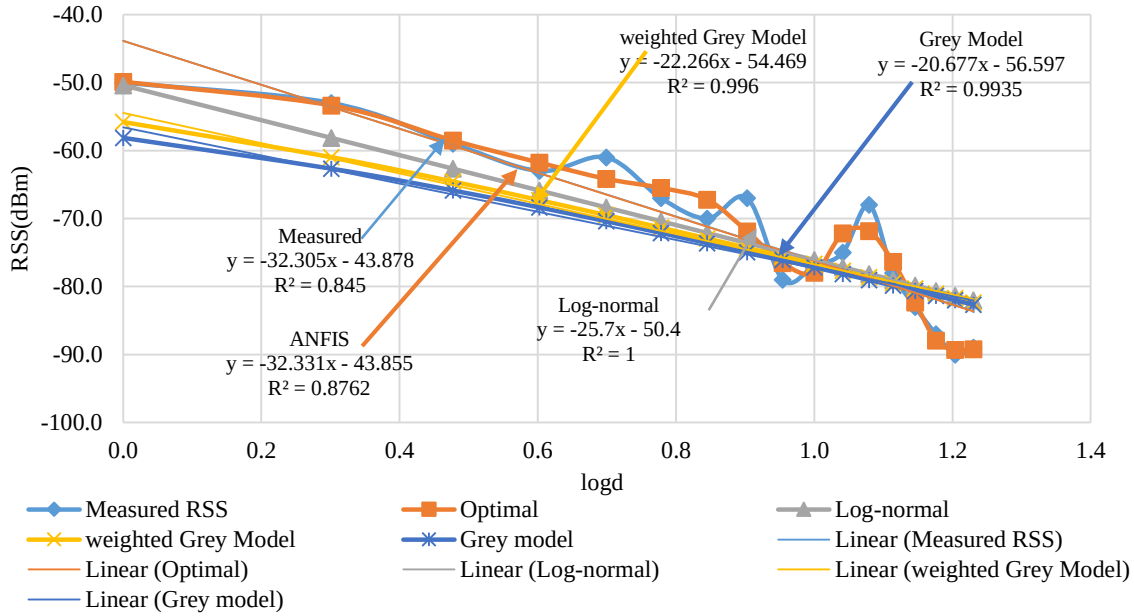

Figure 4.20: RSS versus $\log_{10}(d)$ for Index 6

From Figures 4.21-23, it is seen that the localization or mobility prediction is carried out with some errors as the mobile node (MN) moves away from the base station. A large increase in the prediction error as seen in Figure 4.21 begins to occur at 800m

distance; for Figure 4.22, it occurs at a distance of 1100m; and for Figure 4.23, it occurs at 1200m distance. In each dataset, a rise in the error magnitude is due to the deviation in the RSS values recorded at the MN which slightly or greatly deviates away from the trend of the previously collected data. The error changes as seen in Figures 4.21-23 correlate to the observations made on Figures 4.15-17. By comparing the distance covered by the MN before the RSS becomes erroneous to the entire distance under the study, it is seen that the magnitude of error increases with increase in distance of coverage. Thus, the longer the distance, the larger the error change at the corresponding variable distances is incurred. On average, a large increase in error occurs at 64.82% of the distance in long distance communication environment.

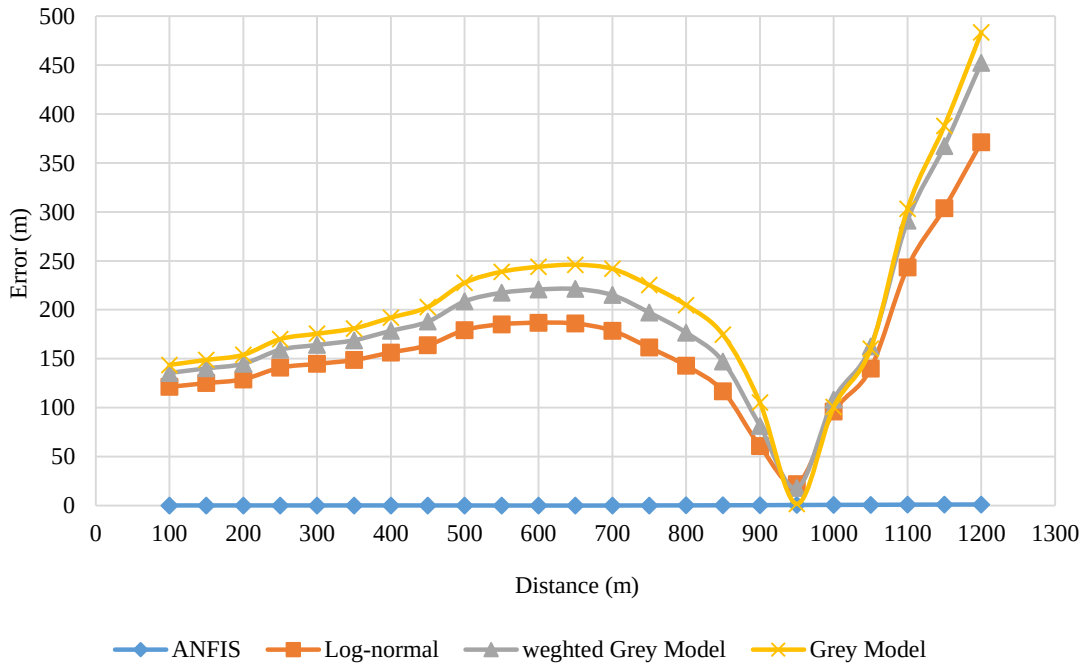

Figure 4.21: Localization Error for the Different Prediction Models for Index 4

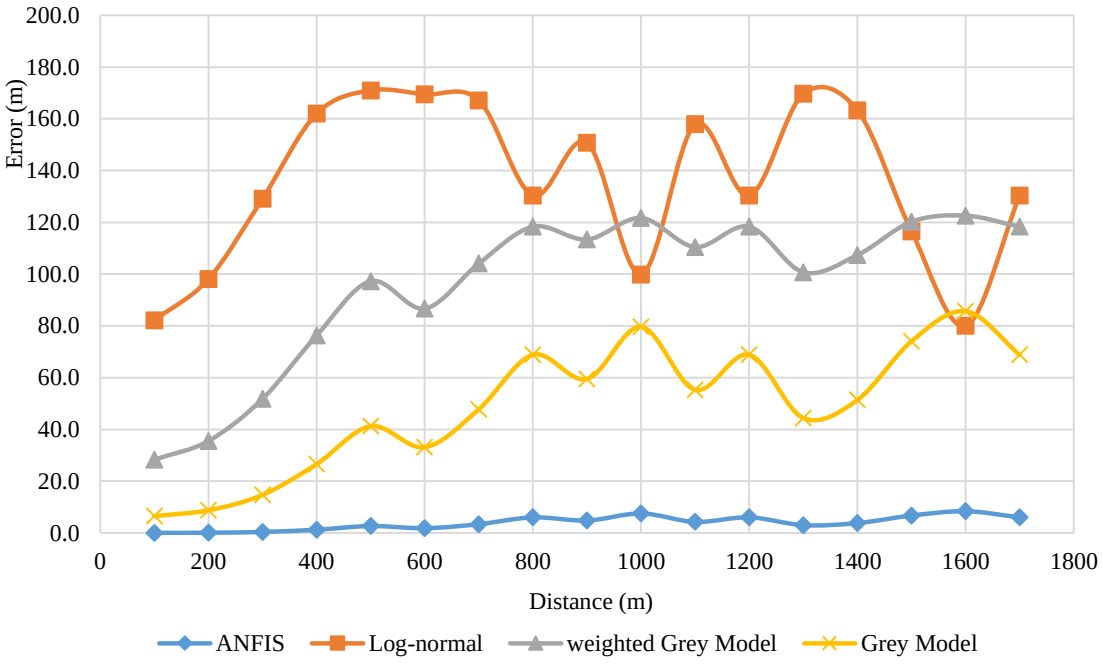

Figure 4.22: Localization Error for the Different Prediction Models for Index 5

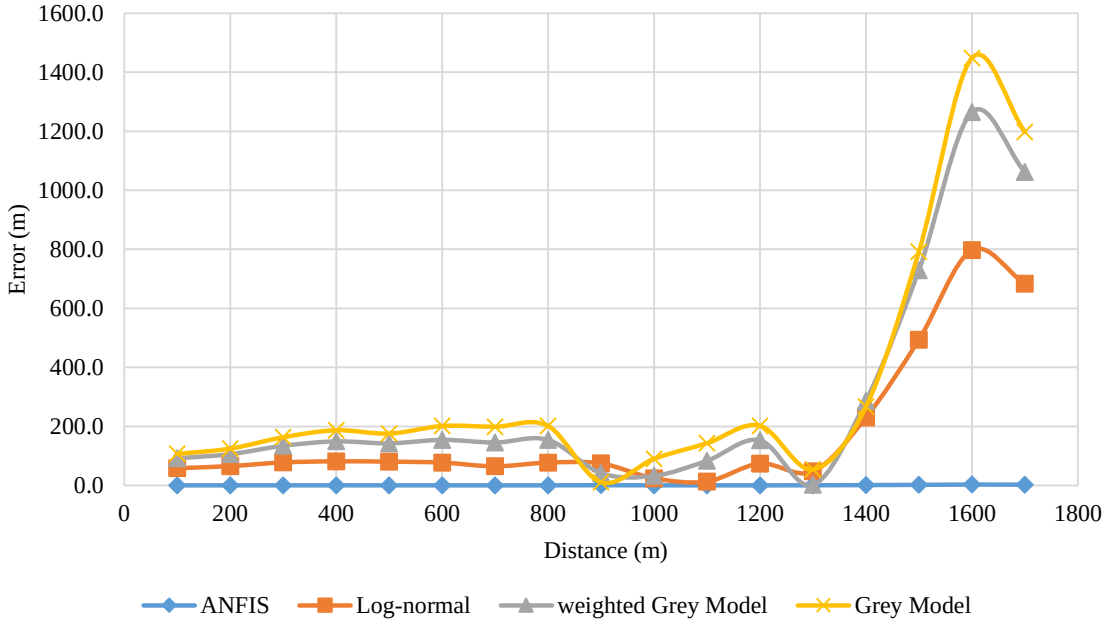

Figure 4.23: Localization Error for the Different Prediction Models for Index 6

Table 4.3: Regression Line Estimations for the Different Prediction Models for Index 4-6

Index, x	Regression line approximation	R^2
4	$RSS_4(dBm) = -49.7 * \log_{10}(d_m) - 31.679$	0.8824
	$RSS_4(dBm) = -49.734 * \log_{10}(d_a) - 31.654$	0.8852
	$RSS_4(dBm) = -31.1 * \log_{10}(d_l) - 51$	1.000
	$RSS_4(dBm) = -28.634 * \log_{10}(d_{wg}) - 53.661$	0.9989
	$RSS_4(dBm) = -27.21 * \log_{10}(d_g) - 55.337$	0.998
5	$RSS_5(dBm) = -28.418 * \log_{10}(d_m) - 62.323$	0.8809
	$RSS_5(dBm) = -28.367 * \log_{10}(d_a) - 62.36$	0.9042
	$RSS_5(dBm) = -35.5 * \log_{10}(d_l) - 53$	1.000
	$RSS_5(dBm) = -30.392 * \log_{10}(d_{wg}) - 59.011$	0.9951
	$RSS_5(dBm) = -28.561 * \log_{10}(d_g) - 61.56$	0.9935
6	$RSS_6(dBm) = -32.305 * \log_{10}(d_m) - 43.878$	0.845
	$RSS_6(dBm) = -32.332 * \log_{10}(d_a) - 43.855$	0.8762
	$RSS_6(dBm) = -25.7 * \log_{10}(d_l) - 50.4$	1.000
	$RSS_6(dBm) = -22.266 * \log_{10}(d_{wg}) - 54.469$	0.996
	$RSS_6(dBm) = -20.677 * \log_{10}(d_g) - 56.597$	0.9935

4.2.2.3 Summary for Short and Long Distance Prediction Performance

From Tables 4.2-3, it is evident that regression line estimates exhibit a general linear equation of a line between two points. This equation is stated as

$$y = mx + b \tag{4.1}$$

Where y denotes RSS, m denotes $-10n$, x denotes $\log_{10}(d_i/d_0)$ and b is the intercept on the y-axis. For all the regression line estimates the approximate distance was calculated using

$$d_i = d_0 * 10^{-\left(\frac{RSS+b}{10n}\right)} \tag{4.2}$$

All the errors and the corresponding root mean square error (RMSE) which are formed by the deviations in distance for different predictions from the measured distance using

the results of Equation 4.2 were computed. These errors are shown in the Figures: 4.12, 4.13, 4.14, 4.21, 4.22 and 4.23. In Table 4.4-5, these errors have been summarized.

Table 4.4: Errors for the Different Prediction Models in Outdoor Environments for Index 1-2

Index, x	Models	Mean Error (m)	RMSE (m)
1	ANFIS	0.690	1.0412
	LNSM	13.068	15.8700
	wGM	14.502	19.7730
	GM	14.794	21.7050
2	ANFIS	0.083	0.1057
	LNSM	0.581	0.6008
	wGM	0.908	0.9826
	GM	0.997	1.1736

Table 4.5: Errors for the Different Prediction Models in Outdoor Environments for Index 3-6

Index, x	Models	Mean Error (m)	RMSE (m)
3	ANFIS	0.368	0.4718
	LNSM	8.061	9.2600
	wGM	8.077	10.1895
	GM	7.266	9.4479
4	ANFIS	0.322	0.4681
	LNSM	161.033	175.8635
	wGM	189.716	208.7665
	GM	204.888	225.5499
5	ANFIS	3.877	4.6456
	LNSM	135.755	139.1499
	wGM	95.955	100.4047
	GM	49.111	54.6076
6	ANFIS	0.630	1.0228
	LNSM	177.564	292.5742
	wGM	278.223	455.1970
	GM	327.125	516.8296

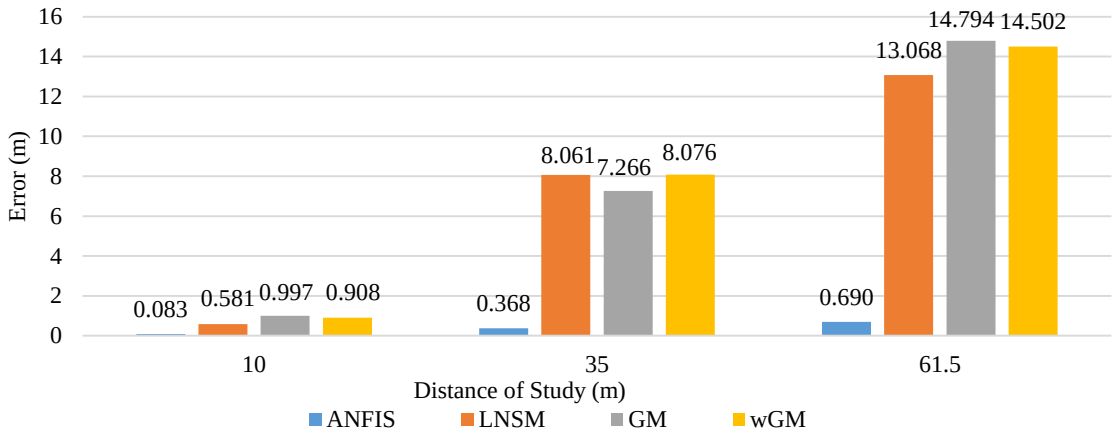

Figure 4.24: Localization Error in Short Distance Outdoor Environment

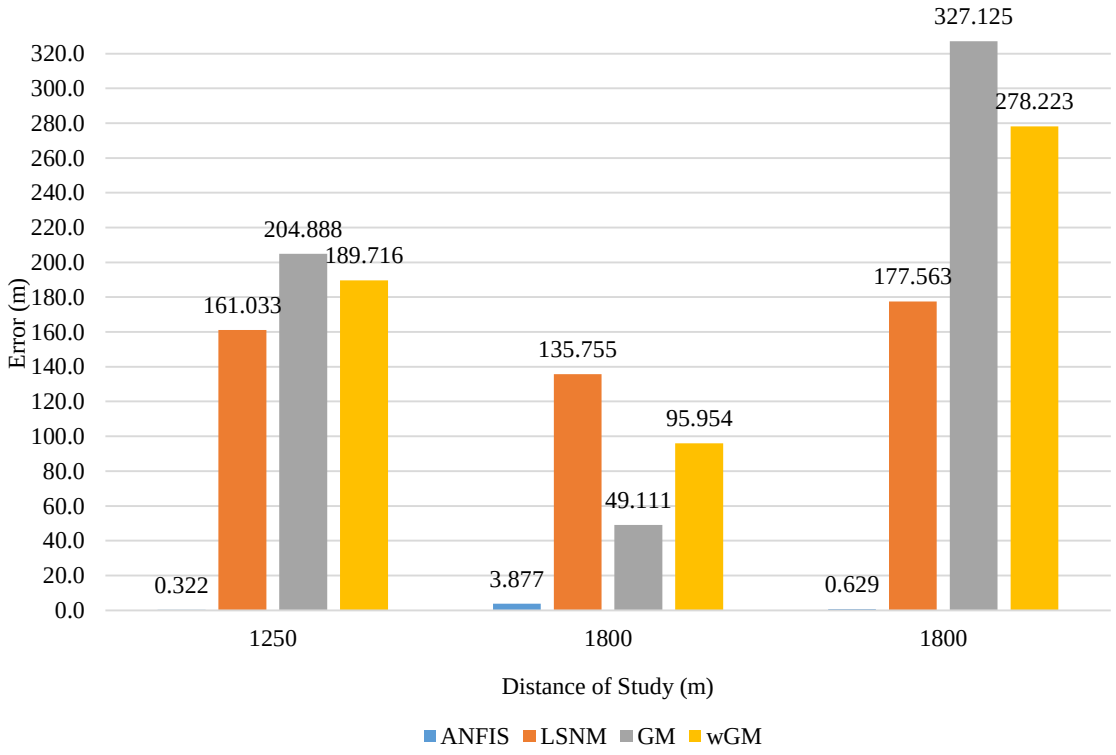

Figure 4.25: Localization Error in Long Distance Outdoor Environment

Figures 4.24-25 show the comparison of error values that were generated by the regression line equations of different models that were studied in this research.

Generally, the mean error in outdoor environments in all the models' estimates increases with increase in distance and with a notably small increase for the ANFIS estimates. This is visible in Figure 4.24. This is attributed to the increase in the error magnitudes of the testing datasets which increase rapidly with increase in distances.

Short distance provided good estimations when using the ANFIS model. The shortest distance provided the best estimation compared to the long distances. This is attributed to the sampling distance of 1m which was used for data corresponding to index 2. Data samples obtained from short distances make it easy for ANFIS to learn about the pattern that exists in them.

For long distances, ANFIS prediction performance for data gathered from suburban environments is better than the performance in an urban environment. Dataset corresponding to index 5 was gathered from a dense urban environment. This is evident in Figure 4.16 and 4.22 (data from urban environment) compared to: Figures 4.15 and 4.21; and Figures 4.17 and Figure 4.23 (data from suburban environment). Urban environments contain high path loss because of the many obstructions; like storey buildings, vehicles, transmitters, which are present in the path of the radio signals and thus measured values and estimated values are at great variance.

Also, in dataset represented by index 5, the ANFIS estimates begin to increase with a high margin at distance of 800m as shown in Figure 4.22. This behavior is different from the rest of the long distance datasets. The data in this dataset was gathered from a dense urban environment with factories, many offices with communication towers, high dense human and vehicular traffic. All these listed items contributed to a high

shadow factor and a poor radio signal reception. The large error at the near end positions is due to the poor learning of ANFIS from the training data.

For long distance ANFIS estimates the mean error between 0.322 and 3.877m, which values are relatively good for long distance localization of mobile nodes. The estimates made from the LNSM had a large error magnitude. The outputs of other prediction models used in this study can't be relied on for the data sets under consideration. The poor prediction of LNSM are spread to the Grey and weighted Grey Models whose inputs are the outputs of the LNSM. The LNSM relies on the theoretical parameters which lead to a large spread between its output and the measured data. The large spread inherent in LNSM estimations, when used as testing data to the ANFIS, gives a different pattern in the trained data output. This impacts the ANFIS estimations negatively since this may increase the error in the output values.

4.2.2.4 A study on the Indoor Environment

An extra study was conducted involving the data captured from the short distance environment [10]. This data is captured in index 7 of Table 3.1. The system was run and the output of this study was analyzed and compared against the outputs of the outdoor short distance.

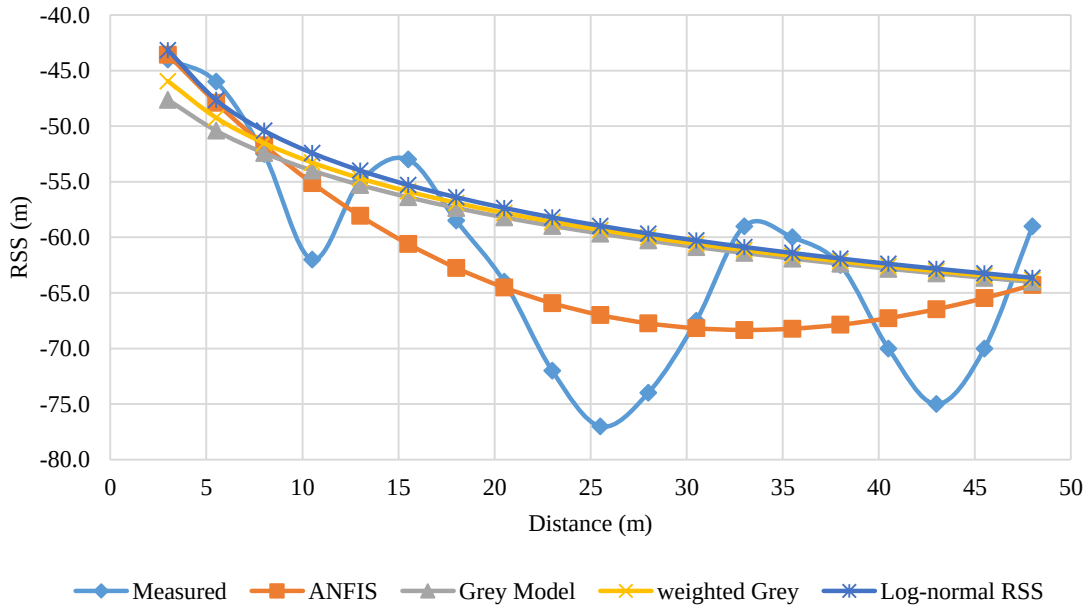

Figure 4.26: RSS versus Distance from the Transmitter for Index 7

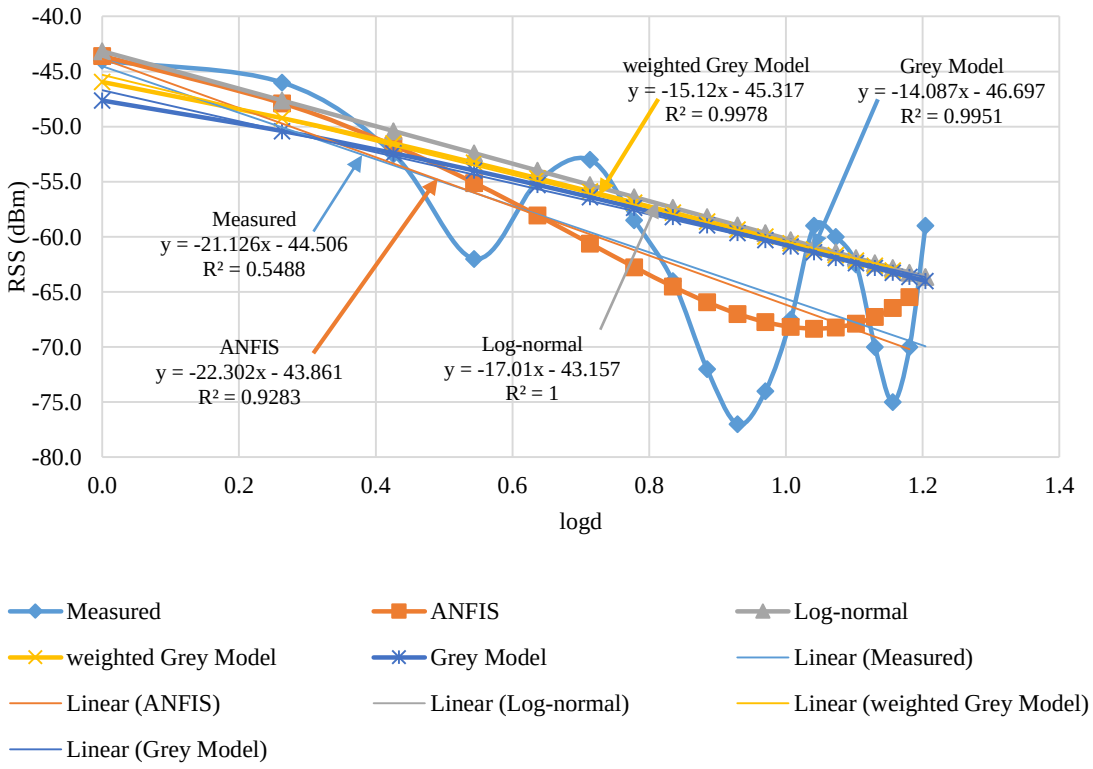

Figure 4.27: RSS versus $\log_{10}(d)$ for Index 7

Figure 4.26 shows plots of RSS versus distance for the four models (ANFIS, LNSM, GM, and wGM) plus a plot for the measured data used in the study. Figure 4.27 shows the regression approximations for the dataset shown in Figures 4.26. Figure 4.28 shows plots of localization error against distance for the same models indicated in Figure 4.26. The Figures 4.26-28 correspond to index 7 of Tables 4.5-6.

In Figure 4.28, there is a great variation in the magnitude of error produced by all the models at distances of 10, 26 and 43m. This was attributed to the reflection of the radio frequency (RF) signals by obstructions like walls, windows, doors and furniture within the hall. At a distance corresponding to 10m, the major contributors of divergence were walls and windows. At 26m distance, the contributors for divergence were doors, windows, and walls. For 43m distance, the contributors were furniture, walls and windows. This explains the reason as to why there are divergences at the three highlighted positions. The magnitude of divergence correlates with number and intensity of obstructions. A high number of reflectors at 26m distance contributed to high divergence. The divergence reduces with the reduction in the reflectors. This is seen at 43m and 10m distances.

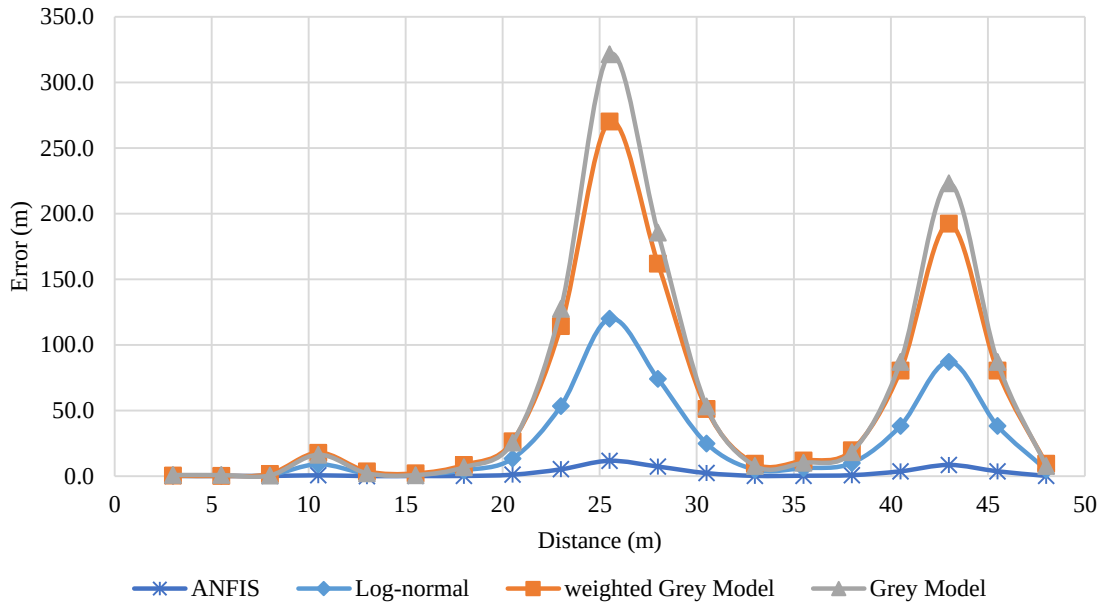

Figure 4.28: Localization Error for the Different Prediction Models for Index 7

In Table 4.6 the regression approximations of different models in indoor environment are summarized whereas the errors resulting from these models have been summarized in Table 4.7.

Table 4.6: Regression Line Estimations for the Different Prediction Models for Index 7

Index, x	Regression line Approximation	R^2
7	$RSS_7(dBm) = -21.126 * \log_{10}(d_m) - 44.506$	0.549
	$RSS_7(dBm) = -22.302 * \log_{10}(d_a) - 43.861$	0.928
	$RSS_7(dBm) = -17.01 * \log_{10}(d_l) - 45.157$	1.000
	$RSS_7(dBm) = -15.12 * \log_{10}(d_{wg}) - 45.317$	0.998
	$RSS_7(dBm) = -14.087 * \log_{10}(d_g) - 46.697$	0.995

Table 4.7: Errors for the Different Prediction Models in Indoor Environment

Index, x	Model	Mean Error (m)	RMSE (m)
7	ANFIS	2.471	4.152
	LNSM	25.992	42.528
	wGM	55.931	93.668
	GM	62.276	108.389

Like in the outdoor environment, the localization error in the ANFIS estimates for indoor environment increases with increase in distance. The ANFIS estimates for the dataset collected from indoor environment deviates from the outdoor one. The absolute error is seen fluctuate rapidly at distances of 10m, 26m and 43m as already explained. This behavior is attributed to the large variation in training dataset. During the learning process of ANFIS, the pattern of the data was hard to be mastered and thus ANFIS output a poor approximation. The regression line for this training was hard to trace and this is seen in its correlation coefficient of 0.5488, which is a poor correlation.

In comparison with results from outdoor environments, the data gathered from an outdoor environment contributed a better prediction than the data gathered from indoor environment. For short distance outdoor environment, the error in ANFIS is in the range of 0.083m to 0.690m whereas the error in short distance indoor environment is 2.472m.

4.3 Evaluation of ANFIS Performance

The performance of ANFIS was evaluated by comparing its localization error, as shown in Table 4.6 and Figure 4.28, with other methods and algorithms which are published in [10] [12] [13] [14] [15].

Table 4.8: Comparison of ANFIS Errors with other Algorithms' Errors

Other Learning Algorithms			**ANFIS**	
Algorithms	**Distance (m)**	**Error (m)**	**Distance (m)**	**Error (m)**
BR, LM	300x300	0.490	1250	0.322
BP	100x100	1.186	1250	0.322
PSO-ANN	65	0.022	65	0.690
NN	50x50	6.500	35	0.368
BP	10x10	0.694	10	0.083

In Table 4.8, a comparison between ANFIS and other algorithms in error performance is presented. BR is the Bayesian Regression, LM is the Levenberg-Marquardt, BP is the Back-propagation, PSO-ANN is the Particle Swarm Optimization-Adaptive Neural Network, and NN is the Neural Network.

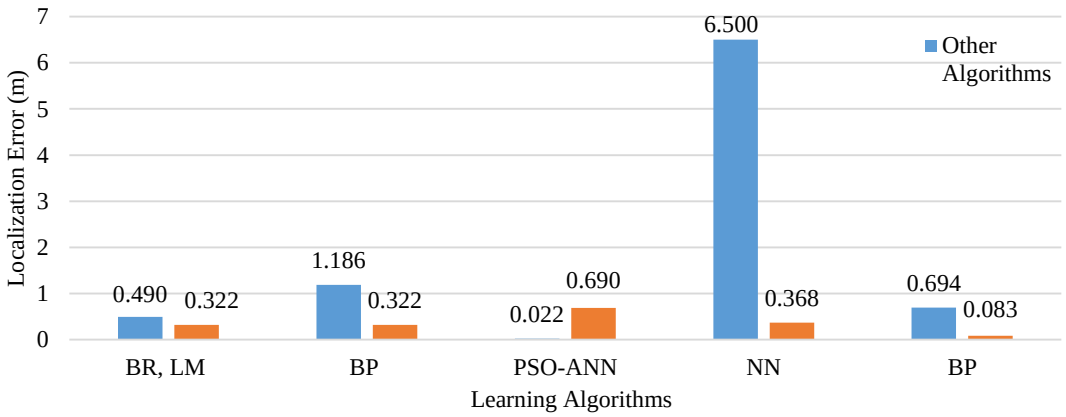

Figure 4.29: Comparison of ANFIS Errors with other Algorithms' Errors.

The study shows that the error ratios of ANFIS to BR and LM, BP, PSO-ANN, NN and BP are; 23:35 (0.670), 161:595 (0.271), 345:11 (31.364), 92:1625 (0.057) and 83:694 (0.120) respectively. A lower error ratio indicates a high prediction performance whereas a high error ratio indicates a poor prediction performance. From this error ratio comparison it is concluded that ANFIS methodology has a superior performance in comparison to many of the highlighted algorithms. For short distances, the performance of ANFIS is comparable to that of Hybrid Particle Swarm Optimization and Adaptive Neural Networks (PSO-ANN) with ANFIS and PSO-ANN having mean errors of 0.083m and 0.022m respectively. The performance of ANFIS in comparison with PSO-ANN is significant at the error ratio of 345:11 which is bigger than the rest of the comparisons with other models, thus training ANFIS with PSO would improve on the results. It is also significant that the error values in long distance

ANFIS estimations are close and some are smaller than the error values in highlighted methods that were used for short distance estimations. For example, using ANFIS methodology at a 1250m distance performed with a mean error of 0.322m which is better than BR and LM which perform with a mean error of 0.490 at a distance of 300m.

The further study showed a poor performance of ANFIS for indoor environment when compared with other methods that were used in indoor localization under closely similar distance of study. Thus ANFIS methodology needs to be integrated with other methods in special cases like indoor environment for optimal prediction performance to be achieved.

CHAPTER FIVE: CONCLUSION AND RECOMMENDATION

5.1 Conclusion

In this work, the objectives of research were met. The application of ANFIS in an optimal mobility prediction was investigated. The study has been made on real data which was gathered from published papers. Prediction algorithms like Log-Normal Shadowing Model (LNSM), Grey Model (GM) and its weighted version have been explored too and their behavior have been critically learned as well. From the design of the ANFIS, it is evident that its algorithm is simple to construct. The convergence time for training this ANFIS methodology, for all the seven datasets, was approximately 120s with an optimal output and an error of 0.083m-3.877m which makes it a fast and reliable mobility prediction methodology in wireless or cellular networks.

During the analysis, the ANFIS output using different sets of testing data exhibited the same behavior. The study and analysis presented in this thesis was based on the testing data produced by the GM. This was due to the negligible difference in the ANFIS outputs. Thus, the localization estimations in this research used the RSS values of the ANFIS model which was tested using RSS extracted from GM outputs.

In long distance outdoor environments, it was seen that ANFIS estimates have mean errors between 0.322m and 3.877m, the values which are relatively good for long distance localization of mobile nodes (MNs) since the maximum error approximates to a size of a small vehicle. For short distances outdoor environments, the error in ANFIS is in the range of 0.083m to 0.690m whereas in short distance indoor

environment, the error value of 2.472m was obtained. The results for outdoor environment were validated and found satisfactory. However, the results for indoor environment were not satisfactory, probably due to insufficient data that were used. This limited ANFIS's ability to learn and adaptive the data supplied to it. Thus it is evident that the data gathered from outdoor environment contributes to a better prediction than the data gathered from indoor environment. This can be attributed to the many and strong sources of signal fluctuation, such as reflection caused by indoor items/structures like furniture, walls, and windows among others.

It has been discovered that ANFIS prediction methodology performs well up to a given distance as the MN traverses. The average approximated distance at which the anomalies in the accuracy of mobility prediction occurs has been noted as 62.33% and 64.82% for short and long distance communication environments respectively. This implies that whenever there is a change in the general trend of ANFIS output values and the measured data, the accuracy in mobility prediction begins to diminish from that point and onwards. In the actual implementation of this ANFIS methodology in smart antenna systems (SAS) such points correspond to critical distances and the beam forming characteristics in the SAS need to be adjusted to counteract the diversion from the normal mobility prediction trend and accuracy.

To validate our methodology, the errors in this prediction were compared with the errors which were reported in other methods as seen in Figure 4.29. The performance of ANFIS in outdoor environment was very good and comparable Particle Swarm Optimization and Adaptive Neural Network (PSO-ANN) which is characterized by complex processes and, thus, executes for a longer time before converging.

The designed methodology therefore is suitable for application in outdoor localization or mobility prediction of MNs and thus it can be integrated in the current and future smart antenna systems. However, the antenna system that will use this methodology needs to have a capability of storing the learned values for future reference so that the learning process on new data may be simplified and therefore use little time to complete the execution.

5.2 Recommendation

The study considered the data gathered from outdoor, short and long, distance environments. The short distance covered 1m-10m, 35m and 61.5m whereas the long distance covered 100m-1250m and 1800m. Generally, prediction error in ANFIS increases with increase in distance between the transmitter and Mobile Node (MN). It is also notable that ANFIS prediction for short distances outperformed its prediction for long distances. This is attributed to the data sampling intervals used in short and long distances; the sampling intervals for short distance was 1m, 1.5m and 2.5m whereas the one for long distance was 50m and 100m. Using data gathered from a small intervals would yield better approximations in long distances.

The gathered data used in this research was assumed to be from reliable sources and was not subjected to any forms of validation before use since it was collected from live environments under consideration at the time the reported researches were carried out.

The values of weights used in Grey Model were the averaged estimates and other variations in values of w_1 and w_2 were not studied. Also the predictions of Grey and

weighted Grey Models depended on the outputs on the LNSM. Further study, where the inputs of Grey and weighted Grey models are measured data, is needed.

The study only considered data gathered from suburban and dense urban environments. Further studies could to be carried out on other environments like rural environment which wasn't covered in the data set considered in this study.

The investigation for indoor environment showed unsatisfactory results due to insufficient data. Hence more research needs to be undertaken.

REFERENCES

[1] S. Venkatachalaiah, R. J. Harris and J. E. Murphy, "Improvement of Handoff in Wireless Networks using Mobility Prediction and Multicasting Techniques," *Centre for Advanced Technology in Telecommunications (CATT)*, vol. 4, no. 2, pp. 195-208, 2005.

[2] B. Liang and Z. J. Haas, "Predictive distance-based mobility management for multidimensional PCS networks," *IEEE/ACM Transactions on Networking*, vol. 11, no. 5, pp. 718-732, 2003.

[3] Z. R. Zaidi and B. L. Mark, "Real-Time Mobility Tracking Algorithms for Cellular Networks Based on Kalman Filtering," *IEEE Transactions on Mobile Computing*, vol. 4, no. 2, pp. 195 - 208, 2005.

[4] K. Zhang, "Traffic pattern prediction in cellular networks," *PhD Thesis, Queen Mary University of London*, 2011.

[5] S. J. Halder, P. Giri and W. Kim, "Advanced Smoothing Approach of RSSI and LQI for Indoor Localization System," *International Journal of Distributed Sensor Networks*, pp. 1-11, 2014.

[6] Z. Fang, Z. Zhao, D. Geng, Y. Xuan, L. Du and X. Cui, "RSSI Variability Characterization and Calibration Method in Wireless Sensor Network,"

Proceedings of the 2010 IEEE International Conference on Information and Automation, pp. 1532-1537, 2010.

[7] S. Hui, F. Yang, Z. Li, Q. Liu and J. Dong, "Application of Grey Model to Forecast," *International Journal of Information and Systems Sciences,* vol. 5, no. 3-4, pp. 522-527, 2009.

[8] E. Kayacan, O. Kaynak and B. Ulutas, "Grey system theory-based models in time series prediction," *Expert Systems with Applications, Elsevier,* vol. 37, p. 1784–1789, 2010.

[9] M. Levy, S. Bose, A. Dinh and D. Kumar, "A novelistic fractal antenna for ultra-wideband (UWB) applications," *Progress In Electromagnetics Research B,* vol. 45, p. 369–393, 2012.

[10] S. K. Gharghan, R. Nordin, M. Ismail and J. A. Ali, "Accurate Wireless Sensor Localization Technique Based on Hybrid PSO-ANN Algorithm for Indoor and Outdoor Track Cycling," *IEEE Sensors Journal,* vol. 16, no. 2, pp. 529 - 541, Jan. 15, 2016.

[11] P. Bilurkar, N. Rao, G. Krishna and R. Jain, "Application of neural network techniques for location predication in mobile networking," *Proceedings of the 9th International Conference on Neural Information,* vol. 5, 2002.

[12] A. Payal, C. S. Rai and B. V. R. Reddy, "Artificial neural networks for developing localization framework in wireless sensor networks," *in Proc IEEE Int. Conf. Data Mining Intell. Comput. (ICDMIC),* pp. 1-6, ep. 2014.

[13] A. Payal, C. S. Rai and B. V. R. Reddy, "Comparative analysis of Bayesian regularization and Levenberg–Marquardt training algorithm for localization in wireless sensor network," *in Proc. IEEE 15th Int. Conf. Adv. Commun. Technol. (ICACT),* pp. 192-194, Jan 2013.

[14] S. Kumar and S. R. Lee, "Localization with RSSI values for wireless sensor networks: An artificial neural network approach," *in Proc. 1st Int. Electron. Conf. Sensors Appl.,* pp. 1-6, Jan. 2014.

[15] P.-J. Chuang and Y.-J. Jiang, "Effective neural network-based node localisation scheme for wireless sensor networks," *IET Wireless Sensor Syst.,* vol. 4, no. 2, pp. 97-103, 2014.

[16] M. A. Sojitra, R. C. Purohit and P. A. Pandya, "Comparative Study of Daily Rainfall Forecasting Models Using Adaptive-Neuro Fuzzy Inference System (ANFIS)," *Curr World Environ.,* vol. 10, no. 2, 2015.

[17] K. V. Rop, D. B. O. Konditi, H. A. Ouma and S. M. Musyoki, "Parameter Optimization In Design Of A Rectangular Microstrip Patch Antenna Using Adaptive Neuro-Fuzzy In ference System Technique," *International Journal on Technical and Physical Problems of Engineering (IJTPE),* vol. 4, no. 3, 2012.

[18] P. Amara and N. Sarma, "Adaptive Beam forming Algorithms for Smart Antenna Systems," *WSEAS Transactions on Communications,* vol. 13, no. 2, pp. 44-50, 2014.

[19] C. Peng, "Cellular Network for Mobile Devices and Applications: Infrastructure Limitations and Solutions," *Computer Science 0201, PhD Thesis - University of Calfonia, Los Angeles,* 2013.

[20] D. M. M. Rahaman, M. M. Hossain and M. M. Rana, "Least Mean Square Least Mean Square," *Universal Journal of Communications and Network,* vol. 1, no. 1, pp. 16-21, 2013.

[21] M. U. Sheikh, J. Lempiainen and A. Hans, "Advanced Antenna Techniques And High Order Sectorization With Novel Network Tessellation For Enhancing Macro Cell Capacity In DcHSDPA Network," *International Journal of Wireless & Mobile Networks (IJWMN),* vol. 5, no. 5, 2013.

[22] A. F. Molisch, Wireless Communications, 2 ed., John Wiley & Sons Ltd, 2011.

[23] S. Hossain, M. Islam and S. Serikawal, "Adaptive beamforming algorithms for smart antenna systems," *International conference on control, automation and systems, ICCAS,* pp. 412-416, 2008.

[24] L. Du, J. Biaham and L. Cuthbert, "A Bubble Oscillation Algorithm for Distributed Geographic Load Balancing in Mobile Networks," *IEEE INFOCOM, Twenty-third AnnualJoint Conference of the IEEE Computer and Communications Societies,* November 2004.

[25] H. Wang, P. Wu, Z. Pan., N. Lui and X. You, "Dynamic load balancing and throughput optimization in 3GPP LTE networks," *In Proceedings of the 6th*

International Wireless Communications and Mobile Computing Conference, ACM, pp. 939-943, 2010.

[26] A. Goldsmith, Wireless Communications, New York: Cambridge University Press, 2005.

[27] P. Chuan-Chin, P. Chuan-Hsian and L. Hoon-Jae, "Indoor Location Tracking Using Received Signal Strength Indicator," *Emerging Communications for Wireless Sensor Networks,* pp. 229-257, 2011.

[28] J. Harri, C. Bonnet and F. Filali, "The Challenges of Predicting Mobility," Eurecom Institute, Sophia-Antipolis, April 2007.

[29] A. Kannan and S. Bose, "Adaptive Multipath Multimedia Streaming Architecture for Mobile Networks with Proactive Buffering Using Mobile Proxies.," *Journal of computing and information technology,* vol. 15, no. 3, pp. 215-226, 2007.

[30] Y.-L. Tang, Y. Yuan, C.-C. Lin and D. -J. Deng, "Dividing Sensitive Ranges Based Mobility Prediction Algorithm in Wireless Networks," *Tamkang Journal of Science and Engineering,* vol. 13, pp. 107-115, 2010.

[31] B. Ng, A. Deng, Y. Qu and W. K. G. Seah, "Changeover prediction model for improving handover support in campus area WLAN," *NOMS 2016 - 2016 IEEE/IFIP Network Operations and Management Symposium,* pp. 265-272, 2016.

[32] C. -C. Pu, C. -H. Pu and H. -J. Lee, Indoor Location Tracking Using Received Signal Strength Indicator, Emerging Communications for Wireless Sensor Networks, A. F. a. A. Foerster, Ed., InTech, 2011.

[33] S. Abbasi, S. Shah, F. Khuhawar, N. Shah and R. Memon, "Optimum Cell Sectorization for Capacity Enhancement," *SindhUniv. Res. Jour. (Sci. Ser.)*, vol. 47, no. 3, pp. 585-590, 2015.

[34] P. Zetterberg, "Performance of three, six, nine and twelve sector sites in CDMA-based on measurements," *IEEE Eighth International Symposium on Spread Spectrum Techniques and Applications*, pp. 394-399, 2004.

[35] A. Sabharwal, D. Avidor and L. Potter, "Sector beam synthesis for cellular systems using phased antenna arrays," *IEEE Transactions on Vehicular Technology*, vol. 49, no. 5, 2000.

[36] L. Ghoutia, T. R. Sheltamia and K. S. Alutaibi, "Mobility Prediction in Mobile Ad Hoc Networks Using Extreme Learning Machines," *The 4th International Conference on Ambient Systems, Networks and Technologies (ANT 2013)*, vol. 19, pp. 305-312, 2013.

[37] O. Dengiz, A. Konak and A. Smith, "Improving Network Connectivity in Ad Hoc Networks Using Particle Swarm Optimization and Agents," in *Wireless Network Design*, vol. 158, 2010, pp. 247-267.

[38] K. V. Rop, D. B. O. Konditi, H. A. Ouma and S. M. Musyoki, "Parameter Optimization In Design Of A Rectangular Microstrip Patch Antenna Using

Adaptive Neuro-Fuzzy Inference System Technique," *International Journal on Technical and Physical Problems of Engineering (IJTPE),* vol. 4, no. 3, pp. 16-23.

[39] K. B. Ariffin, "On Neuro-Fuzzy Applications for Automatic Control, Supervision, and Fault Diagnosis for Water Treatment Plant," A Thesis submitted to the Faculty of Electrical Engineering, Universiti Teknologi, Malaysia, 2007.

[40] T. N. Kapetanakis, I. O. V. G. S. Liodakis and A. Maras, "Solving the Inverse Loop Antenna Radiation Problem Using a Hybrid Neuro-Fuzzy System," *20th Telecommunications forum TELFOR 2012 Serbia, Belgrade,* p. 1189–1192, Nov. 2012.

[41] J. J. Cárdenas, A. García, J. L. Romeral and K. Kampouropoulos, "Evolutive ANFIS Training for Energy Load Profile Forecast for an IEMS in an Automated Factory," *Emerging Technologies & Factory Automation (ETFA), 2011 IEEE 16th Conference on, Toulouse,* pp. 1-8, 2011.

[42] S. Sharma, U. Kalra, S. Srivathsan, K. Rana and V. Kumar, "Efficient Air Pollutants Prediction using ANFIS Trained by Modified PSO Algorithm," *Reliability, Infocom Technologies and Optimization (ICRITO) (Trends and Future Directions), 2015 4th International Conference on, Noida,* pp. 1-6, 2015.

[43] E. A. Ubom, V. E. Idigo, A. O. C. Azubogu, C. O. Ohaneme and T. L. Alumona, "Path loss Characterization of Wireless Propagation for South – South Region of

Nigeria," *International Journal of Computer Theory and Engineering,* vol. 3, no. 3, pp. 360-364, June 2011.

[44] L. Ghoutia, T. R. Sheltamia and K. S. Alutaibi, "Mobility Prediction in Mobile Ad Hoc Networks Using Extreme Learning Machines," *The 4th International Conference on Ambient Systems, Networks and Technologies (ANT 2013),* vol. 19, pp. 305-312, 2013.

[45] I. Khider, F. Wang and W. Yin, "Study on Indoor and Outdoor Environment for Mobile Ad Hoc Network Supported with Base Stations," *International Conference on Wireless Communications, Networking and Mobile Computing,* vol. 4, pp. 1470-1474, 2007.

[46] N. Meghanathan, "Impact of the Gauss-Markov Mobility Model on Network Connectivity, Lifetime and Hop Count of Routes for Mobile Ad hoc Networks," *Journal Of Networks,* vol. 5, no. 5, pp. 509-516, 2010.

[47] N. V. Okorogu, U. D. Onyishi., C. G. Nwalozie and N. N. Utebor, "Empirical Characterization of Propagation Path Loss and Performance Evaluation for Co-Site Urban Environment," *International Journal of Computer Applications (0975 – 8887),* vol. 70, no. 10, pp. 34 - 41, May 2013.

[48] O. S. Oguejiofor, V. N. Okorogu, A. Adewale and B. O. Osuesu, "Outdoor Localization System Using RSSI Measurement of Wireless Sensor Network," *International Journal of Innovative Technology and Exploring Engineering (IJITEE),* vol. 2, no. 2, pp. 1 - 6, 2013.

[49] E. Ifeagwu, M. Alor and G. Obi, "Received Signal Strength Estimation in Wireless Local Area Network (WLAN) Environment," *International Journal of Scientific Research in Science, Engineering and Technology* , vol. 1, no. 3, p. 183–186, 2015.

[50] S. Y. Seidel and T. Rappaport, "914 MHz Path Loss Prediction Models for Indoor Wireless Communications in Multifloored Building," *IEEE Transactions on Antennas and Propagation*, vol. 40, no. 2, p. 207–217, 1992.

[51] Y. Lin and S. Liu, "A Historical Introduction to Grey Systems Theory," *2004 IEEE InternationalConference on Systems, Man and Cybernetics*, vol. 3, pp. 2403-2408, 2005.

[52] S. Zhaozheng, J. Qingzhe and J. Yanjun, "The Combined Model of Gray Theory and Neural Network which is based on Matlab Software for Forecasting of Oil Product Demand," *Scientific Research,* p. 155–160, 2010.

[53] L. Xiaofei and H. Renfang, "Interpolation Optimization Interpolation Optimization," *SHS Web of Conferences,* vol. 6, no. 03003, pp. 1-6, 2014.

[54] P. Zhou, B. W. Ang and K. L. Poh, "A trigonometric grey prediction approach to forecasting electricity energy demand," *Energy,* vol. 31, no. 14, pp. 2839-2847, 2006.

[55] D. T. A., L. A. U. and U. Salisu, "A comparative Study between Modelled and Received Mobile," *The International Journal Of Engineering And Science (IJES),* vol. 3, no. 7, pp. 38-45, 2014.

[56] E. Akujobi, O. Nosiri and U. Lazarus, "Path Loss Characterization of 3G Wireless Signal for Urban and Suburban Environments in Port Harcourt City, Nigeria.," *International Research Journal of Engineering and Technology (IRJET)*, vol. 3, no. 3, pp. 16-22, March 2016.

[57] M. Bernas and B. Płaczek, "Fully Connected Neural Networks Ensemble with Signal Strength Clustering for Indoor Localization in Wireless Sensor Networks," *International Journal of Distributed Sensor Networks*, vol. 2015, pp. 1 - 10, 2015.

APPENDICES

Appendix A: Matlab Code

Appendix A-1: Matlab Code for LNSM, GM and w-GM models

```
function begin = trainingparameters1
tic
clc
clear all
clf
d0=1.5;%Reference distance for outdoor propagation environment
n1=1.613; %Path loss exponent according to Rappaport
s=65+d0;
std=0.451; %Standard deviation
j=27;
w1=0.5;w2=0.5; % weights for creating weighted averages
%%%%%%%
pt=0.001;%(in Watts)
pt_d=10*log10(pt);%in dB
prdBm=-39;%RSS at a refernce distance, d0=1m, in dBm
prW=0.001*10.^(prdBm/10);
PL0=10*log10(pt/prW); %PL0 in dB at refernece distance)
d=d0:2.5:s;
for i=1:j
   RSS_0(i)=pt_d-PL0-10*n1*log10(d(i)/d0)-std;
```

```
end
for i=1:j
   rss_0(i)=10.^(-RSS_0(i)/10);
end
sum=0;
for i=1:j
   sum=sum+rss_0(i);
   rss_1(i)=sum; %AGO application
end
for i=1:j-1
   B(i,1)=-1/2.*(rss_1(i)+rss_1(i+1)); %Background value calculation
end
B(:,2)=1; % the second column of the (B and B2)-matrix is 1
yn=(rss_0(2:j))'; %Application of AGO on the iregular data sequence
v=inv(B'*B)*(B*yn)';%Application of square method
%%%%%%%
a=v(1);% Row one of the result of square method
b=v(2);% Row one of the result of square method
for i=1:j
   prss_1(i)=rss_1(i);
   prss_1(i+1)=(rss_0(i)-b/a)*exp(-a*j)+(b/a); %Solution for the conventional Grey
Model
   %%%
   prss_0(i)=rss_0(i);
```

```
    prss_0(i+1)=prss_1(i+1)-prss_1(i); %Obtaining the predicted value of the
primitive data at time (i+1),
    %the IAGO is used.
end
for i=1:j
PRSS_0(1:j)=-10*log10(prss_0(2:j+1)); %converted to dB
end
for i=1:j
    prss_2(i)=w1*rss_0(i)+w2*prss_0(i+1);%Predicted value after applying the
weigted average method
end
for i=1:j
PRSS_2(1:j)=PRSS_0(1:j);%converted back to dB
end
for i=1:j
PR1(i:j-1)=10*log10((10.^(PRSS_2(i:j-1)/10))/0.001);%Conversion to dBm
end
for i=1:j
d1(i:j-1)=d(i:j-1);
end
trncolumn1 = d1';
%%%%%%
for i=1:j
PR00(i:j-1)=10*log10((10.^(RSS_0(i:j-1)/10))/0.001);%Conversion to dBm
```

```
%rs_0(1:j-1)=awgn(PR0(1:j-1),d0-0.5);
end
PR0=PR00';
trncolumn2 =PR1';
%%%%%%%%%%%%%%
t=ones(26,1);
tn1=n1*t;
tPL01=PL0*t;%dB
%%%%%%%%%%%%%%
begin = [tn1 tPL01 trncolumn1 trncolumn2 PR0];
save begin
end
function begin2 = trainingparameters2
tic
clc
clear all
clf
d0=1;%Reference distance for outdoor propagation environment
n2=2.2; %Path loss exponent according to Rappaport
s=10+d0;%in m
std=0.2721; %Standard deviation
j=11;
w1=0.5;w2=0.5; % weights for creating weighted averages
%%%%%%%
```

```
pt=0.001;%(in Watts)=-3.802 dB
pt_d=10*log10(pt);%in dB
prdBm=-45;%RSS at a refernce distance, d0=1m, in dBm
prW=0.001*10.^(prdBm/10);
PL02=10*log10(pt/prW); %PL0 in dB at reference distance
d2=d0:1:s;
for i=1:j
   RSS_0(i)=pt_d-PL02-10*n2*log10(d2(i)/d0)-std;
end
for i=1:j
   rss_0(i)=10.^(-RSS_0(i)/10);
end
sum=0;
for i=1:j
   sum=sum+rss_0(i);
   rss_1(i)=sum; %AGO application
end
for i=1:j-1
   B(i,1)=-1/2.*(rss_1(i)+rss_1(i+1)); %Background value calculation
end
B(:,2)=1; % the second column of the (B and B2)-matrix is 1
yn=(rss_0(2:j))'; %Application of AGO on the iregular data sequence
v=inv(B'*B)* (B*yn)';%Application of square method
%%%%%%%
```

```
a=v(1);% Row one of the result of square method
b=v(2);% Row one of the result of square method
for i=1:j
   prss_1(i)=rss_1(i);
   prss_1(i+1)=(rss_0(i)-b/a)*exp(-a*j)+(b/a); %Solution for the conventional Grey
Model
   %%%
   prss_0(i)=rss_0(i);
   prss_0(i+1)=prss_1(i+1)-prss_1(i); %Obtaining the predicted value of the
primitive data at time (i+1),
   %the IAGO is used.
end
for i=1:j
PRSS_0(1:j)=-10*log10(prss_0(2:j+1)); %converted to dB
end
for i=1:j
   prss_2(i)=w1*rss_0(i)+w2*prss_0(i+1);%Predicted value after applying the
weighted average method
end
for i=1:j
PRSS_2(1:j)=PRSS_0(1:j);%converted back to dB
end
for i=1:j
PR1(i:j-1)=10*log10((10.^(PRSS_2(i:j-1)/10))/0.001);%Conversion to dBm
```

```
end
for i=1:j
dd2(i:j-1)=d2(i:j-1);
end
trncolumn12 = dd2';
 %%%%%%
for i=1:j
PR00(i:j-1)=10*log10((10.^(RSS_0(i:j-1)/10))/0.001);%Conversion to dBm
end
PR02=PR00';
trncolumn22 = PR1';
%%%%%%%%%%%%%%%
t2=ones(10,1);
tn2=n2*t2;
%tPL02=(10*log10((10.^(PL02/10))/0.001))*t2;%dBm
tPL02=PL02*t2;%dBm
%%%%%%%%%%%%%%%
begin2 = [tn2 tPL02 trncolumn12 trncolumn22 PR02];
save begin2
end
function begin3 = trainingparameters3
tic
clc
clear all
```

```
clf
 d0=2.5;%Reference distance for outdoor propagation environment
n3=3.8; %Path loss exponent according to Rappaport (In buildings)
s=35+d0;%in m
std=0.727; %Standard deviation
j=15;
w1=0.5;w2=0.5; % weights for creating weighted averages
%%%%%%%
pt=0.0024;%(in Watts)
pt_d=10*log10(pt);%in dB
prdBm=-43.5;%RSS at a refernce distance, d0=1m, in dBm
prW=0.001*10.^(prdBm/10);
PL02=10*log10(pt/prW); %PL0 in dB at reference distance)
d2=d0:2.5:s;
for i=1:j
   RSS_0(i)=pt_d-PL02-10*n3*log10(d2(i)/d0)-std;
end

for i=1:j
   rss_0(i)=10.^(-RSS_0(i)/10);
end
sum=0;
for i=1:j
   sum=sum+rss_0(i);
```

```
    rss_1(i)=sum; %AGO application
end
for i=1:j-1
    B(i,1)=-1/2.*(rss_1(i)+rss_1(i+1)); %Background value calculation
end
B(:,2)=1; % the second column of the (B and B2)-matrix is 1
yn=(rss_0(2:j))'; %Application of AGO on the iregular data sequence
v=inv(B'*B)* (B*yn)';%Application of square method
%%%%%%%
a=v(1);% Row one of the result of square method
b=v(2);% Row one of the result of square method
for i=1:j
    prss_1(i)=rss_1(i);
    prss_1(i+1)=(rss_0(i)-b/a)*exp(-a*j)+(b/a); %Solution for the conventional Grey
Model
    %%%
    prss_0(i)=rss_0(i);
    prss_0(i+1)=prss_1(i+1)-prss_1(i); %Obtaining the predicted value of the
primitive data at time (i + 1),
    %the IAGO is used.
end
for i=1:j
PRSS_0(1:j)=-10*log10(prss_0(2:j+1)); %converted to dB
end
```

```
for i=1:j
    prss_2(i)=w1*rss_0(i)+w2*prss_0(i+1);%Predicted value after applying the
weigted average method
end
for i=1:j
PRSS_2(1:j)=PRSS_0(1:j);%converted back to dB
end
for i=1:j
PR1(i:j-1)=10*log10((10.^(PRSS_2(i:j-1)/10))/0.001);%Conversion to dBm
end
for i=1:j
d3(i:j-1)=d2(i:j-1);
end
trncolumn13 = d3';
 %%%%%%
for i=1:j
PR00(i:j-1)=10*log10((10.^(RSS_0(i:j-1)/10))/0.001);%Conversion to dBm
end
PR03=PR00';
trncolumn23 = PR1';
%%%%%%%%%%%%%%%
t3=ones(14,1);
tn3=n3*t3;
tPL03=PL02*t3;%dB
```

```
%%%%%%%%%%%%%%%
begin3 = [tn3 tPL03 trncolumn13 trncolumn23 PR03];
save begin3
end
function begin4 = trainingparameters4
tic
clc
clear all
clf
%%
d0=3;%Reference distance for outdoor propagation environment
n3=1.701; %Path loss exponent according to Rappaport (In buildings)
s=50+d0;%in m
std=2.157; %Standard deviation
j=20;
w1=0.5;w2=0.5; % weights for creating weighted averages
%%%%%%%
pt=0.001;%(in Watts)
pt_d=10*log10(pt);%in dB
prdBm=-41;%RSS at a refernce distance, d0=1m, in dBm
prW=0.001*10.^(prdBm/10);
PL02=10*log10(pt/prW); %PL0 in dB at reference distance) %(PL0=41.04dB)
d2=d0:2.5:s;
for i=1:j
```

```
    RSS_0(i)=pt_d-PL02-10*n3*log10(d2(i)/d0)-std;
end
 for i=1:j
    rss_0(i)=10.^(-RSS_0(i)/10);
end
sum=0;
for i=1:j
    sum=sum+rss_0(i);
    rss_1(i)=sum; %AGO application
end
for i=1:j-1
    B(i,1)=-1/2.*(rss_1(i)+rss_1(i+1)); %Background value calculation
end
B(:,2)=1; % the second column of the (B and B2)-matrix is 1
yn=(rss_0(2:j))'; %Application of AGO on the iregular data sequence
v=inv(B'*B)* (B*yn)';%Application of square method
%%%%%%%
a=v(1);% Row one of the result of square method
b=v(2);% Row one of the result of square method
for i=1:j
    prss_1(i)=rss_1(i);
    prss_1(i+1)=(rss_0(i)-b/a)*exp(-a*j)+(b/a); %Solution for the conventional Grey
Model
    %%%
```

```
    prss_0(i)=rss_0(i);
    prss_0(i+1)=prss_1(i+1)-prss_1(i); %Obtaining the predicted value of the
primitive data at time (i + 1),
    %the IAGO is used.
end
for i=1:j
PRSS_0(1:j)=-10*log10(prss_0(2:j+1)); %converted to dB
end
for i=1:j
    prss_2(i)=w1*rss_0(i)+w2*prss_0(i+1);%Predicted value after applying the
weigted average method
end
for i=1:j
PRSS_2(1:j)=PRSS_0(1:j);%converted back to dB
end
for i=1:j
PR1(i:j-1)=10*log10((10.^(PRSS_2(i:j-1)/10))/0.001);%Conversion to dBm
end
for i=1:j
d3(i:j-1)=d2(i:j-1);
end
trncolumn14 = d3';
 %%%%%%
for i=1:j
```

```
PR00(i:j-1)=10*log10((10.^(RSS_0(i:j-1)/10))/0.001);%Conversion to dBm
end
PR04=PR00';
trncolumn24 = PR1';
%%%%%%%%%%%%%%%
t3=ones(19,1);
tn4=n3*t3;
tPL04=PL02*t3;%dB
begin4 = [tn4 tPL04 trncolumn14 trncolumn24 PR04];
save begin4
end
function begin5 = trainingparameters5
tic
clc
clear all
clf
d0=100;%Reference distance for outdoor propagation environment
n=3.11; %Path loss exponent according to Rappaport
s=1250;
std=6; %Standard deviation
j=24;
w1=0.5;w2=0.5; % weights for creating weighted averages
pt=30;%(in Watts)
pt_d=10*log10(pt);%in dB
```

```
prdBm=-45;%RSS at a refernce distance, d0=100, in dBm
prW=0.001*10.^(prdBm/10);
PL0=10*log10(pt/prW); %PL0 in dB at refernece distance) %PL0=75;%dB
d=d0:50:s;
for i=1:j
   RSS_0(i)=pt_d-PL0-10*n*log10(d(i)/d0)-std;
end
for i=1:j
   rss_0(i)=10.^(-RSS_0(i)/10);
end
sum=0;
for i=1:j
   sum=sum+rss_0(i);
   rss_1(i)=sum; %AGO application
end
for i=1:j-1
   B(i,1)=-1/2.*(rss_1(i)+rss_1(i+1)); %Background value calculation
end
B(:,2)=1; % the second column of the (B and B2)-matrix is 1
yn=(rss_0(2:j))'; %Application of AGO on the iregular data sequence
v=inv(B'*B)* (B*yn)';%Application of square method
a=v(1);% Row one of the result of square method
b=v(2);% Row one of the result of square method
for i=1:j
```

```
    prss_1(i)=rss_1(i);
    prss_1(i+1)=(rss_0(i)-b/a)*exp(-a*j)+(b/a); %Solution for the conventional Grey
Model
    prss_0(i)=rss_0(i);
    prss_0(i+1)=prss_1(i+1)-prss_1(i); %Obtaining the predicted value of the
primitive data at time (i + 1),
    %the IAGO is used.
end
for i=1:j
PRSS_0(1:j)=-10*log10(prss_0(2:j+1)); %converted to dB
end
for i=1:j
    prss_2(i)=w1*rss_0(i)+w2*prss_0(i+1);%Predicted value after applying the
weigted average method
end
for i=1:j
PRSS_2(1:j)=PRSS_0(1:j);%converted back to dB
end
for i=1:j
PR1(i:j-1)=10*log10((10.^(PRSS_2(i:j-1)/10))/0.001);%Conversion to dBm
end
 for i=1:j
d1(i:j-1)=d(i:j-1);
end
```

```
trncolumn15 = d1';
 for i=1:j
PR00(i:j-1)=10*log10((10.^(RSS_0(i:j-1)/10))/0.001);%Conversion to dBm
end
PR05=PR00';
trncolumn25 = PR1';
t5=ones(23,1);
tn5=n*t5;
tPL05=t5*PL0;
begin5 = [tn5 tPL05 trncolumn15 trncolumn25 PR05];
save begin5
end
function begin6 = trainingparameters6
tic
clc
clear all
clf
d0=100;%Reference distance for outdoor propagation environment
n2=3.55; %Path loss exponent according to Rappaport
s=1800;
std=8; %Standard deviation
j=18;
w1=0.5;w2=0.5; % weights for creating weighted averages
pt=0.001;%(in Watts)
```

```
pt_d=10*log10(pt);%in dB
prdBm=-45;%RSS at a refernce distance, d0=100, in dBm
prW=0.001*10.^(prdBm/10);
PL02=10*log10(pt/prW); %PL0 in dB at refernece distance)
d2=d0:100:s;
for i=1:j
   RSS_0(i)=pt_d-PL02-10*n2*log10(d2(i)/d0)-std;
end
for i=1:j
   rss_0(i)=10.^(-RSS_0(i)/10);
end
sum=0;
for i=1:j
   sum=sum+rss_0(i);
   rss_1(i)=sum; %AGO application
end
for i=1:j-1
   B(i,1)=-1/2.*(rss_1(i)+rss_1(i+1)); %Background value calculation
end
B(:,2)=1; % the second column of the (B and B2)-matrix is 1
yn=(rss_0(2:j))'; %Application of AGO on the iregular data sequence
v=inv(B'*B)* (B*yn)';%Application of square method
a=v(1);% Row one of the result of square method
b=v(2);% Row one of the result of square method
```

```
for i=1:j
    prss_1(i)=rss_1(i);
    prss_1(i+1)=(rss_0(i)-b/a)*exp(-a*j)+(b/a); %Solution for the conventional Grey
Model
    prss_0(i)=rss_0(i);
    prss_0(i+1)=prss_1(i+1)-prss_1(i); %Obtaining the predicted value of the
primitive data at time (i + 1),
    %the IAGO is used.
end
for i=1:j
PRSS_0(1:j)=-10*log10(prss_0(2:j+1)); %converted to dB
end
for i=1:j
    prss_2(i)=w1*rss_0(i)+w2*prss_0(i+1);%Predicted value after applying the
weigted average method
end
for i=1:j
PRSS_2(1:j)=PRSS_0(1:j);%converted back to dB
end
for i=1:j
PR1(i:j-1)=10*log10((10.^(PRSS_2(i:j-1)/10))/0.001);%Conversion to dBm
end
for i=1:j
dd2(i:j-1)=d2(i:j-1);
```

```
end
trncolumn16 = dd2';
for i=1:j
PR00(i:j-1)=10*log10((10.^(RSS_0(i:j-1)/10))/0.001);%Conversion to dBm
end
PR06=PR00';
trncolumn26 = PR1';
t6=ones(17,1);
tn6=n2*t6;
tPL06=t6*PL02;
begin6 = [tn6 tPL06 trncolumn16 trncolumn26 PR06];
save begin6
end
function begin7 = trainingparameters7
tic
clc
clear all
clf
d0=100;%Reference distance for outdoor propagation environment
n3=2.57; %Path loss exponent according to Rappaport
s=1800;
std=5.4; %Standard deviation
j=18;
w1=0.5;w2=0.5; % weights for creating weighted averages
```

```
pt=0.001;%(in Watts)
pt_d=10*log10(pt);%in dB
prdBm=-45;%RSS at a refernce distance, d0=100, in dBm
prW=0.001*10.^(prdBm/10);
PL02=10*log10(pt/prW); %PL0 in dB at refernece distance)
d2=d0:100:s;
for i=1:j
   RSS_0(i)=pt_d-PL02-10*n3*log10(d2(i)/d0)-std;
end
for i=1:j
   rss_0(i)=10.^(-RSS_0(i)/10);
end
sum=0;
for i=1:j
   sum=sum+rss_0(i);
   rss_1(i)=sum; %AGO application
end
for i=1:j-1
   B(i,1)=-1/2.*(rss_1(i)+rss_1(i+1)); %Background value calculation
end
B(:,2)=1; % the second column of the (B and B2)-matrix is 1
yn=(rss_0(2:j))'; %Application of AGO on the iregular data sequence
v=inv(B'*B)* (B*yn)';%Application of square method
a=v(1);% Row one of the result of square method
```

```
b=v(2);% Row one of the result of square method
for i=1:j
   prss_1(i)=rss_1(i);
   prss_1(i+1)=(rss_0(i)-b/a)*exp(-a*j)+(b/a); %Solution for the conventional Grey
Model
   prss_0(i)=rss_0(i);
   prss_0(i+1)=prss_1(i+1)-prss_1(i); %Obtaining the predicted value of the
primitive data at time (i + 1),
   %the IAGO is used.
end
for i=1:j
PRSS_0(1:j)=-10*log10(prss_0(2:j+1)); %converted to dB
end
for i=1:j
   prss_2(i)=w1*rss_0(i)+w2*prss_0(i+1);%Predicted value after applying the
weigted average method
end
for i=1:j
PRSS_2(1:j)=PRSS_0(1:j);%converted back to dB
end
for i=1:j
PR1(i:j-1)=10*log10((10.^(PRSS_2(i:j-1)/10))/0.001);%Conversion to dBm
end
for i=1:j
```

```
d3(i:j-1)=d2(i:j-1);
end
trncolumn17 = d3';
for i=1:j
PR00(i:j-1)=10*log10((10.^(RSS_0(i:j-1)/10))/0.001);%Conversion to dBm
end
PR07=PR00';
trncolumn27 = PR1';
t3=ones(17,1);
tn7=n3*t3;
tPL07=t3*PL02;
begin7 = [tn7 tPL07 trncolumn17 trncolumn27 PR07];
save begin7
end
```

Appendix A-2: Matlab Code for Training Data

```
%% Training Dataset
function check = testingdata
chkcolumn1 = [
%%%Testing Data for Index 1
1.0 -40;3.5 -46.5;6.0 -54;8.5 -55.8;11.0 -56.5;13.5 -57.6;16.0 -58;18.5 -58.6;21.0 -
60;23.5 -60.5;26.0 -61.4;28.5 -60.7;31.0 -64.5;33.5 -64;36.0 -63;38.5 -63.5;41.0 -
66.1;43.5 -65.8;46.0 -66.2;48.5 -66;51.0 -65.5;53.5 -65.7;56.0 -65.4;58.5 -68.5;61.0 -
69.5;63.5 -69.7; ...
%%%% Testing Data for Index 2
```

```
1.0 -45;2.0 -47.5;3.0 -48.5;4.0 -53;5.0 -55.6;6.0 -62;7.0 -67.5;8.0 -67;9.0 -69;10.0 -
67.7;…
%%% Testing Data for Index 3
2.5 -43.5;5.0 -62;7.5 -67;10.0 -73.5;12.5 -78.0;15.0 -84.5;17.5 -85.5;20.0 -87;22.5 -
85;25.0 -83;27.5 -88;30.0 -93;32.5 -90;35.0 -93;...
%%% Testing Data for Index 7
3.00 -44;5.50 -46;8.00 -52.5;10.5 -62.0;13.0 -55;15.5 -53;18.0 -58.5;20.5 -64.0;23.0 -
72.0;25.5 -77;28.0 -74;30.5 -67.5;33.0 -59;35.5 -60;38.0 -62.5;40.5 -70.0;43.0 -
75.0;45.5 -70.0;48.0 -59.0;… %
%%% Testing Data for Index 4
100 -45;150 -46;200 -47;250 -50;300 -51;350 -52;400 -54;450 -56;500 -61;550 -
64;600 -66;650 -68;700 -71;750 -74;800 -76;850 -78;900 -81;950 -84;1000 -86;1050
-87;1100 -89;1150 -90;1200 -91;…
%%% Testing Data for Index 5
100 -62;200 -66;300 -73;400 -81;500 -87;600 -84;700 -89;800 -94;900 -92;1000 -
96;1100 -91;1200 -94;1300 -88;1400 -90;1500 -95;1600 -97;1700 -94;…
%%% Testing Data for Index 6
100 -50;200 -53;300 -59;400 -63;500 -61;600 -67;700 -70;800 -67;900 -79;1000 -
77;1100 -75;1200 -68;1300 -78;1400 -83;1500 -87;1600 -90;1700 -89
];
%%%
c=ones(26,1);
n=1.613;
cn1=n*c;
```

```
%%
c2=ones(10,1);
n2=2.2;
cn2=n2*c2;
%%
c3=ones(14,1);
n3=3.8;
cn3=n3*c3;
%%
c4=ones(19,1);
n4=1.701;
cn4=n4*c4;
%%
c5=ones(23,1);
n5=3.11;
cn5=n5*c5;
%%
c6=ones(17,1);
n6=3.5;
cn6=n6*c6;
%%
c7=ones(17,1);
n7=2.57;
cn7=n7*c7;
```

```
%%
cPL01=39*c;%dB
cPL02=45*c2;
cPL03=47.3*c3;
cPL04=41.04*c4;
%%
cPL05=89.7712*c5;
cPL06=106*c6;
cPL07=95*c7;
%%
check = [[cn1;cn2;cn3;cn4;cn5;cn6;cn7]
[cPL01;cPL02;cPL03;cPL04;cPL05;cPL06;cPL07] chkcolumn1];
save check
end
```

Appendix A-3: Matlab Code for ANFIS Program

```
%ANFIS (GANFIS) Optmization of RSS at the Mobile Node using Grey model
%output as the testing data
tic
clc
clear all
run trainingparameters1
run trainingparameters2
run trainingparameters3
```

```
run trainingparameters4
run trainingparameters5
run trainingparameters6
run trainingparameters7
run testingdata
load begin.mat
load begin2.mat
load begin3.mat
load begin4.mat
load begin5.mat
load begin6.mat
load begin7.mat
load check.mat
chkdata=[[tn1;tn2;tn3;tn4;tn5;tn6;tn7]
[tPL01;tPL02;tPL03;tPL04;tPL05;tPL06;tPL07]...
[trncolumn1;trncolumn12;trncolumn13;trncolumn14;trncolumn15;trncolumn16;trnco
lumn17]...
[trncolumn2;trncolumn22;trncolumn23;trncolumn24;trncolumn25;trncolumn26;trnco
lumn27;]];
trndata=[[cn1;cn2;cn3;cn4;cn5;cn6;cn7]
[cPL01;cPL02;cPL03;cPL04;cPL05;cPL06;cPL07] chkcolumn1];
%%%%% A plot training data and checking data versus mobile distance
plot(trndata(:,3),trndata(:,4),'-.*',chkdata(:,3),chkdata(:,4),'-.x');
legend('Training data','Checking data')
```

```
grid
xlabel('Distance from the antenna(m)')
ylabel('Received Signal Strength in dBm')
title('Received Signal Versus MNs distance for Training and Checking')
numMFs=[4 4 5];
mfType='gbellmf';
fismat=genfis1(trndata,numMFs,mfType);
showfis(fismat)
showrule(fismat)
ruleview(fismat)
ruleedit(fismat)
fismat = setfis(fismat, 'name','RSS');
fismat = setfis(fismat, 'input',1,'name','Path loss exponent');
fismat = setfis(fismat, 'input',2,'name','Path loss at refernce distance');
fismat = setfis(fismat, 'input',3,'name','MN distance from the Antenna');
fismat = setfis(fismat, 'output',1,'name','Received Signal Strength');
figure
plotfis(fismat);
figure
for input_index=1:3,
subplot(2,2,input_index)
[x,y]=plotmf(fismat,'input',input_index);
plot(x,y)
axis([-inf inf 0 1.2]);
```

```
xlabel(['Input ' int2str(input_index)]);
title('Initial Membership Values')
end
numEpochs=800;
[fismat1,trnErr,ss,fismat2,chkErr]=anfis(trndata,fismat,[numEpochs 0 0.04 0.9
1.1],...
   NaN,chkdata,1);
trnOut=evalfis([trndata(:,1) trndata(:,2) trndata(:,3)], fismat1);
trnRMSE=norm(trnOut-trndata(:,4))/sqrt(length(trnOut));
fprintf('trnRMSE: %s \n', trnRMSE);
%drawing error curves
epoch=1:numEpochs;
figure
plot(epoch, trnErr,'+', epoch, chkErr,'x');
ylabel('RMSE'); xlabel('Epochs'); legend('Training error','Testing error');
hold on;
plot(epoch, [trnErr chkErr]);
hold off;
%step size during training
figure
plot(epoch, ss,'*',epoch,ss,'x');
ylabel('Step Size');
xlabel('Epochs');
%membership function after training
```

```
figure
for input_index=1:3,
subplot(2,2,input_index)
[x,y]=plotmf(fismat1,'input',input_index);
plot(x,y)
axis([-inf inf 0 1.2]);
xlabel(['Input ' int2str(input_index)]);
title('Final Membership Values')
end
optrss = trnOut;
save optrss
orig_rss=PR0;
orig_rss2=PR02;
orig_rss3=PR03;
orig_rss4=PR04;
orig_rss5=PR05;
orig_rss6=PR06;
orig_rss7=PR07;
%%
mm=trndata(:,4);
%%
allparameters = {'n' 'PLO' 'Dist' 'Log-Normal' 'Pred_RSS_GM' 'Opt_RSS_ANFIS'
'Measured_RSS';...
   tn1 tPL01 trncolumn1 orig_rss trncolumn2 optrss mm};
```

```
allt = [[tn1;tn2;tn3;tn4;tn5;tn6;tn7]
[tPL01;tPL02;tPL03;tPL04;tPL05;tPL06;tPL07]...
[trncolumn1;trncolumn12;trncolumn13;trncolumn14;trncolumn15;trncolumn16;trnco
lumn17]...
   [orig_rss;orig_rss2;orig_rss3;orig_rss4;orig_rss5;orig_rss6;orig_rss7]...
[trncolumn2;trncolumn22;trncolumn23;trncolumn24;trncolumn25;trncolumn26;trnco
lumn27] optrss mm];
save allparameters
s1 = xlswrite('rssvalues.xls',allparameters,'simulation','A1');
s2 = xlswrite('rssvalues.xls',allt,'simulation','A3');
toc
```

Appendix B: Raw Results Data

The table below contains the raw data used in the study. RSS denotes the Received Signal Strength, LNSM denotes the Log-Normal Shadowing Model, GM denotes the Grey Model, wGM denotes the weighted Grey Model, ANFIS denotes Adaptive Neuro-Inference System and Measured denotes the column for data extracted from published papers.

Path Loss Exponent, n	Path Loss, PL	Distance (m)	RSS				
			LNSM	GM	wGM	ANFIS	Measured
1.613	39	1.5	-39.4510	-46.3219	-44.1234	-44.2566	-40.0
1.613	39	4	-46.3219	-49.7229	-48.3472	-47.4289	-46.5
1.613	39	6.5	-49.7229	-52.0026	-51.0106	-50.2394	-54.0
1.613	39	9	-52.0026	-53.7197	-52.9455	-52.7094	-55.8
1.613	39	11.5	-53.7197	-55.0977	-54.4631	-54.8611	-56.5
1.613	39	14	-55.0977	-56.2487	-55.7112	-56.7172	-57.6
1.613	39	16.5	-56.2487	-57.2369	-56.7709	-58.3008	-58.0
1.613	39	19	-57.2369	-58.1029	-57.6915	-59.6358	-58.6
1.613	39	21.5	-58.1029	-58.8735	-58.5052	-60.7461	-60.0

1.613	39	24	-58.8735	-59.5676	-59.2344	-61.6564	-60.5
1.613	39	26.5	-59.5676	-60.1991	-59.8948	-62.3914	-61.4
1.613	39	29	-60.1991	-60.7784	-60.4984	-62.9762	-60.7
1.613	39	31.5	-60.7784	-61.3134	-61.0541	-63.4361	-64.5
1.613	39	34	-61.3134	-61.8104	-61.5690	-63.7967	-64.0
1.613	39	36.5	-61.8104	-62.2745	-62.0487	-64.0839	-63.0
1.613	39	39	-62.2745	-62.7098	-62.4976	-64.3238	-63.5
1.613	39	41.5	-62.7098	-63.1195	-62.9195	-64.5427	-66.1
1.613	39	44	-63.1195	-63.5067	-63.3174	-64.7674	-65.8
1.613	39	46.5	-63.5067	-63.8735	-63.6940	-65.0250	-66.2
1.613	39	49	-63.8735	-64.2221	-64.0513	-65.3430	-66.0
1.613	39	51.5	-64.2221	-64.5542	-64.3913	-65.7495	-65.5
1.613	39	54	-64.5542	-64.8712	-64.7156	-66.2734	-65.7
1.613	39	56.5	-64.8712	-65.1745	-65.0255	-66.9443	-65.4
1.613	39	59	-65.1745	-65.4652	-65.3223	-67.7927	-68.5
1.613	39	61.5	-65.4652	-65.7443	-65.6070	-68.8507	-69.5
1.613	39	64	-65.7443	-66.0128	-65.8806	-70.1514	-69.7
2.2	45	1	-45.2721	-51.8948	-49.7396	-43.0104	-45.0
2.2	45	2	-51.8948	-55.7688	-54.2501	-47.1521	-47.5
2.2	45	3	-55.7688	-58.5174	-57.3570	-51.0201	-48.5
2.2	45	4	-58.5174	-60.6494	-59.7130	-54.6105	-53.0
2.2	45	5	-60.6494	-62.3914	-61.6072	-57.9194	-55.6
2.2	45	6	-62.3914	-63.8643	-63.1900	-60.9426	-62.0
2.2	45	7	-63.8643	-65.1401	-64.5489	-63.6761	-67.5
2.2	45	8	-65.1401	-66.2654	-65.7391	-66.1156	-67.0
2.2	45	9	-66.2654	-67.2721	-66.7979	-68.2571	-69.0
2.2	45	10	-67.2721	-68.1827	-67.7512	-70.0960	-67.7
3.8	47.3	2.5	-44.2270	-55.6661	-52.9570	-51.1976	-43.5
3.8	47.3	5	-55.6661	-62.3576	-60.1903	-58.5694	-62.0
3.8	47.3	7.5	-62.3576	-67.1053	-65.3503	-65.1492	-67.0
3.8	47.3	10	-67.1053	-70.7879	-69.3257	-70.9506	-73.5
3.8	47.3	12.5	-70.7879	-73.7967	-72.5478	-75.9874	-78.0
3.8	47.3	15	-73.7967	-76.3407	-75.2524	-80.2736	-84.5
3.8	47.3	17.5	-76.3407	-78.5444	-77.5809	-83.8231	-85.5
3.8	47.3	20	-78.5444	-80.4882	-79.6242	-86.6496	-87.0
3.8	47.3	22.5	-80.4882	-82.2270	-81.4441	-88.7666	-85.0
3.8	47.3	25	-82.2270	-83.7999	-83.0843	-90.1870	-83.0
3.8	47.3	27.5	-83.7999	-85.2359	-84.5770	-90.9234	-88.0
3.8	47.3	30	-85.2359	-86.5568	-85.9464	-90.9876	-93.0
3.8	47.3	32.5	-86.5568	-87.7799	-87.2113	-90.3910	-90.0
3.8	47.3	35	-87.7799	-88.9185	-88.3864	-89.1440	-93.0
3.11	89.8	100	-51.0000	-56.4764	-54.5497	-44.5315	-45.0
3.11	89.8	150	-56.4764	-60.3620	-58.8400	-46.6385	-46.0
3.11	89.8	200	-60.3620	-63.3759	-62.1253	-47.7248	-47.0
3.11	89.8	250	-63.3759	-65.8385	-64.7795	-48.5451	-50.0
3.11	89.8	300	-65.8385	-67.9205	-67.0031	-50.1896	-51.0
3.11	89.8	350	-67.9205	-69.7241	-68.9152	-52.4276	-52.0
3.11	89.8	400	-69.7241	-71.3149	-70.5919	-54.9167	-54.0
3.11	89.8	450	-71.3149	-72.7380	-72.0845	-57.5837	-56.0
3.11	89.8	500	-72.7380	-74.0253	-73.4291	-60.3744	-61.0
3.11	89.8	550	-74.0253	-75.2005	-74.6525	-63.1228	-64.0
3.11	89.8	600	-75.2005	-76.2816	-75.7746	-65.6451	-66.0

3.11	89.8	650	-76.2816	-77.2825	-76.8109	-68.1814	-68.0
3.11	89.8	700	-77.2825	-78.2144	-77.7734	-71.0368	-71.0
3.11	89.8	750	-78.2144	-79.0861	-78.6721	-73.7874	-74.0
3.11	89.8	800	-79.0861	-79.9049	-79.5148	-76.2050	-76.0
3.11	89.8	850	-79.9049	-80.6769	-80.3081	-78.5410	-78.0
3.11	89.8	900	-80.6769	-81.4072	-81.0574	-81.0329	-81.0
3.11	89.8	950	-81.4072	-82.1000	-81.7674	-83.5365	-84.0
3.11	89.8	1000	-82.1000	-82.7590	-82.4420	-85.6787	-86.0
3.11	89.8	1050	-82.7590	-83.3873	-83.0845	-87.4383	-87.0
3.11	89.8	1100	-83.3873	-83.9877	-83.6979	-88.9739	-89.0
3.11	89.8	1150	-83.9877	-84.5625	-84.2846	-89.8626	-90.0
3.11	89.8	1200	-84.5625	-85.1139	-84.8470	-91.0458	-91.0
3.55	45	100	-53.0000	-63.6866	-61.0321	-62.2058	-62.0
3.55	45	200	-63.6866	-69.9378	-67.8514	-65.2170	-66.0
3.55	45	300	-69.9378	-74.3731	-72.6987	-74.9947	-73.0
3.55	45	400	-74.3731	-77.8134	-76.4254	-80.3518	-81.0
3.55	45	500	-77.8134	-80.6244	-79.4425	-83.9819	-87.0
3.55	45	600	-80.6244	-83.0010	-81.9733	-86.9242	-84.0
3.55	45	700	-83.0010	-85.0597	-84.1512	-89.4127	-89.0
3.55	45	800	-85.0597	-86.8756	-86.0619	-91.6061	-94.0
3.55	45	900	-86.8756	-88.5000	-87.7633	-93.6384	-92.0
3.55	45	1000	-88.5000	-89.9694	-89.2966	-94.9439	-96.0
3.55	45	1100	-89.9694	-91.3109	-90.6918	-93.3521	-91.0
3.55	45	1200	-91.3109	-92.5450	-91.9716	-90.8427	-94.0
3.55	45	1300	-92.5450	-93.6875	-93.1537	-89.5115	-88.0
3.55	45	1400	-93.6875	-94.7512	-94.2519	-89.9506	-90.0
3.55	45	1500	-94.7512	-95.7463	-95.2772	-94.9903	-95.0
3.55	45	1600	-95.7463	-96.6809	-96.2387	-96.8816	-97.0
3.55	45	1700	-96.6809	-97.5622	-97.1439	-94.0911	-94.0
2.57	45	100	-50.4000	-58.1365	-55.8021	-49.8841	-50.0
2.57	45	200	-58.1365	-62.6620	-60.9638	-53.3669	-53.0
2.57	45	300	-62.6620	-65.8729	-64.5577	-58.4992	-59.0
2.57	45	400	-65.8729	-68.3635	-67.2944	-61.7682	-63.0
2.57	45	500	-68.3635	-70.3985	-69.4991	-64.1583	-61.0
2.57	45	600	-70.3985	-72.1190	-71.3434	-65.4892	-67.0
2.57	45	700	-72.1190	-73.6094	-72.9278	-67.2096	-70.0
2.57	45	800	-73.6094	-74.9240	-74.3163	-71.9034	-67.0
2.57	45	900	-74.9240	-76.1000	-75.5517	-76.5272	-79.0
2.57	45	1000	-76.1000	-77.1638	-76.6644	-77.9812	-77.0
2.57	45	1100	-77.1638	-78.1350	-77.6765	-72.1554	-75.0
2.57	45	1200	-78.1350	-79.0283	-78.6046	-71.8372	-68.0
2.57	45	1300	-79.0283	-79.8555	-79.4616	-76.3812	-78.0
2.57	45	1400	-79.8555	-80.6255	-80.2576	-82.3332	-83.0
2.57	45	1500	-80.6255	-81.3459	-81.0006	-87.9476	-87.0
2.57	45	1600	-81.3459	-82.0225	-81.6974	-89.3251	-90.0
2.57	45	1700	-82.0225	-82.6605	-82.3532	-89.2255	-89.0
1.701	41	3	-43.1570	-47.6347	-45.9491	-43.5831	-44.0
1.701	41	5.5	-47.6347	-50.4027	-49.2356	-47.8866	-46.0
1.701	41	8	-50.4027	-52.4116	-51.5223	-51.7235	-52.5
1.701	41	10.5	-52.4116	-53.9893	-53.2717	-55.1107	-62.0
1.701	41	13	-53.9893	-55.2887	-54.6874	-58.0659	-55.0
1.701	41	15.5	-55.2887	-56.3934	-55.8761	-60.6069	-53.0

1.701	41	18	-56.3934	-57.3541	-56.9002	-62.7518	-58.5
1.701	41	20.5	-57.3541	-58.2042	-57.7999	-64.5190	-64.0
1.701	41	23	-58.2042	-58.9664	-58.6020	-65.9268	-72.0
1.701	41	25.5	-58.9664	-59.6573	-59.3256	-66.9938	-77.0
1.701	41	28	-59.6573	-60.2891	-59.9847	-67.7386	-74.0
1.701	41	30.5	-60.2891	-60.8711	-60.5898	-68.1794	-67.5
1.701	41	33	-60.8711	-61.4106	-61.1492	-68.3348	-59.0
1.701	41	35.5	-61.4106	-61.9133	-61.6692	-68.2231	-60.0
1.701	41	38	-61.9133	-62.3840	-62.1550	-67.8623	-62.5
1.701	41	40.5	-62.3840	-62.8265	-62.6109	-67.2707	-70.0
1.701	41	43	-62.8265	-63.2439	-63.0402	-66.4662	-75.0
1.701	41	45.5	-63.2439	-63.6391	-63.4460	-65.4667	-70.0
1.701	41	48	-63.6391	-64.0142	-63.8307	-64.2900	-59.0

Appendix C: Publication

The paper was accepted for publication by the Journal of Sustainable Research in Engineering (JSRE). The reference and abstract of the paper are shown below:

Reference

N. Nkamwesiga, D. B. O. Konditi and H. A. Ouma, "Mobility Prediction Optimization of Mobile Hosts in Smart Antenna Systems Using Adaptive Neuro-Fuzzy Inference System," *Journal of Sustainable Research in Engineering (JSRE)*, to be published.

Abstract

MOBILITY PREDICTION OPTIMIZATION OF MOBILE HOSTS IN SMART ANTENNAS SYSTEM USING ADAPTIVE NEURO-FUZZY INFERENCE SYSTEM

Nicholas Nkamwesiga[1*], Dominic B. O. Konditi[2], Heywood A. Ouma[2]

[1]Department of Electrical Engineering, Pan African University, P. O. Box 62000-00200, Nairobi, Kenya

[2]Faculty of Telecommunication and Information Engineering, Technical University of Kenya, P. O. Box 52428-00200, Nairobi, Kenya

[3]*Department of Electrical and Information Engineering, University of Nairobi, P. O. Box 30197-00100, Nairobi, Kenya*

**Corresponding Author - E-mail: nkamwesiga.nicholas@students.jkuat.ac.ke*

Abstract – Owing to the growing demand for wireless communication, the communication network should have better coverage, improved capacity, and higher transmission quality, which contribute to better Quality of Service (QoS). The use of smart antenna systems (SASs) is one of the promising technologies in achieving this demand. The SASs achieve this by dynamically radiating shaped signal beams to the mobile terminals in response to received signals. This has the effect of enhancing the performance characteristics such as capacity and hand-over in wireless systems. By using machine learning methods, it is possible to predict upcoming changes in the mobile terminal location at an early stage and then carry out beam forming optimization to alleviate the reduction in network performance. Prediction of Received Signal Strength (RSS) in wireless networks offers a strong base for mobility prediction and localization with minimal effort. The need for mobility prediction is significant and calls for the use of artificial intelligence approaches to make precise and efficient predictions.

This paper presents the use of Grey Prediction model (GM) which is associated with benefits of reduced overheads in wireless cellular networks and Adaptive Neuro-Fuzzy Inference System (ANFIS) in improving mobility prediction. In this methodology, the ANFIS uses both measured data and the theoretical data used by Log-Normal Shadowing Model (LNSM) to achieve a better estimation of mobility. Mobility is based on the RSS at the mobile node (MN) as it moves towards or away from the

transmitting antenna. The approach also takes into account the factors that contribute to the RSS including; path loss exponent, path loss at reference distance and distance of the MN from the transmitter. The results show that ANFIS achieves prediction with a mean absolute error (MAE); between 0.083m and 0.690m for short distances (1m-65m), and between 0.322m and 3.877m for long distance (100m-1800m). The results were compared against those from other models including the LNSM, GM and generic weighted GM which were found to achieve prediction with larger MAE than ANFIS.

Keywords-Adaptive Neuro-Fuzzy Inference System, Grey Prediction Model, Mobility Prediction, Path Loss, Received Signal Strength.